Markers and Mechanisms of β-cell Dedifferentiation

Jason Fan

Submitted in partial fulfillment of the
requirements for the degree of
Doctor of Philosophy
under the Executive Committee
of the Graduate School of Arts and Sciences

COLUMBIA UNIVERSITY

2018

ABSTRACT

Markers and Mechanisms of β cell Dedifferentiation

Jason Fan

Human and murine diabetes is characterized by pancreatic β-cell dedifferentiation, a process in which β-cells lose expression of markers of maturity and gain those of endocrine progenitors. Failing β-cells inappropriately metabolize lipids over carbohydrates and exhibit impaired mitochondrial oxidative phosphorylation. Therefore, pathways involved in mitochondrial fuel selection and catabolism may represent potential targets for the prevention or reversal of dedifferentiation.

In chapter I of this dissertation, we isolated and functionally characterized failing β-cells from various experimental models of diabetes. We found a striking enrichment in the expression of aldehyde dehydrogenase 1 isoform A3 (Aldh1a3) as β-cells become dedifferentiated. Flow-sorted Aldh1a3-expressing (ALDH+) islet cells demonstrate impaired glucose-induced insulin secretion, are depleted of Foxo1 and MafA, and include a Neurogenin3-positive subset. RNA sequencing analysis demonstrated that ALDH+ cells are characterized by: (i) impaired oxidative phosphorylation and mitochondrial complex I, IV, and V; (ii) activated RICTOR; and (iii) progenitor cell markers. We propose that impaired mitochondrial function marks the progression from metabolic inflexibility to dedifferentiation in the natural history of β-cell failure.

In chapter II of this dissertation, we report that cytochrome b5 reductase 3 (Cyb5r3) is a FoxO1-regulated mitochondrial oxidoreductase critical to β cell function. Expression of Cyb5r3 is greatly decreased in multiple murine models of diabetes, and *in vitro* Cyb5r3 knockdown leads to increased ROS generation and impairment of

respiration, mitochondrial function, glucose-stimulated insulin secretion, and calcium mobilization. *In vivo*, mice with β-cell-specific ablation of Cyb5r3 (B-Cyb5r3) display impaired glucose tolerance with decreased insulin secretion, and their islets have significantly lower basal respiration and glucose-stimulated insulin secretion. B-Cyb5r3 β-cells lose expression of Glut2, MafA, and Pdx1 expression despite a compensatory increase in FoxO1 expression. Our data suggest that Cyb5r3 is a critical mediator of FoxO1's protective response in β-cells, and that loss of Cyb5r3 expression is an early event in β-cell failure.

TABLE OF CONTENTS

LIST OF FIGURES

Neurogenin3 (g). ALDH1A3+/ Neurog3^{+} cells are indicated by the white arrows. Neurog3/ALDH1a3 stainings were performed on consecutive sections. To better assess Neurog3/ALDH1A3-positive cells, we provide two representative sections from Foxo knockout mice.

Fig. 3 ALDH gain-of-function in β cells. *a*, Effect of Foxo1 overexpression on *Aldh1a3* mRNA in Min6 cells. Foxo-DN is a truncated mutant that is unable to drive gene expression and competes with endogenous Foxo for DNA binding. Foxo-DBD is a mutant unable to bind the Foxo response element, but can still function as a coregulator of gene expression [2]. ***b,*** Western blot analysis of ALDH1A3 levels following lentiviral transduction in Min6 cells. ***c,*** Gene expression in Min6 cells stably-expressing GFP or ALDH1a3. ***d,*** Insulin secretion expressed as fold-increase from 5 to 20 mM glucose in MIN6 cells expressing either GFP or ALDH1A3 (n=8). ***e,*** Insulin secretion in primary islets from C57Bl/6J mice expressing either GFP or ALDH1A3 adenovirus (n=3). ***f,*** Insulin secretion (expressed as in panel d) in islets isolated from *db/db* mice and their wild-type controls following treatment with the ALDH inhibitor DEAB at the doses indicated (n=4). Each experiment was performed with pooled islets from 5 mice per genotype. ***g,*** Area under the curve of oxygen consumption rates measured in Min6 cells stably expressing either GFP or ALDH1A3 (n=4 per group). One asterisk indicates $p<0.05$ by one-factor ANOVA.

Fig. 4 Isolation and characterization of ALDH^{+} cells. *a*, Enrichment procedure to isolate ALDH-expressing islet cells. β cells are labeled red by Rip-cre-activated Tomato.

Cells are incubated with aldefluor, and selected for tomato and aldefluor, yielding $ALDH^-$ (low) and $ALDH^+$ (high) cells. ***b-c***, Experimental validation. Islets from 6-month-old β cell-specific (Rip-cre) Foxo knockouts and littermate controls were sorted as described. The different circles denote the three cell populations used in further studies: RFP^-ALDH^-, RFP^+ALDH^-, and RFP^+ALDH^+. ***d,*** Quantification of RFP^+ALDH^+ cells in repeated sorts (n=5) of wild-type and Rip-Foxo knockout animals. ***e,*** Insulin secretion in RFP^-ALDH^- (GFP_FITC, PE TR subset 2), RFP^+ALDH^- (GFP_FITC, PE TR subset), and RFP^+ALDH^+ (GFP_FITC, PE TR subset 1) cells isolated from Rip-Foxo knockout mice (n=3). ***f-n***, qPCR analysis of selected transcripts in the different fractions isolated from islet cell preparations. One asterisk indicates $p<0.05$ by one-factor ANOVA.

Fig. 5 Comprehensive analysis of ALDH isoform expression in flow-sorted $ALDH^+$ and $ALDH^-$ cells. ***a,*** Data from RNA sequencing of all ALDH transcripts are represented as column Z-scores, with red indicating high expression and blue indicating low expression. Each row represents a different ALDH isoform, and each column an individual population from a single mouse used for analysis. RFP^+ALDH^-: JD001 through JD014, and RFP^+ALDH^+: JD003 through JD015. Aldh1a3 is boxed for reference. ***b,*** Model of the relationship between changes in Foxo levels and gene expression signature of $ALDH^+$ cells.

Table 2. Curated list of differentially expressed transcripts in wild-type $ALDH^-$ vs. $ALDH^+$ cells. This table lists a subset of genes differentially expressed between $ALDH^-$ and $ALDH^+$ cells, arranged by functional category.

Table 3. Pathway analysis of RNA sequencing in wild-type and Foxo knockout β cells. The table summarizes top pathways from transcriptome analysis of $ALDH^-$ vs. $ALDH^+$ cells.

Table 4. Progenitor-like features of $ALDH^+$ cells. Z-score analysis of transcriptional networks involved in pancreas development in $ALDH^+$ cells.

Table 5. Top 25 differentially expressed transcripts in $ALDH^+$ cells from wild-type and Foxo knockout mice. This table lists a subset of genes differentially expressed between wild-type and triple Foxo-deficient $ALDH^+$ cells, arranged by p-value.

Table 6. Overview of key differential changes in transcript profile of wild-type and Foxo knockout $ALDH^+$ cells. Category list of principal genes altered in $ALDH^+$ cells as a function of Foxo genotype. Upward arrows indicate genes with increased expression, downward arrows indicate genes with decreased expression. Arrows in the Foxo column indicate that the change is specific to Foxo knockout $ALDH^+$ cells.

CHAPTER II

Fig. 6 Expression of Cyb5r3 in Islets from Diabetic Mice (A) Cyb5r3 mRNA levels in Aldh-low (Aldh-) and Aldh-high (Aldh+) β-cells from RIP-Cre^+ (Ctrl) vs. RIP-Cre^+ $FoxO1/3/4^{fl/fl}$ (β-FoxO) mice (n=5 per group). (B) Co-Immunofluorescence of insulin (red), Aldh1a3 (blue), Cyb5r3 (green), and DAPI (white) in control vs. β-FoxO mice. (C)

ChIP-qPCR at the *Cyb5r3* promoter using anti-FoxO1 or control antibody in Min6 cell lysates. (D) *Cyb5r3* expression in Min6 cells treated with adenovirus expressing GFP, constitutively active FoxO1-ADA, or dominant negative FoxO1-DN256. All data in all panels are presented as means ± SEM. **p < 0.05, **p < 0.01, ***p < 0.001 by Student's t-test.

Fig. 7 Effects of Cyb5r3 Knockdown on Insulin Secretion, Respiration, ETC, NAD/NADH and ROS Generation. (A) Insulin secretion in Min6 cells treated with Ad-shCyb5r3 or Ad-shScramble at indicated glucose concentrations. (B) Basal respiration in Min6 cells stably expressing GFP, shCyb5r3, or shCyb5r4. (C-F) Mitochondrial ETC complex I-IV activity in isolated mitochondria from Ad-shCyb5r3 or Ad-shScr-treated Min6 cells. (G) ROS levels in Min6 cells treated with Ad-shCyb5r3 or Ad-shScr with or without 0.5mM palmitate. (H) NAD/NADH ratio and (I) NADH levels in Min6 cells treated with Ad-shScr, Ad-shCyb5r3, or Ad-Cyb5r3-GFP. (J) Lactate levels in Min6 cells treated with Ad-shCyb5r3 or Ad-shScr following incubation with 0.5mM palmitate. All data in all panels are presented as means ± SEM. **p < 0.05, **p < 0.01, ***p < 0.001 by Student's t-test.

Fig. 8 Effects of Cyb5r3 Knockdown in Primary Islets. (A) Glucose-stimulated insulin secretion and (B) insulin content in wildtype islets treated with Ad-shCyb5r3 or Ad-shScr. (C) Representative calcium flux traces from Insulin2-Gfp β-cells treated with Ad-shCyb5r3 or Ad-shScr measured by Fura2AM

fluorescence (n=10-20 per group). Black arrow denotes point at which perfusion changed from 2.8mM to 16.8mM glucose. Red arrow denotes change from 16.8mM glucose to 40mM KCl. (D) Averaged maximal peak heights of the 340/380 ratio from the same experiment (n=3 plates per treatment, with 10-30 beta cells counted per plate). All data in all panels are presented as means ± SEM. **p < 0.05, **p < 0.01, ***p < 0.001 by Student's t-test.

Fig. 9 Islet Cell Markers in Pancreata from 2-month-old mice. (A) Insulin (red), Cyb5r3 (green), and DAPI (blue) immunostaining in B-Cyb5r3 vs. RIP-Cre^{+} control mice. (B) Insulin (red), glucagon (green), somatostatin with pancreatic polypeptide (SMS+PP) (Blue), and DAPI (white). (C) Insulin (red), Glut2 (green), and DAPI (blue). (D) Insulin (red), MafA (green), and DAPI (blue). (E) Insulin (red), Cyb5r3 (green), Pdx1 (blue), and DAPI (white).

Fig. 10 Islet Cell Markers in Pancreata from 6-month-old mice. (A) Insulin (red), glucagon (green), somatostatin with pancreatic polypeptide (SMS+PP) (Blue), and DAPI (white) immunostaining in B-Cyb5r3 vs. RIP-Cre^{+} control mice. (B) Insulin (red), Glut2 (green), and DAPI (blue). (C) Insulin (red), MafA (green), and DAPI (blue). (D) Insulin (red), Cyb5r3 (green), Pdx1 (blue), and DAPI (white). (E) FoxO1 (green) and DAPI (blue).

Fig. 11 Metabolic Characterization of B-Cyb5r3 Mice. (A) Intraperitoneal glucose tolerance test (IPGTT) in 4-month-old female and (B) male B-Cyb5r3

mice vs. RIP-Cre+ controls. (C) 1hr refed serum insulin levels normalized to insulin after 4hr-fast in female B-Cyb5r3 mice. (D) Insulin tolerance test in 4-month-old female and (E) male B-Cyb5r3 mice vs. RIP-Cre+ controls. (F) Blood glucose in female B-Cyb5r3 vs. RIP-Cre+ control mice fed high fat diet for 1 week. (G) IPGTT in 4-month-old female and (H) male B-Cyb5r3 mice vs. RIP-Cre+ controls fed HFD for 8 weeks. (I) Insulin levels 15 and 30 minutes during IPGTT normalized by fasting levels in 4-month-old B-Cyb5r3 mice vs. RIP-Cre+ controls, both fed HFD for 8 weeks. All data in all panels are presented as means ± SEM. **p < 0.05, **p < 0.01, ***p < 0.001 by Student's t-test.

Fig. 12 Hyperglycemic Clamps (A) Blood glucose, (B) body weight, (C-D) glucose infusion rate, and (E-F) serum insulin in female B-Cyb5r3 vs. RIP-Cre+ control mice during the clamp. (D) and (F) are AUC quantifications of (C) and (E), respectively. All data in all panels are presented as means ± SEM. **p < 0.05, **p < 0.01, ***p < 0.001 by Student's t-test.

Fig. 13 B-Cyb5r3 Islet Function. (A) Glucose- and (B) secretagogue-stimulated insulin secretion in primary islets from B-Cyb5r3 vs. RIP-Cre+ controls (n=4 samples each containing 5 islets from 3 mice for GSIS, n=6 wells each containing 70 islets for islet respiration). (C) Time course of oxygen consumption rate measured in primary islets from B-Cyb5r3 vs. RIP-Cre+ controls. "Glucose" indicates the addition of 25mM glucose media. Oligomycin inhibits ATP synthase, FCCP is an uncoupler, and rotenone is an inhibitor of complex I. Islets from 5

mice were pooled in n=9 wells per genotype, with each well containing ~70 islets. All data in all panels are presented as means ± SEM. **p < 0.05, **p < 0.01, ***p < 0.001 by Student's t-test.

Supplemental Fig.1 Cyb5r3 Expression in Islets of Multiple Murine Models of Diabetes or Insulin Resistance. (A) Insulin (green), Cyb5r3 (blue), and DAPI (white) expression in Glut4-Cre Insulin Receptor Knockout (GIRKO) mice compared to Glut4-Cre+ Controls. (B) Insulin (red), Cyb5r3 (green), Pdx1 (blue), and DAPI (white) staining in mice fed normal chow or HFD for 20 weeks (C) Insulin (red), Cyb5r3 (green), Pdx1 (blue), and DAPI (white).staining in S961-treated (1wk) mice.

Supplemental Fig. 2 Knockdown Efficiency of shCyb5r3 Adenovirus. (A) Cyb5r3 mRNA levels in Min6 cells treated with shCyb5r3 vs. shScramble at varying MOIs of shCyb5r3 adenovirus. (B) Cyb5r4 mRNA expression in the same samples. (C) Densitometry of Cyb5r3 protein expression in samples treated with shScr vs. varying MOIs of shCyb5r3 adenovirus. (D) Western blot used for densitometry shown in (C). Rat Ins1 cells were used as a negative control for the mouse-specific shCyb5r3 sequence.

Supplemental Fig. 3 Metabolic Phenotyping Experiments Performed on B-Cyb5r3 mice. (A-B) Magnetic Resonance Imaging (MRI) of B-Cyb5r3 vs. RIP-Cre+ control mice fed (A) normal chow and (B) HFD. (C-D) Oral glucose tolerance test (OGTT) of 4-month old B-Cyb5r3 (C) female and (D) male mice fed

normal chow. (E) Fasting and refed serum triglycerides and non-esterified free fatty acids (NEFAs) in male and female B-Cyb5r3 mice fed normal chow. (D) IPGTT in S961-treated B-Cyb5r3 and RIP-Cre+ control mice (5 months old, n=6 per group).

Supplemental Fig. 4 Islet Cyb5r3 Staining and GTT in Male B-Cyb5r3 mice. (A) Insulin (red), Cyb5r3 (green), Pdx1 (blue), and DAPI (white) immunostaining in B-Cyb5r3 vs. RIP-Cre^{+} control mice. (B) IPGTT in 8-month-old male B-Cyb5r3 mice.

Supplemental Fig. 5 Islet Cell Quantification in B-Cyb5r3 Mice. (A) Insulin, glucagon, and somatostatin+pp area normalized to total islet area as determined by immunohistochemistry. Data shown for 2 month and 6 month old B-Cyb5r3 mice vs. RIP-Cre^{+} controls.

Supplemental Fig. 6 Progenitor Cell Marker Immunohistochemistry in B-Cyb5r3 Mice (A) Insulin (red), Neurog3 (green), and DAPI (white) immunostaining in B-Cyb5r3 vs. RIP-Cre^{+} control mice. (B) Insulin (red), Aldh1a3 (green), and DAPI (white).

Supplemental Table 1: List of Antibodies Used in this Study

ACKNOWLEDGMENTS

I am grateful to members of the Accili laboratory for insightful data discussions and for making the Accili lab a wonderful environment to make friends and perform excellent research: Jinsook Son, Diana Kuo, Takumi Kitamoto, Michael Kraakman, Wendy McKimpson, Liheng Wang, Joshua Cook, Fanny Langlet, Noemie Druelle, and Emi Ishida. A special thanks to Ja Young Kim-Muller, Utpal Pajvani, Li Qiang, Hongxia Ren, and Rebecca Haeusler, alums of the Accili lab that helped mentor and guide me. I thank Thomas Kolar, Ana Flete-Castro, Jun B. Feranil, Lumei Xu, and Q. Xu (Columbia University) for outstanding technical support. I thank Travis Morgenstern and Dr. Henry Colecraft (Columbia University) for providing the training and equipment for calcium flux imaging. I thank Drs. William Blaner and Seung-Ah Lee for helping with the quantification of retinoic acid species. I thank Drs. Lori Sussel and Rachel Kim for help analyzing RNA sequencing data. I thank Dr. Delfina Larrea for assisting with Seahorse respirometry and Dr. Magali Mondin (U. Nice) for providing us with the islet immunostaining quantification macro for ImageJ. I thank Dr. Läuge Schaffer (Novo Nordisk) for providing us with S961 InsR antagonist. I thank Enrique Garcia (Columbia University) for insightful discussion. I'd also like to thank the members of my thesis defense committee, Drs. Remi Creusot, Dieter Egli, Ron Liem, and Jeffrey Pessin for all their guidance and advice these past few years.

DEDICATION

I would like to dedicate my PhD dissertation to God, my wife, Sarah Elizabeth Stone Fan, and my daughter, Nicola Stone Fan. To Sarah: Thank you for patiently and lovingly standing by my side for the past 9 years. I am so lucky to have you as my partner in life. Thank you for helping to create our wonderful little family and for bearing and raising Nico. I hope our remaining time together will be filled with as much joy and love as we have already experienced. To Nico: Thank you for being the most wonderful little baby girl I could have ever hoped for. Thank you for already being so cute, quirky, and funny at the age of two. You bring so much joy into our lives, and I am so excited to see what kind of person you grow up to be.

CHAPTER I

INTRODUCTION

Diabetes arises as a consequence of combined abnormalities in insulin production and function [3]. Although alterations in either arm of this homeostatic loop can result in full-blown disease, in most individuals, the two abnormalities coexist. While target organs show an impaired response to insulin (so-called insulin resistance), β-cells of diabetics show a blunted and mistimed response to nutrients [4]. During the natural history of the disease, β-cell function markedly deteriorates [5]. In fact, an intrinsic susceptibility of the β–cell to functional exhaustion–what is commonly referred to as "β-cell failure"–sets apart those individuals who go on to develop diabetes from those that, at the same level of insulin resistance, don't [5]. Abnormalities of islet cell function in diabetes include an impaired insulin response to stimulus, a reduced number of β-cells, and an inappropriate glucagon response [6]. This occurs despite the fact that reversal of hyperglycemia can partly restore β-cell function, even in patients with advanced disease [7]. Treatments range from preserving β-cell function by reducing the metabolic demand on β-cells, to increasing β-cell performance to meet the increased metabolic demand [4]. Notwithstanding this evidence, it is unclear whether the two primary components of β-cell failure, impaired insulin secretion and reduced β-cell mass, are mechanistically linked. We have shown that genetic ablation of Foxo function in β-cells impairs metabolic flexibility, i.e., the ability to switch from glucose to lipids as a source of acetyl-CoA for mitochondrial oxidative phosphorylation, paving the way for β-cell dedifferentiation [8-11]. These two processes bookend β-cell failure, but we don't know what happens in between. The work described in this thesis attempts to characterize

the progression of β-cell failure and dedifferentiation. Central to our study is the transcription factor FoxO1, a critical mediator of β-cell function and identity.

Foxo in insulin action and β-cell function

Foxo 1, 3a, and 4 are three genes encoding forkhead-type transcription factors. There are over one hundred forkhead domain-containing genes in the human genome [12], but there are compelling differences that account for the selective involvement of the "O" subfamily in hormone action, a concept first discovered in *C.elegans* [13, 14]. Unique among the forkhead domain-containing proteins, Foxo change their subcellular localization and hence their activity in response to Akt-dependent phosphorylation as well as NAD^+-dependent acetylation [15]. The latter is thought to reflect the intracellular ratio of reduced NAD equivalents. Thus, Foxo can be viewed as a relay of metabolic signals to the nucleus. The overarching physiologic role of Foxo is to enable metabolic flexibility, i.e., the ability to switch from glucose to lipid utilization depending on nutrient availability [10, 16]. However, at a more granular level, this general property morphs into a more nuanced mode of action. Thus, in the central nervous system Foxo integrates energy intake with energy expenditure through its actions on neuropeptide production, processing, and signaling [17-19]. In liver, Foxo regulates hepatic glucose and lipid production, and in adipocytes, free fatty acid turnover [16, 20, 21]. In the vasculature, it regulates nitric oxide production and inflammatory responses [22-24]. In addition, Foxo has seemingly distinct functions in tissue differentiation and lineage determination that are best illustrated by its role to maintain stability of insulin-producing β-cells and prevent their dedifferentiation during diabetes progression [9, 25].

Our interest in this area was driven by the observation that Foxo subcellular localization changes in β-cells, depending on their pathophysiologic state[8, 26]. In the "resting" β-cell, under physiological conditions, Foxo is seemingly inactive. When β-cells are exposed to increased glucose and/or fatty acids levels [8, 27], or to cytokines and other inflammatory agents [28], Foxo undergoes nuclear translocation. This is due to different post-translational modifications that include phosphorylation and acetylation [15, 29]. The residence of Foxo in the nucleus leads to activation of certain pathways and inhibition of others. The net outcome of this response is described below. However, it's equally important to note that Foxo activation is limited in time, as the deacetylated nuclear protein has decreased stability [30]. As Foxo levels decrease, the stage is set for dedifferentiation through the loss of gene expression networks necessary to the maintenance of β-cell characteristics [31].

Insulin secretion and β-cell function

Our understanding of the regulation of β-cell function has been shaped by the metabolic paradigm, according to which insulin secretion responds to metabolic cues [32]. More controversial is the role of insulin itself as a regulator of β-cell function. The concept that insulin controls its own secretion remains debated, but the thrust of our work is that FoxOs integrate insulin/hormone-dependent pathways with glucose/nutrient-dependent pathways [8], thus superseding the debate on whether insulin or glucose are to blame for abnormal β-cell function.

There are two main phases to insulin secretion: an ATP-dependent first phase [32], and a second–or amplifying–phase, variously assumed to be controlled by pyruvate

cycling [33], NADH shuttle [34], long-chain acyl-CoAs [35], glutamate [36], or NADPH [37, 38]. Substrate for mitochondrial oxidative phosphorylation can be derived from glucose, amino acids, and lipids.

During the first phase of insulin secretion, glucose from the blood equilibrates across the β-cell's plasma membrane and is phosphorylated by glucokinase. Glucose-6-phosphate enters the glycolytic pathway to produce pyruvate, which then enters the mitochondria to be metabolized by the TCA cycle. Reducing equivalents produced by the TCA cycle then hyperpolarize the mitochondrial membrane to generate a protein gradient that drives ATP synthase. The ATP produced by this process is released into the cytosol and triggers closure of the K_{ATP}-channel, leading to depolarization of the cell membrane. Depolarization then triggers opening of the voltage-dependent Ca^{2+} channels, increasing cytosolic Ca^{2+} to promote exocytosis of stored insulin granules.

The second phase of insulin release sustains insulin production/secretion and requires the action of metabolic coupling factors, many of which originate from the mitochondria. For example, alpha-ketoglutarate formed by the TCA cycle can be converted by glutamate dehydrogenase to glutamate, which enhances glucose-stimulated insulin secretion.[39] However, in the state of metabolic excess, increased mitochondrial metabolism is a double-edged sword: reactive oxygen species (ROS) are a natural by-product of respiration and can damage mitochondrial inner membrane components. Extreme ROS production can even trigger apoptosis.

The balance between glucose and lipid oxidation is very important: during fasting, fatty acid oxidation allows β-cells to maintain a trickle of insulin secretion; after a meal, the rise in plasma glucose drives mitochondrial energy generation for ATP

production and insulin release [6]. Experimental animal studies show that Foxo activation in the early phases of diabetes preserves the balance between glucose and lipids in the generation of acyl-CoA for mitochondrial oxidation. Foxo maintains the activation state of the Maturity Onset Diabetes of Youth (MODY) genes Hnf4, Hnf1, and Pdx1, and suppresses the fatty acid oxidation network supervised by nuclear receptor Pparα, to curtail generation of lipid-derived acyl-CoA[10, 31, 40].

This stress response aims to preserve the physiologic balance of mitochondrial substrate, and keeps β-cells from "overheating" [10, 40]; but again, it is not unlimited. There is a penalty to be paid for Foxo activation: it becomes rapidly degraded, leading to its depletion if hyperglycemia does not resolve [10]. As Foxo expression wanes, β-cells switch from glucose oxidation-driven energy generation to lipid oxidation-driven energy generation for insulin secretion, becoming "blind" to glucose. Excessive lipid oxidation leads to generation of toxic products, primarily ROS and peroxides, and impairs ATP production, calcium mobilization, and insulin secretion. Interestingly, loss of Foxo is also associated with increased Pparγ and triglyceride synthesis [6]. We have suggested that this increase is compensatory in nature, and is meant to divert acyl-CoA toward lipid synthesis, to alleviate mitochondrial overload. The inability of the β-cell to adapt from lipid to glucose utilization is similar to what has been described in other tissues as metabolic inflexibility [41]. We have proposed that this inflexibility is a key step in β-cell failure [10].

What are the long-term consequences of metabolic inflexibility? Gradually β-cells lose, along with insulin secretion, their terminally differentiated features. This conclusion was arrived at using lineage-tracing studies to monitor the fate of β-cells during diabetes

development [9]. Talchai *et al.* (2012) subjected insulin promoter Ins2-Cre^{+}:FoxO1$^{fl/fl}$:Rosa26-GFP mice to various physiological stressors (multiparity, aging, etc.), and followed their fate. The expectation of these experiments was that, if diabetic β-cells died of apoptosis, they would simply disappear over time. Instead, GFP+ β-cells were still present, but lost their defining features (Insulin, MafA, and Pdx1 expression) while gaining features of endocrine progenitor/stem cells (Neurog3, L-Myc, and Oct4 expression). Moreover, a subset of these "dedifferentiated" cells then turned into glucagon-producing cells, providing a potential explanation for the hyperglucagonemia of diabetes [9]. This observation has now been reproduced [42-46], and significantly advanced by the demonstration that in rodents, non-human primates, and human islets dedifferentiation is reversible by insulin and other treatments [25, 44, 47-50]. Although insulin treatment of humans has not been found to result in significant restoration of β-cell dysfunction [51], the data raise the possibility that new agents, acting on different mechanisms, might prevent or reverse β–cell failure.

Dedifferentiation: a cellular hypothesis rooted in clinical observation

From the studies described above, it can be concluded that as β-cells lose their identity, they come to resemble endocrine progenitor cells [9, 25, 42, 43]. The notion that β-cells might become dedifferentiated during diabetes progression has parallels in the daily clinical reality of treating diabetic patients. Beginning in the 1980's, with the advent of glucose clamp techniques, the idea that type 2 diabetes could be subsumed under the paradigm of insulin resistance became commonplace. And certainly treating insulin resistance is a large unmet medical need [52]. But prior to that, diabetes treatment was primarily viewed

as addressing the need to improve insulin secretion. Astute clinicians knew that insulin secretion becomes worse with each passing year, and early clinical studies showed the benefits of β-cell "rest" [7, 53, 54]. Beginning with the UKDPS [55], these findings became settled law, jumpstarting a search for treatments that would "protect" the β-cells and "modify" the course of the disease. Thus, the concept of dedifferentiation provides an underpinning for the reversibility of β-cell failure in the early phases of diabetes, and at the same time an explanation for the slow decline of β-cell function.

An important step in the process of determining the role of β-cell dedifferentiation was to test the human relevance of the mouse observations. While one cannot easily assess cellular plasticity of the endocrine pancreas in living humans, it's however possible to use animal studies to formulate testable hypotheses on the expected features of dedifferentiated human β-cells [56, 57]. With this goal in mind, our lab undertook a survey of human diabetic pancreata from organ donors to assess if β-cells become dedifferentiated. The assumptions were that dedifferentiated β-cells would no longer contain insulin, or other pancreatic hormones, to exclude cells arising from converted β-cells. However, dedifferentiated cells would retain endocrine as well as progenitor cell features that could be detected by immunohistochemical techniques [9]. Under these assumptions, Cinti *et al*. were able to confirm the prediction that β-cells become dedifferentiated in patients with type 2 diabetes. They found that all features of murine dedifferentiation occur in the human islets: ~40% of β-cells were dedifferentiated according to these criteria, and displayed patterns of transcription factor expression reminiscent of murine islets, with decreased Foxo1, Nkx6.1, and MafA. In addition, 4% of β-cells were degranulated, as assessed by electron microscopy.

Relevant to this issue is whether dedifferentiating β-cells do indeed have progenitor cell-like features. To address this question it's necessary to first discover biomarkers that can be used to isolate and characterize "failing" β cells. In Chapter I, we report the discovery of an isoform of the enzyme aldehyde dehydrogenase (ALDH1A3) as a biomarker of dysfunctional β cells. We isolated and characterized ALDH1A3-expressing islet cells, and compared their gene expression profiles in normal and diabetic mice. The data indicate that two reciprocal processes unfold in failing β cells: a decrease of mitochondrial function with (likely compensatory) RICTOR activation, associated with activation of progenitor cell-like features. We identify a narrow set of candidate genes that may affect the transition from a healthy to a dysfunctional β cell. The significance of this work consists in the discovery of a biomarker of β cell dysfunction that can also be used to isolate failing cells; and in the identification of a pathogenic mechanism and a narrow set of potential effectors that can be tested for therapeutic relevance.

MATERIALS AND METHODS

We performed genotyping as described.[58, 59] Mice were maintained on a *mixed* 129J-C57BL/6 background. We derived control genotypes from the same litters. Owing to the complexity of genotyping the 6 mutant alleles (five Foxo alleles and Rip-cre), we used different combinations of Foxo1, 3 and 4 floxed mice without Rip-cre transgene or Rip-cre mice without Foxo floxed alleles [60]. Sample size calculations were based on the variance observed in prior experiments [10, 31]. These mice were indistinguishable from *mixed* 129J-C57BL/6 mice in all metabolic tests. All mice were fed normal chow and maintained on a 12–hour light–dark cycle (lights on at 7 AM). The Columbia University Institutional Animal Care and Utilization Committee approved all experiments.

Cell lines. We used the mouse insulinoma cell line MIN6, obtained from ATCC, and previously characterized for its ability to secrete insulin [8].

RNA profiling. We used GeneChip Mouse Exon arrays (Affymetrix) and performed data analysis with Partek Genomics Suite (Partek, Inc.) and Ingenuity Pathway Analysis (Ingenuity Systems, Inc.). For the analyses shown in this study, we used a threshold of $p < 0.05$ and >1.3-fold change ($n = 4$ WT, 3 KO per group). Each array was performed with pooled islets from 3 mice per genotype [10]. Data have been deposited as in the GEO database as GSE78966.

Fluorescence-Activated Cell Sorting. We isolated islets by collagenase digestion from 6-month-old *Rip-cre Foxo1,3a,4*$^{lox/lox}$;*RFP (ROSA-Tomato)* and *Rip-cre*

Foxo1,3a,4$^{+/+}$;*RFP* mice (10-20 animals per genotype) as described [10]. We incubated cells with the fluorescent ALDH substrate BODIPY™-aminoacetaldehyde (aldefluor) for 1hr prior to flow cytometry. Thereafter, cells were applied to a BD Influx sorter and analyzed with a BD LSRII instrument. We gated cells for RFP (red) and aldefluor (green) fluorescence, and sorted three sub-populations: $RFP^{-}ALDH^{-}$ (non-β cells), $RFP^{+}ALDH^{-}$ (β cells), and $RFP^{+}ALDH^{+}$ (ALDH-positive β cells).

Immunoblot and immunohistochemistry. We performed immunoblotting and immunohistochemistry as previously described[9]. We used the following antibodies: rabbit primary antibodies to FoxO1 (Santa Cruz, Cell Signaling), somatostatin (DAKO), Aldh1a3 (Novus), Neurog3 (Beta Cell Biology Consortium), and MafA (Bethyl); guinea pig primary antibodies to insulin and glucagon (DAKO), and Pdx1 (Millipore); sheep primary antibodies to Somatostatin (Novus); goat primary antibodies to Pancreatic Polypeptide (Novus and Abcam), Somatostatin (Santa Cruz), Nkx6.1 (Santa Cruz), and L-Myc (R&D) ; and mouse primary antibodies to Aldh1a3 (LSBio) and Glucagon (Sigma) [58].

Mitochondrial function. We used the XF24-3 respirometer (Seahorse Bioscience) with 24-well plates. We used the F_1F_0 ATP synthase inhibitor oligomycin to assess uncoupling, FCCP to estimate maximum respiration, and rotenone to measure non-mitochondrial respiration [61].

RNA measurements. We used standard techniques for mRNA isolation and SYBR green quantitative PCR. PCR primer sequences have been published [9]. Data have been deposited as GEO (number pending).

Statistical analyses and general methods. Sample sizes were estimated from expected effect size based on previous experiments. No randomization or blinding was used. We present data as means ± SEM. We used two-tailed Student's t-test, one-way ANOVA, or two-way ANOVA for data analysis, and the customary threshold of $p < 0.05$ to declare statistically significant differences.

RESULTS

Elevated ALDH1A3 is a common feature of diabetic β cells. We reasoned that critical changes in gene expression during β cell failure would be shared across multiple models of diabetes. We used two permutations of a genetic approach involving triple Foxo knockouts (Foxo1, 3a, and 4) at two distinct developmental stages: (*i*) in pancreatic precursors (generated using *Pdx1-cre*-mediated gene knockout) [11]; (*ii*) in terminally differentiated β-cells (generated using *RIP-cre*) [9]. The triple Foxo knockout faithfully replicates human MODY, a genetic form of diabetes caused by an intrinsic β-cell abnormality [62]. When we compared transcriptomes of islets from these models, a swath of genes was uniformly affected across the board. Among them was aldehyde dehydrogenase isoform 1A3 (ALDH1A3), expression of which increased 3 to 6-fold with robust adjusted *p* values (Table 1). We tested the expression of ALDH1A3 in other models of diabetes including aging, diet-induced, and *db/db* mutants, and found it to be increased too (Fig. 1a). We sought independent confirmation of this observation in the literature, and found that similar increases of ALDH1A3 had been observed in diabetic Nkx6.1 (Ref [43]) and MafA knockout mice [63], as well as in a cross of diabetes-sensitive *vs*. resistant mice [64]. ALDH1A3 is notably absent from normal β cells [65]. In a recent study inspired by these findings, we found that ALDH1A3 is also elevated in islets from patients with type 2 diabetes [66].

Chapter I, Figure 1

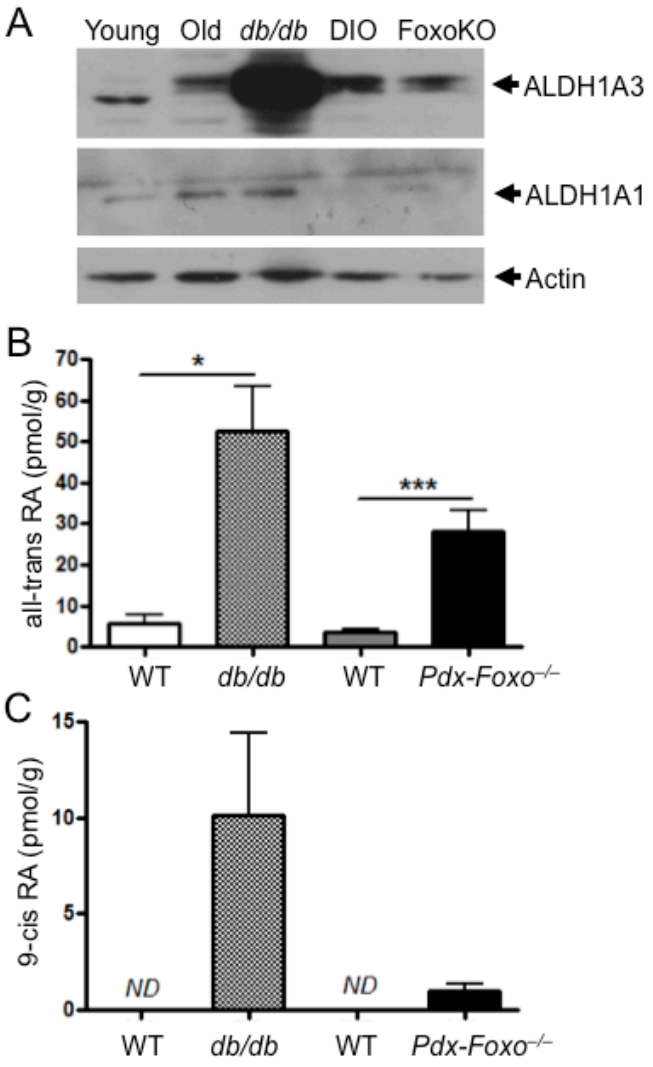

Figure 1

Table 1. Comparison of the top 10 transcripts in two models of Foxo knockout β cells

β cell-specific triple FoxO knockout (Rip-cre)				Pan-pancreatic triple FoxO knockout (Pdx-cre)			
Gene symbol	*RefSeq*	*P*	*Fold change*	*Gene symbol*	*RefSeq*	*P*	*Fold change*
Serpina7	NM_177920	0.0303021	6.10514	Serpina7	NM_177920	0.00421694	11.2331
Ly96	NM_016923	0.0397911	3.54036	Penk	NM_001002927	1.90E-05	9.24023
Asb11	NM_026853	0.00436504	2.9386	Aldh1a3	NM_053080	4.83E-06	5.59631
Aldh1a3	NM_053080	2.89E-05	2.87677	Aass	NM_013930	0.00140689	5.29716
Fabp3	NM_010174	0.0280225	2.7083	Fabp3	NM_010174	0.00458626	3.49306
Aass	NM_013930	0.0199395	2.58233	Zfp423	NM_033327	6.73E-05	3.40006
Gnpda2	NM_001038015	0.0486419	2.54645	Ly96	NM_016923	0.0395544	3.39488
Tmed6	NM_025458	0.0427281	2.52494	Asb11	NM_026853	0.0019639	3.36892
Arsk	NM_029847	0.0290211	2.5013	Tmed6	NM_025458	0.00459613	3.29786
4930432O21Rik	NM_001025373	0.0434902	2.47144	Mc5r	NM_013596	0.0167905	3.28699

List of the 10 top overexpressed genes from microarray analysis of β cells isolated from β cell-specific and pan-pancreatic Foxo triple Foxo knockouts compared to their relevant wild-type controls.

ALDH1A3 had two attractive features: ALDH1 activity marks human cancer progenitor cells [67-70], and ALDH1A3 has been recognized as the isoform conveying increased ALDH1 activity in lung, ovary, breast, head and neck cancer, and melanoma [71-73]. This fits with the notion that dedifferentiating β cells have progenitor-like features [25, 43, 74]. Moreover, ALDH-expressing cells can be readily isolated using live cell assays [75]. ALDH1A3 is one of 20 murine genes encoding $NAD(P)^+$-dependent enzymes that

catalyze aldehyde oxidation. ALDHs also have additional catalytic (*e.g.*, esterase and reductase) and non-catalytic activities. ALDH1A3 is also known as retinaldehyde dehydrogenase (RALDH3) owing to its ability to synthesize retinoic acid (RA) from retinal.

The increase was specific to ALDH1A3, as other isoforms showed little if any change (Fig. 1a and data not shown). Measurements of all-trans-RA and 9-cis-RA production in islets confirmed a correlation between ALDH1A3 levels and RA generation, indicating that the enzyme is catalytically active (Fig. 1b-c). We localized ALDH1A3 in islets using immunohistochemistry. ALDH1A3-positive cells were rare in normal islets (Fig. 2a). We studied a classic model of diabetes secondary to extreme obesity, *db/db* mice, as well as mice that develop diabetes as a consequence of extreme peripheral insulin resistance, brought about by targeted knockout of Insulin Receptor in muscle, fat, and brain (GIRKO) [1]. Of note, the latter mice have no intrinsic β cell abnormalities, but develop diabetes as a result of their inability to compensate for insulin resistance. In both models, the number of ALDH1A3-expressing cells rose considerably (Fig. 2a-b). There was heterogeneity of immunohistochemical signal intensity among ALDH1A3-expressing cells. We empirically defined them as ALDH1A3^{low} and ALDH1A3^{hi} cells. ALDH1A3 immunoreactivity showed a reciprocal pattern with insulin immunoreactivity such that ALDH1A3^{hi} cells were insulin-negative, while ALDH1A3^{low} cells retained some insulin immunoreactivity (Fig. 2a-b). We didn't detect strongly insulin-immunoreactive cells that were also ALDH1A3-positive, nor did we detect any other endocrine cell type that co-localized with ALDH1A3 in mouse islets (Fig. 2b). These data show that ALDH1A3-expressing cells are heterogeneous and are

comprised of insulin-producing cells as well as hormone-negative cells that can potentially represent a progenitor-like population.

Chapter I, Figure 2

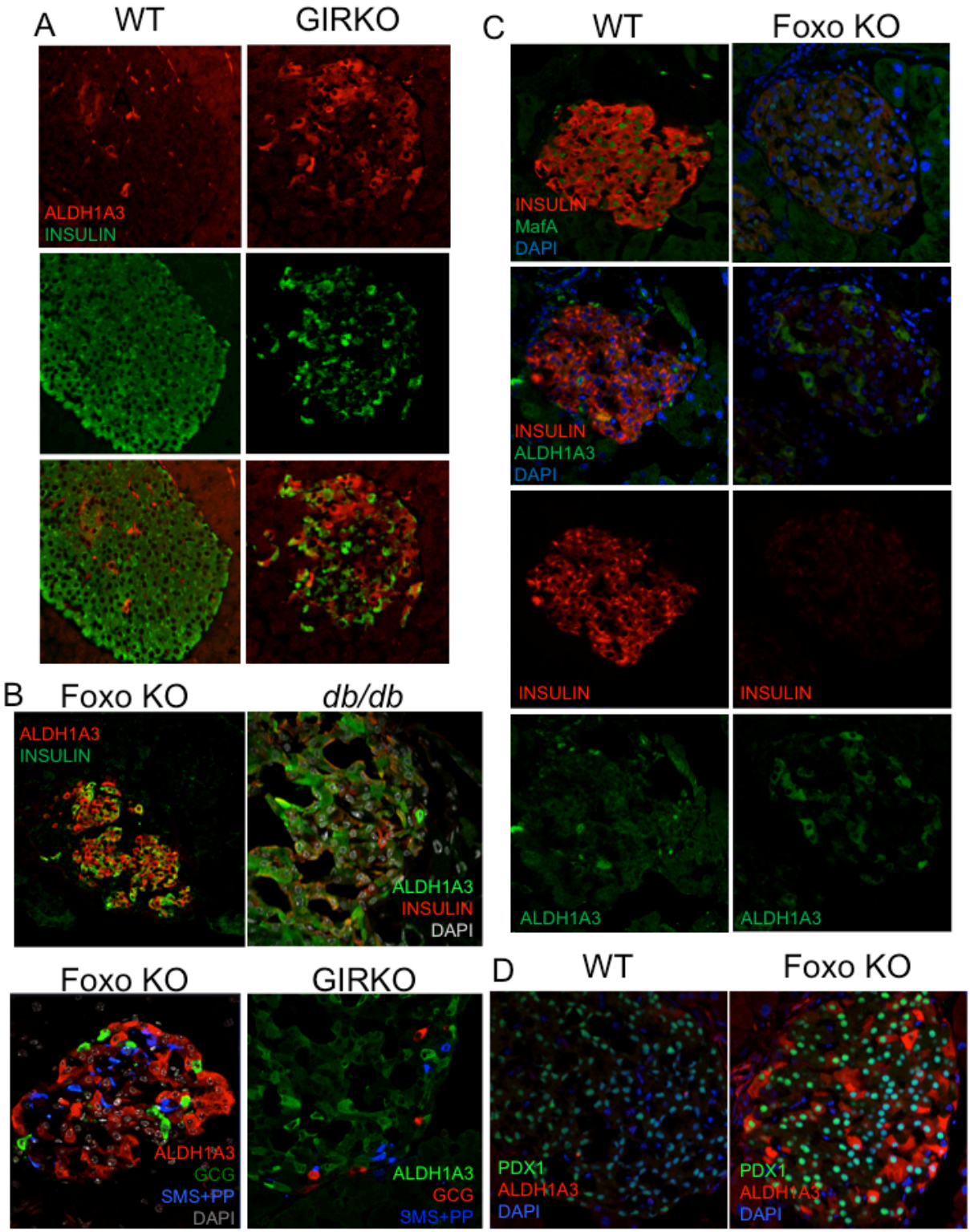

Figure 2

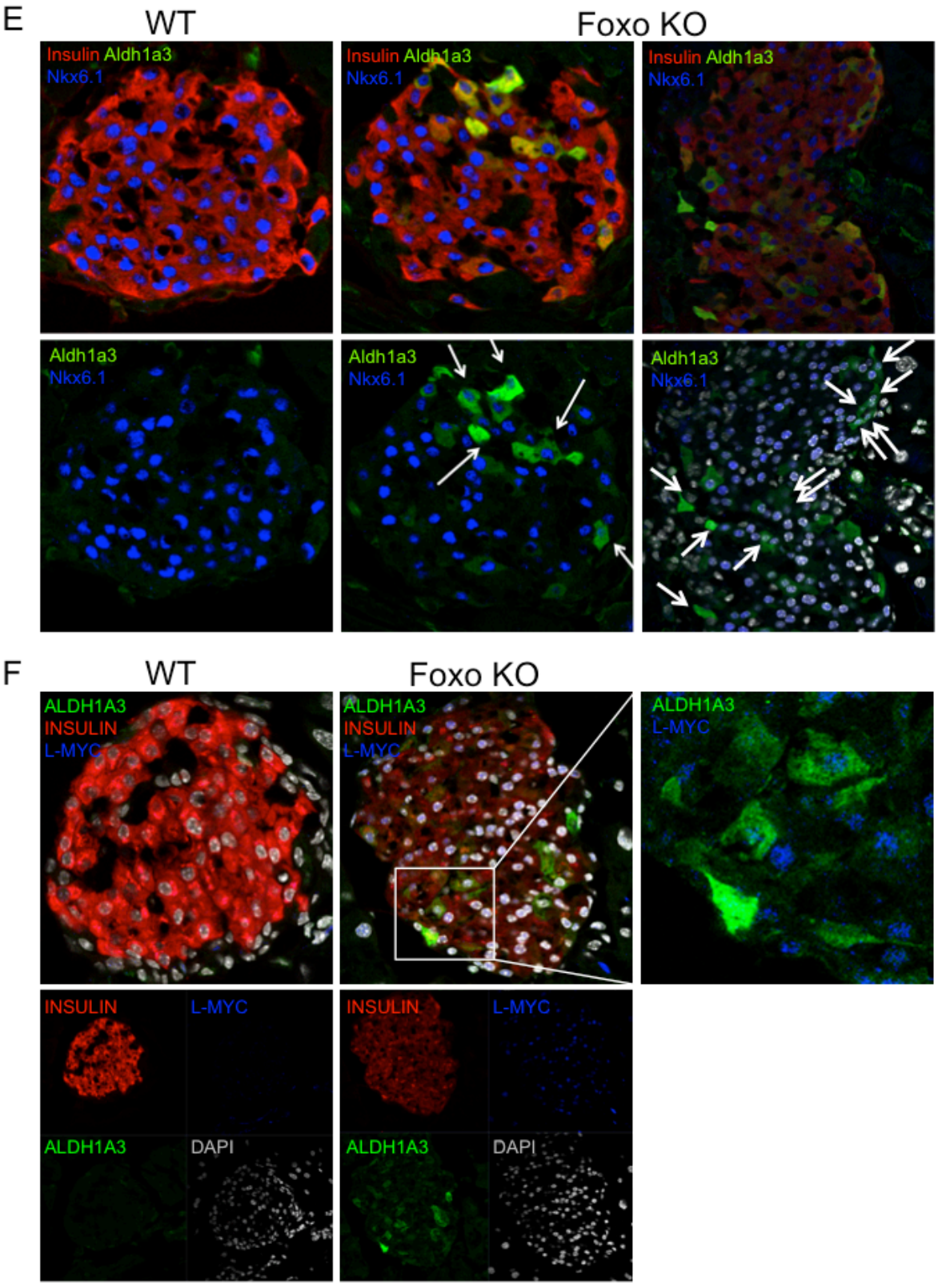

Chapter I, Figure 2 Continued

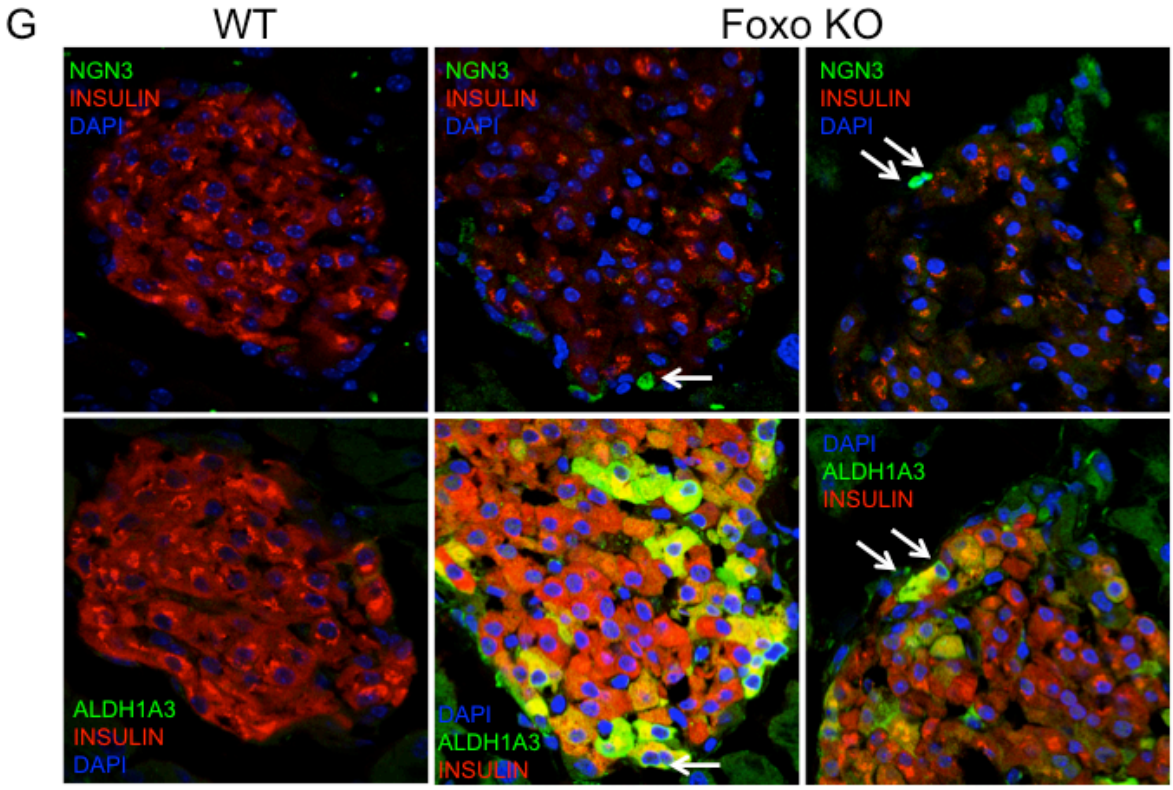

Chapter I, Figure 2 Continued

We tested the expression of various β cell markers in ALDH1A3-positive cells. They had weak MafA immunoreactivity (Fig. 2c), but retained Pdx1 immunoreactivity (Fig. 2d). We examined Nkx6.1 expression by staining adjacent sections with insulin and Nkx6.1 or ALDH1A3 and Nkx6.1 and found that Nkx6.1 was generally reduced (Fig. 2e, left and middle panels). We then performed co-staining with ALDH1A3 and Nkx6.1 antibodies on the same section, and found that Nkx6.1 was absent in a subset of ~10% of ALDH1A3-positive cells (Fig. 2e, right panels, white arrows). We also examined two progenitor cell markers, L-myc and Neurogenin3. Consistent with previous results, we found that L-myc expression increased in Foxo knockout islets and that ALDH1A3-

positive cells were L-myc-positive (Fig. 2f). Moreover, there was a subset of ALDH1A3-positive/Neurog3^{+} cells (Fig. 2g, white arrows). These data provide immunohistochemical evidence that ALDH1A3 marks a heterogeneous cell population, with features of incipient β cell failure (reduced insulin), and including a subset of dedifferentiating (low MafA or Nkx6.1) or dedifferentiated cells (L-myc and Neurog3-expressing) [9, 25, 43].

ALDH1A3 overexpression does not impair insulin secretion. As Foxo1 loss-of-function is associated with increased ALDH1A3 levels, we asked whether Foxo1 regulates ALDH1A3 in MIN6 insulinoma cells. We transfected wild-type and two different mutant Foxo1 constructs to investigate this point. The first mutant is a dominant-negative that binds to DNA but lacks the transactivation domain, preventing binding of RNA polymerase, hence transcription. When over-expressed, it outcompetes endogenous Foxo (1, 3a, and 4) and effectively mimics the effect of a knockout [76]. The second mutant, DNA-binding deficient (DBD), doesn't bind to DNA, and fails to activate Foxo targets for which DNA binding is required [2]. Inhibition of Foxo1 by the dominant-negative mutant resulted in a ~ 30-fold increase in *Aldh1a3* mRNA, while the DBD mutant Foxo1 failed to activate *Aldh1a3* expression (Fig. 3a). This experiment shows that Foxo1 inhibits *Aldh1a3* independently of DNA binding, likely acting as a co-repressor [2, 77]. These data are consistent with the possibility that activation of ALDH1A3 expression is an early correlate of reduced Foxo1 function.

Reduced RA signaling in islets has been linked to defective insulin secretion [78]. To test whether elevated ALDH1A3 activity affects β cell function, we overexpressed

ALDH1A3 in MIN6 cells using either transient transduction with adenovirus (Fig. 3b) or the derivation of stably transfected clones, and then measured expression of genes that are important for β cell function or glucose-stimulated insulin secretion. In either case, we found no defects in gene expression (Fig. 3c) or insulin secretion (Fig. 3d). Moreover, we transduced islets of wild-type C57Bl/6J mice with ALDH1A3 adenovirus and found a small, but statistically significant increase of glucose-induced insulin secretion (Fig. 3e). ALDH1A3 activity can be inhibited by the irreversible inhibitor N,N-diethylaminobenzaldehyde (DEAB) [75]. We performed insulin secretion experiments in MIN6 cells overexpressing ALDH1A3, as well as in *db/db* mice with endogenously elevated ALDH1A3, in the presence of DEAB. But we didn't detect an effect of this compound to change insulin secretion (Fig. 3f). Finally, we measured oxygen consumption in MIN6 cells overexpressing ALDH1A3 as a surrogate of mitochondrial function, and found a modest decrease (Fig. 3g). However, in light of the fact that insulin secretion was normal (in MIN6) or slightly elevated (in primary islets), we suppose that this slight oxidative defect is unlikely to result in a functional change. These data showing that acute gain-of-function of ALDH1A3 doesn't compromise β cell function suggest that ALDH1A3 is a marker, rather than a cause of β cell dysfunction.

Chapter I, Figure 3

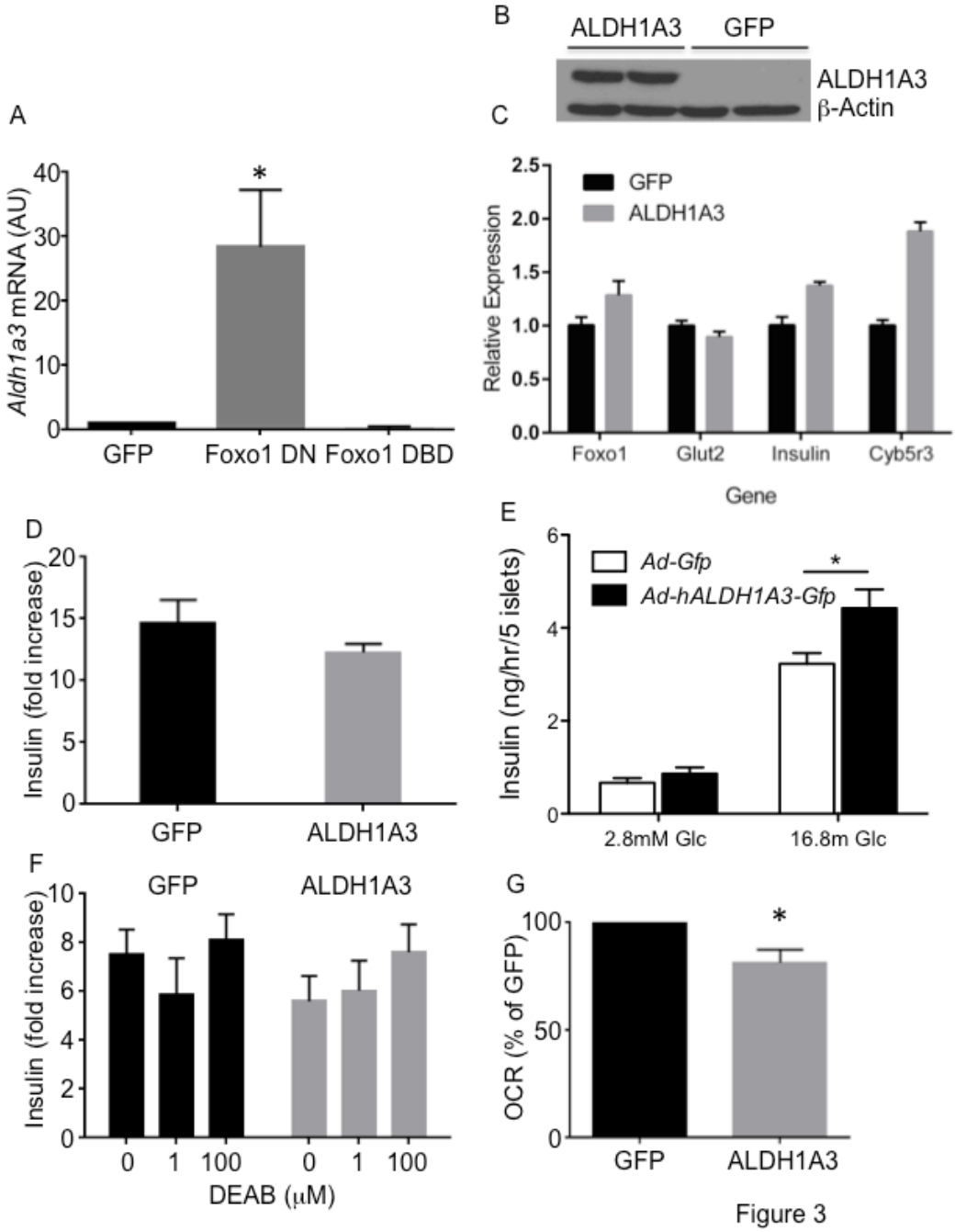

Figure 3

Chapter I, Figure 4

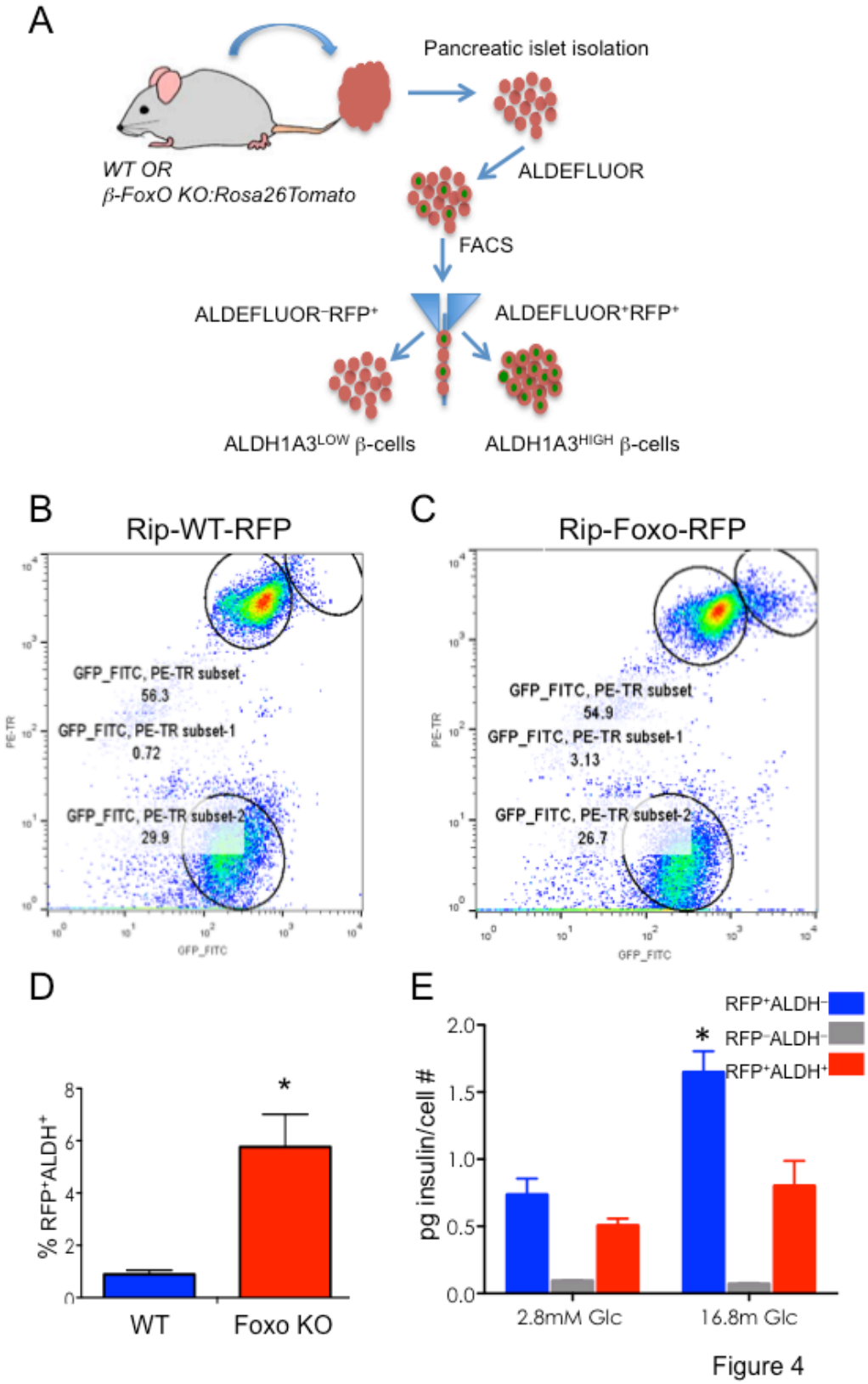

Figure 4

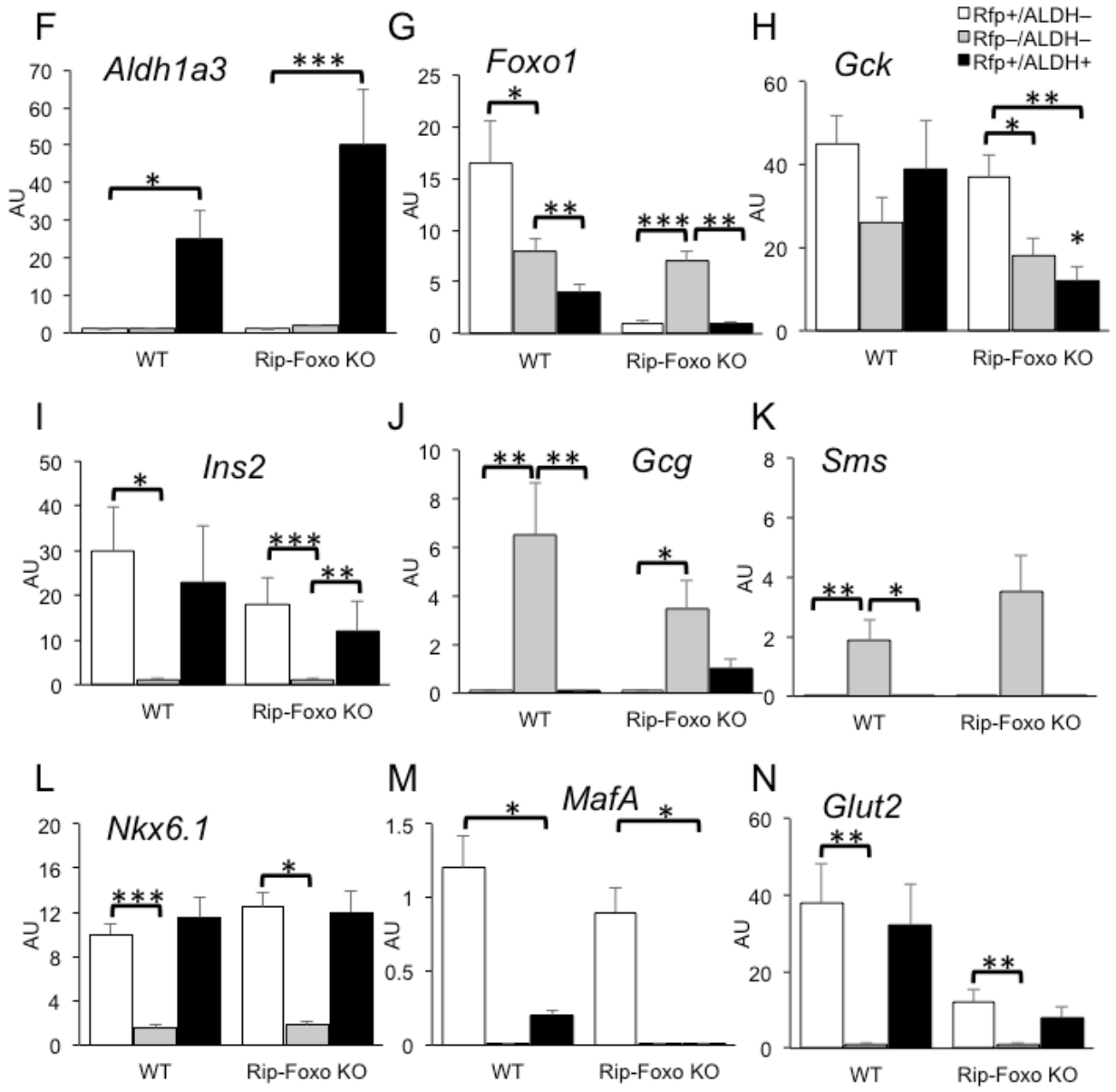

Figure 4

Chapter I, Figure 4 Continued

Isolation and functional characterization of ALDH1A3-expressing islet cells. We used a vital assay of ALDH activity to isolate ALDH1A3-expressing cells from mouse islets (Fig. 4a). The cell-permeable fluorescent ALDH substrate BODIPY™-aminoacetaldehyde (aldefluor) is metabolized to the non-releasable derivative BODIPY™-aminoacetate (BAA), thus permanently labeling ALDH-expressing cells. We used RFP to label β (or former β) cells by cre-mediated recombination [9]. Thereafter, we incubated cells with aldefluor, and selected for RFP (red) and aldefluor (green) fluorescence, yielding $ALDH^-$ and $ALDH^+$ β cells. The latter should include dysfunctional/dedifferentiating β cells. In wild-type mice, we obtained three sub-populations: RFP^-ALDH^- (non-β cells), RFP^+ALDH^- (healthy β cells), and RFP^+ALDH^+ (dysfunctional β cells) (Fig. 4b). The latter represented less than 1% of total cells in normal islets. In separate experiments, we isolated RFP^+ALDH^+ cells from animals with β cell-specific (RIP-cre) triple Foxo1 knockouts [10]. As predicted, the RFP^+ALDH^+ sub-population increased about 7-fold in this model (Fig. 4c-d).

We performed a preliminary characterization of $ALDH^-$ and $ALDH^+$ cells by measuring insulin secretion and gene expression. The predicted outcome of these experiments was that $ALDH^+$ cells would be: (*i*) enriched in ALDH1A3; (*ii*) impaired in their ability to secrete insulin; (*iii*) depleted of markers of functional β cells, including Foxo1 [10]. All predictions were borne out by the data. In glucose-stimulated insulin release experiments using $ALDH^-$ *vs.* $ALDH^+$ cells, we found that only the former responded to glucose, providing critical evidence for a functional impairment of $ALDH^+$ cells (Fig. 4e). *Aldh1a3* mRNA was restricted to the RFP^+ALDH^+ population in both wild-

type and triple Foxo knockout mice (Fig. 4f). *Foxo1* was reduced by ~70% in $ALDH^+$ cells from wild-type mice (Fig. 4g). *Glucokinase* was nearly equally represented in all fractions, but was decreased in $ALDH^+$ cells of triple Foxo knockouts (Fig. 4h), similar to previously reported single knockouts [9]. *Insulin2* and *Nkx6.1* expression were greatly enriched in the RFP^+ population, while *glucagon* and *somatostatin* were enriched in the RFP^- population (Fig. 4i-l), providing another key element to support the identity of these cells. Foxo1 target *MafA* was enriched in the RFP^+ALDH^- population and drastically reduced in RFP^+ALDH^+ cells. These data are consistent with the notion that $ALDH^+$ cells are β cells that have lost key functional features (Fig. 4m). Finally, *Glut2* expression was restricted to RFP^+ cells, regardless of their ALDH status, and was significantly decreased in Foxo knockouts, consistent with prior findings (Fig. 4n) [9].

Chapter I, Figure 5

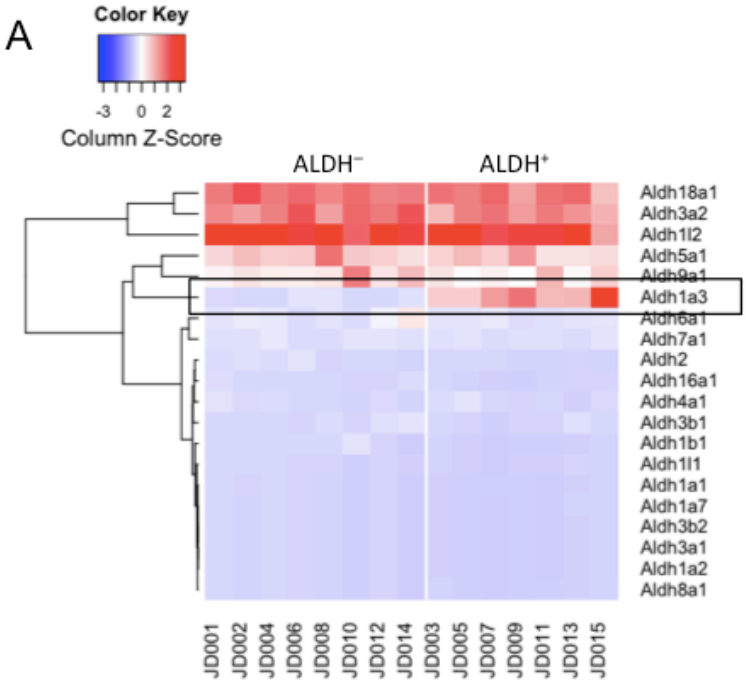

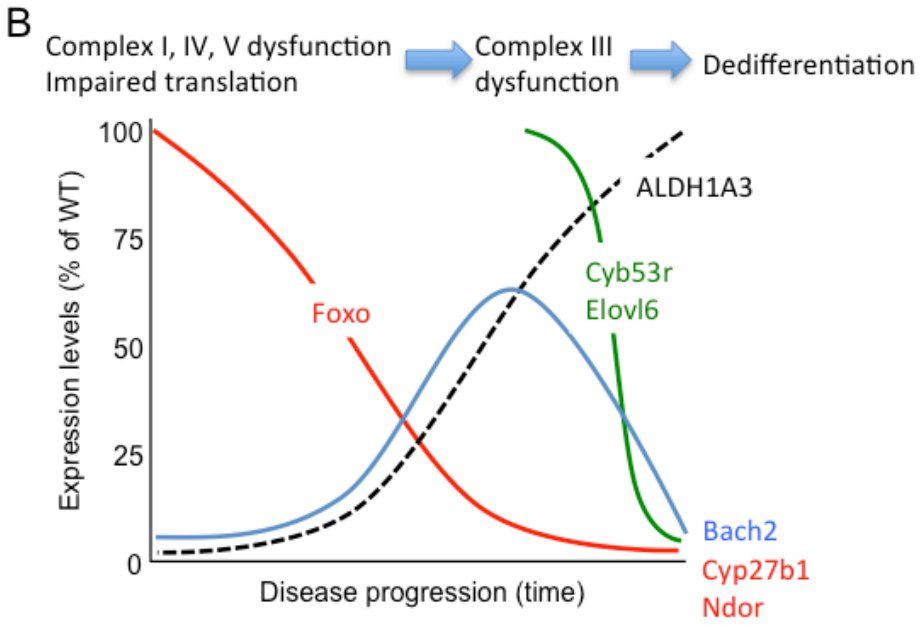

Figure 5

Transcriptome of ALDH$^+$ cells and progression of β cell failure. We carried out RNA sequencing analyses comparing ALDH$^+$ with ALDH$^-$ β cells (RFP$^+$), as well as other islet cell types (RFP$^-$) in wild-type mice. Moreover, we compared wild-type ALDH$^+$ cells with triple Foxo-deficient ALDH$^+$ cells generated by knocking out Foxo in mature β-cells [10]. As a quality control, we interrogated expression of all 20 *Aldh* transcripts, and found that only *Aldh1a3* showed differential expression in the ALDH$^+$ population (Fig. 5a). Moreover, in all comparisons between ALDH$^+$ and ALDH$^-$ cells, *Aldh1a3* was among the top differentially expressed genes (Table 2). This finding confirms the specificity and robustness of the enrichment technique.

First, we analyzed differences in the levels of individual transcripts expressed in ALDH$^+$ vs. ALDH$^-$ cells of wild-type mice. Using $p<0.05$ adjusted for multiple comparisons as threshold, we found 671 differentially expressed transcripts. A curated sub-list is shown in Table 2 and a complete list in Supplemental Table 1. The transcripts fell into three broad categories: terminal differentiation of β cells, mitochondrial oxidative phosphorylation, and ribosomal subunits. ALDH$^+$ cells were depleted of transcripts encoding insulin, IAPP, Cpe, transthyretin, as well as other pancreatic hormones commonly found at low levels in β cells [79], and were enriched in transcripts encoding markers of uncommitted endocrine progenitors, such as Pax6, Rfx6, Rfx7, Mlxipl, as well as transcription factors associated with progenitor cell differentiation, such as Ncor, Hic1, and Bach2. Next, there was a striking decrease of selected mitochondrial components: ~30% of complex I NADH dehydrogenase subunits (13 of 41), complex IV cytochrome C oxidase subunits (8 of 25), and complex V F_1 ATP synthase subunits (15 of 54) were substantially decreased. In addition, ~30% of genes (28 of 92) encoding

ribosomal 40S and 60S subunits were coordinately decreased (Table 2 and Supplemental Table 1). Interestingly, 6 of the top 12 differentially expressed transcripts were long noncoding RNAs that have been associated with β cell dysfunction: Malat1, Neat1, Meg3, Peg3, Sngh11, and Kcnq1ot1 [80, 81]. These highly abundant transcripts increased from 2.5 to 12-fold in ALDH$^+$ cells (Table 2).

Table 2. Curated list of differentially expressed transcripts in wild-type ALDH$^-$ vs. ALDH$^+$ cells

Gene	ALDH$^-$	ALDH$^+$	Fold change	Log_2 Fold Change	P	P adjusted	Function
Aldh1a3	43.89	1016.56	23.16	4.53	6.71E-24	1.13E-20	Biomarker
Ins1	2590036.28	1940536.28	0.75	-0.42	0.000930546	0.027522748	Hormone production
Gcg	8148.96	3014.79	0.37	-1.43	5.72E-05	0.00332584	
Ppy	2650.81	496.46	0.19	-2.42	1.23E-21	1.55E-18	
Pyy	5362.39	860.08	0.16	-2.64	3.61E-37	1.10E-33	
Gipr	158.22	527.98	3.34	1.74	0.000249629	0.010434218	
Malat1	28383.66	317323.72	11.18	3.48	3.39E-60	5.14E-56	LncRNA
Meg3	1394.28	14866.79	10.66	3.41	3.32E-52	2.52E-48	
Neat1	1293.07	8685.24	6.72	2.75	1.34E-30	2.91E-27	
Peg3	10847.19	26432.85	2.44	1.29	6.41E-22	9.35E-19	
Snhg11	142.49	2397.86	16.82	4.07	4.52E-43	1.71E-39	
Kcnq1ot1	775.61	5750.38	7.41	2.89	1.90E-30	3.61E-27	
Bach2	16.18	238.66	14.75	3.88	5.61E-06	0.000512996	Cellular differentiation
Mlxipl	1521.05	6819.86	4.48	2.16	1.35E-33	3.42E-30	
Hic2	58.41	260.05	4.45	2.15	0.001977283	0.046291597	
Ncor1	3821.50	6625.10	1.73	0.79	1.41E-06	0.000162812	
Pax6	2560.43	4087.64	1.60	0.67	0.000270125	0.010988238	
Rfx6	1409.36	2881.95	2.04	1.03	1.46E-06	0.000166394	
Rfx7	916.06	1825.98	1.99	1.00	8.29E-05	0.004444825	
Sall1	94.36	0.00	0.00	INF	8.19E-05	0.004414367	
Atp1a1	9889.83	6215.32	0.63	-0.67	1.55E-05	0.001206084	Complex V
Atp1b3	1251.14	575.26	0.46	-1.12	0.000162268	0.007646262	
Atp5a1	6810.79	3792.69	0.56	-0.84	0.000857639	0.025870698	
Atp5c1	2636.63	1433.09	0.54	-0.88	0.000205123	0.009162496	

Atp5e	1589.03	326.47	0.21	-2.28	4.43E-14	3.05E-11	
Atp5g1	1096.95	567.38	0.52	-0.95	0.00203175	0.047209409	
Atp5g3	1859.61	960.27	0.52	-0.95	0.001441708	0.037046485	
Atp5j	1475.00	831.94	0.56	-0.83	0.002127738	0.048474728	
Atp5o	865.54	342.23	0.40	-1.34	0.000171152	0.007869345	
Atp6v0d1	2455.93	1463.49	0.60	-0.75	0.00077602	0.024052844	
Atp6v0e	1202.47	538.11	0.45	-1.16	0.000130094	0.006429695	
Atp6v1b2	3943.01	2468.79	0.63	-0.68	0.000378227	0.014275718	
Atp6v1c1	1737.43	1004.18	0.58	-0.79	0.001718365	0.042052834	
Atp6v1e1	1431.67	598.90	0.42	-1.26	1.06E-05	0.000867355	
Atp6v1f	634.28	162.11	0.26	-1.97	0.000947641	0.027859186	
Cox17	750.09	184.62	0.25	-2.02	6.45E-07	8.30E-05	Complex IV
Cox4i1	1686.10	526.86	0.31	-1.68	1.82E-09	4.67E-07	
Cox6a1	1830.11	875.84	0.48	-1.06	2.98E-05	0.001962504	
Cox6b1	1089.61	258.92	0.24	-2.07	6.69E-05	0.003759072	
Cox6c	884.60	370.38	0.42	-1.26	0.000315848	0.012447694	
Cox7a2	1190.38	303.96	0.26	-1.97	1.45E-07	2.10E-05	
Cox7b	1696.32	749.76	0.44	-1.18	8.68E-06	0.000739806	
Cox8a	1783.45	988.42	0.55	-0.85	0.000706031	0.022364515	
Cyp27b1	3.75	233.03	62.20	5.96	5.50E-09	1.27E-06	
Ndufa11	966.85	229.66	0.24	-2.07	1.31E-08	2.62E-06	Complex I
Ndufa13	817.24	334.35	0.41	-1.29	0.00038447	0.014368374	
Ndufa2	602.15	164.36	0.27	-1.87	2.40E-05	0.001645658	
Ndufa5	230.83	20.26	0.09	-3.51	2.27E-05	0.001566944	
Ndufb10	742.86	319.72	0.43	-1.22	0.001246519	0.033123357	
Ndufb11	944.43	369.25	0.39	-1.35	8.00E-05	0.004381781	
Ndufb2	416.34	126.09	0.30	-1.72	0.000918555	0.027274428	
Ndufb3	396.07	126.09	0.32	-1.65	0.001797277	0.043148871	
Ndufb8	813.88	219.52	0.27	-1.89	0.000579175	0.019313885	
Ndufb9	1211.79	431.17	0.36	-1.49	1.97E-06	0.000210659	
Ndufc2	1486.70	614.67	0.41	-1.27	5.86E-06	0.000532564	
Ndufs6	376.69	64.17	0.17	-2.55	1.64E-05	0.001253071	
Ndufv3	828.81	390.64	0.47	-1.09	0.002157213	0.048852832	
Ndor1	209.90	782.40	3.73	1.90	2.66E-06	0.000269397	
Rpl13a	1619.13	636.05	0.39	-1.35	9.07E-07	0.000111832	Ribosomal subunits
Rpl14	1448.69	471.69	0.33	-1.62	4.09E-08	6.95E-06	
Rpl22	1352.84	681.09	0.50	-0.99	0.000488305	0.017393076	
Rpl22l1	742.74	272.43	0.37	-1.45	0.000170912	0.007869345	
Rpl29	977.46	466.06	0.48	-1.07	0.001104889	0.03059486	
Rpl32	3663.74	1316.01	0.36	-1.48	1.61E-12	7.87E-10	

Rpl36al	1651.97	891.60	0.54	-0.89	0.000614025	0.020206063
Rpl38	301.12	47.28	0.16	-2.67	6.52E-05	0.003690809
Rpl41	9232.17	3217.42	0.35	-1.52	6.15E-09	1.37E-06
Rpl8	3049.55	1108.87	0.36	-1.46	4.04E-11	1.57E-08
Rplp0	1081.18	529.11	0.49	-1.03	0.000975463	0.028353845
Rplp1	2091.32	552.75	0.26	-1.92	2.97E-13	1.73E-10
Rps11	1754.68	761.01	0.43	-1.21	4.37E-06	0.000416959
Rps14	1438.54	333.23	0.23	-2.11	3.75E-05	0.002361914
Rps15	2313.78	865.71	0.37	-1.42	4.51E-09	1.07E-06
Rps15a	1076.58	395.14	0.37	-1.45	9.87E-06	0.000831648
Rps17	704.56	307.33	0.44	-1.20	0.001832148	0.043778235
Rps20	1126.82	388.39	0.34	-1.54	2.17E-06	0.000225538
Rps21	1023.31	452.56	0.44	-1.18	0.000289137	0.011636817
Rps24	1994.06	717.11	0.36	-1.48	9.24E-09	1.95E-06
Rps25	1320.93	670.95	0.51	-0.98	0.000635685	0.020609513
Rps27l	936.36	274.69	0.29	-1.77	8.32E-07	0.000104333
Rps28	447.27	119.33	0.27	-1.91	0.000196341	0.008813862
Rps3	3520.68	1400.45	0.40	-1.33	2.01E-10	6.61E-08
Rps4x	2240.30	701.35	0.31	-1.68	2.39E-11	9.56E-09
Rps5	4075.84	1368.92	0.34	-1.57	1.36E-14	9.85E-12
Rps6kb2	137.19	466.06	3.40	1.76	0.000448689	0.016209421
Rps9	1981.66	722.74	0.36	-1.46	1.44E-08	2.84E-06

This table lists a subset of genes differentially expressed between $ALDH^-$ and $ALDH^+$ cells, arranged by functional category.

We next used the “upstream regulator analysis” function of the Ingenuity Analysis program to identify contributors to the phenotype of $ALDH^+$ cells based on coordinated changes affecting their downstream effectors and regardless of whether the regulator’s own expression levels changed. Z-scores were used to predict activation or inhibition of individual networks [10]. This analysis confirmed that the main differences between $ALDH^+$ and $ALDH^-$ cells could be subsumed under mitochondrial oxidative phosphorylation and revealed a strong potential activation of the RICTOR branch of

mTOR signaling. Importantly, the same top five pathways were altered in $ALDH^+$ cells isolated from wild-type and triple Foxo knockout mice, confirming that most differences between wild-type and Foxo-deficient $ALDH^+$ cells are of a quantitative, rather than qualitative nature (Table 3).

Table 3. Pathway analysis of RNA sequencing in wild-type and Foxo knockout β cells

Wild-type $ALDH^-$ vs. $ALDH^+$	*p*
Oxidative Phosphorylation	$8.58E^{-27}$
Mitochondrial Dysfunction	$1.02E^{-23}$
EIF2 Signaling	$1.31E^{-15}$
mTOR signaling	$1.81E^{-10}$
Regulation of eIF4 and p70S6K Signaling	$7.17E^{-10}$
Foxo knockout $ALDH^-$ vs. $ALDH^+$	
EIF2 Signaling	$6.88E^{-08}$
Oxidative Phosphorylation	$1.29E^{-07}$
Mitochondrial Dysfunction	$2.14E^{-06}$
Regulation of eIF4 and p70S6K Signaling	$1.05E^{-04}$
mTOR signaling	$3.78E^{-04}$

The table summarizes top pathways from transcriptome analysis of $ALDH^-$ vs. $ALDH^+$ cells.

Transcription factor network analyses indicated that $ALDH^+$ cells have stem/progenitor cell properties, based on the combination of activated GATA, Wnt, Nanog, and Neurog3 [82] and decreased Foxo and Notch signaling (Table 4 and Supplemental Table 2). Of note was also the marked inhibition of two master regulators of mitochondrial biogenesis and function, NFE2L2 and NRF1, consistent with the data in Table 2. NRF1 activates expression of EIF2A1 as well as genes required for mitochondrial biogenesis, function, and mitochondrial DNA transcription [83]. The inhibition of NRF1 is consistent with the decrease of Tfam and Eif2 signaling in $ALDH^+$

cells (Supplemental Table 2). NFE2L2 is involved in NRF2-mediated oxidative stress and unfolded protein response [84].

Table 4. Progenitor-like features of ALDH$^+$ cells

Transcription factor	*Z-score*	*P*
GATA4	2.607	1.00 x10^{-1}
GATA6	2.111	1.00 x10^{-1}
NKX6.1	1.969	2.68 x10^{-2}
PDX1	1.575	2.11 x10^{-6}
NANOG	1.508	1.62 x10^{-2}
GLIS3	1.384	8.57 x10^{-4}
CTNNB1	1.366	2.66 x10^{-2}
HNF1A	1.028	1.39 x10^{-2}
NEUROD1	0.741	4.70 x10^{-4}
NEUROG3	0.791	1.38 x10^{-4}
RBPJ	–2.130	1.00 x10^{-1}
FOXO1	–1.811	4.91 x10^{-3}
FOXO3	–1.400	2.92 x10^{-3}
FOXO4	–0.640	1.87 x10^{-2}
HNF4A	–1.212	1.39 x10^{-2}
NKX2.2	–1.000	2.65 x10^{-4}

Z-score analysis of transcriptional networks involved in pancreas development in ALDH$^+$ cells.

This analysis also indicated activation of RICTOR (mTORC2) signaling. RICTOR promotes β cell growth and insulin secretion[85]. However, other features of ALDH$^+$ cells suggest that the activation of RICTOR is compensatory in nature. For example, ATF4-mediated signaling is inhibited, thus leading to decreased unfolded protein response and apoptotic signaling in response to endoplasmic reticulum stress. There are impairments in insulin and IGF1 receptor signaling, as well as inhibition of the transcriptional network overseen by nuclear receptor NR4A3, which is required for β cell growth (Supplemental Table 2) [86]. The decrease in insulin/IGF receptor signaling is consistent with the homeostatic role of Foxo in these pathways, such that low Foxo

would be expected to result in impaired insulin/IGF receptor signaling [23]. In addition, the mild activation of Src and EGF receptor signaling observed in ALDH$^+$ cells suggests that cells are shifting from a fully differentiated phenotype maintained through insulin receptor/Foxo signaling, to a less differentiated phenotype dependent on oncogene signaling with features of progenitor cells (Supplemental Table 2).

Two other features of ALDH$^+$ cells deserve mention: the decrease in estrogen receptor signaling, and activation of inflammation pathways, including NFKB1, MYD88, TICAM1, IFRD1, TLR7, CXCL12, and IL6 (Supplemental Table 2).

Comparing wild-type and Foxo knockout ALDH$^+$ cells. Next, we compared ALDH$^+$ cells from wild-type and triple Foxo-deficient mice. The rationale was threefold: first, although ALDH1A3 expression is a marker of reduced Foxo activity, Foxo is *not* absent in the majority of these cells, and complete Foxo ablation may exacerbate their phenotype; second, it may reduce heterogeneity of ALDH$^+$ cells; and third, because Foxo-deficient mice develop a MODY-like form of diabetes, this comparison might reveal qualitative differences between ALDH$^+$ cells isolated from euglycemic *vs*. diabetic animals. One can hypothesize that complete genetic ablation of Foxo mimics the final stages in the progression of the fate of ALDH$^+$ cells and that, by analyzing differences between wild-type and Foxo-deficient ALDH$^+$ cells, it's possible to identify genes that mark the mechanistic progression to an advanced phase of cellular failure, or a tipping point toward dedifferentiation (Fig. 5b).

When we compared transcriptomes of wild-type *vs*. triple Foxo knockout ALDH$^+$ cells, we found few differentially expressed genes, as predicted (Tables 5 and 6). The

dearth of differences between wild-type and Foxo-deficient ALDH$^+$ cells is wholly consistent with the concept that in diabetes there is a "spontaneous" loss of Foxo [8-10], and that Foxo normally restrains ALDH1A3 expression (Fig. 3). Nonetheless, these genes indicated potential pathogenic processes unfolding in failing β cells. A striking aspect of the gene expression profile of Foxo-deficient ALDH$^+$ cells is the decrease in Cyb5r3. This gene encodes cytochrome b5 reductase isoform 3, one of four b5 reductase subunits (r1 through 4). Its expression is regulated by Foxo and Nrf, consistent with our findings [87]. Cyb5r3 has a membrane-bound and a soluble form, the latter of which is restricted to erythrocytes. It utilizes NADH and NADPH to synthesize long-chain fatty acids, and it's also required for mitochondrial complex III function. Cyb5r3-deficient cells show decreased NAD$^+$/NADH ratios, mitochondrial respiration rate, ATP production, and mitochondrial electron transport [87]. Notably, knockout of the related isoform Cyb5r4 causes early-onset β cell failure in mice independent of peripheral insulin sensitivity [88].

Other interesting genes that are specifically altered in Foxo-deficient ALDH$^+$ cells include: *Elovl6*, *Ndor*, and *Cyp27b1*. *Elovl6* is a long chain fatty acid elongase that plays an important role in liver [89]. In β cells, its expression pattern mirrors Cyb5r3, and can potentially act in concert with the latter to synthesize long-chain FA. Similarly, the NAPDH-dependent oxidoreductase *Ndor*, whose expression levels track closely those of Foxo in ALDH$^+$ cells, could also be involved in mitochondrial processes related to Cyb5r3. Cyp27b1 is required for the synthesis of 1,25-OH vitamin D3, and there is some evidence that it participates in β cell dysfunction in diabetes [90]. Finally, there were two transcripts that showed opposite changes in wild-type vs. Foxo-deficient ALDH$^+$ cells:

the lncRNA Peg3, a parentally imprinted transcript whose methylation correlates with human islet function [91], and Bach2, a transcription factor that has been implicated in type 1 diabetes susceptibility [92, 93], as well as β cell stress [94] (Table 6).

Table 5. Top 25 differentially expressed transcripts in ALDH$^+$ cells from wild-type and Foxo knockout mice

Gene	Wild-type	Foxo knockout	Fold Change	$\log_2$ Fold Change	*P*	Adjusted *P*
Foxo1	1005.01	131.37	0.13	-2.94	2.23E-11	3.47E-07
Cyb5r3	5076.01	1742.73	0.34	-1.54	8.29E-09	6.46E-05
Cyp27b1	206.80	4.83	0.02	-5.42	5.10E-07	0.002649712
Elovl7	384.62	38.27	0.10	-3.33	1.46E-06	0.005684329
Hip1r	1463.56	467.44	0.32	-1.65	2.98E-06	0.009288892
Bach2	211.79	11.73	0.06	-4.17	2.45E-05	0.052959279
Ctsl	2272.77	5237.71	2.30	1.20	3.39E-05	0.052959279
Etl4	1573.45	590.80	0.38	-1.41	3.21E-05	0.052959279
Muc4	3932.14	763.76	0.19	-2.36	3.32E-05	0.052959279
Ptprt	753.26	181.42	0.24	-2.05	2.71E-05	0.052959279
Dnahc17	112.89	1.32	0.01	-6.41	3.87E-05	0.054903167
Spp1	3933.14	1896.47	0.48	-1.05	0.000104638	0.136037989
Gpc6	72.93	0.00	0.00	N/A	0.000119737	0.14369393
Cxcl13	71.93	0.00	0.00	N/A	0.000135081	0.150528447
Prnd	93.91	1.06	0.01	-6.47	0.000149671	0.155667934
2010015L04Rik	249.75	32.76	0.13	-2.93	0.000188906	0.173360099
Ncam1	2471.57	1148.98	0.46	-1.11	0.000183578	0.173360099
Jam2	437.57	97.38	0.22	-2.17	0.000207049	0.179454216
Galntl4	316.69	53.81	0.17	-2.56	0.000328609	0.269822705
D0H4S114	613.40	190.91	0.31	-1.68	0.000492415	0.351638321
Hcn1	76.92	0.60	0.01	-7.01	0.000495868	0.351638321
Nog	61.94	0.00	0.00	N/A	0.000451442	0.351638321
Cox6b1	229.77	695.81	3.03	1.60	0.000553818	0.362501015
Krba1	424.58	108.79	0.26	-1.96	0.000565259	0.362501015

This table lists a subset of genes differentially expressed between wild-type and triple Foxo-deficient ALDH$^+$ cells, arranged by p-value.

Table 6. Overview of key differential changes in transcript profile of wild-type and Foxo knockout ALDH$^+$ cells

Change	*Gene or network*	*Wild-type*	*Foxo KO*
↑↑↑	ALDH1A3		
↑	Differentiation Factors	Bach2 Pax6 Rfx6 Rfx7 Hic2 NcoR	↓
	LncRNA	Malat1 Meg3 Peg3 Neat1 KcQ1ot1 Sngh11	↓
↓	Gpcrs	Gipr Gpr116 Gpr137 Gpr98	
	Cytochrome	Cyp27b1 Ndor	↓↓↓ ↓↓ Cyb5r3 Elovl6
	Ribosomes	40S Subunit 60S Subunit	
	Mitochondria	Complex I Complex IV Complex V	Complex III
	Differentiation markers	Insulin IAPP Cpe ChgB Gcg Pyy Npy	

Category list of principal genes altered in ALDH$^+$ cells as a function of Foxo genotype. Upward arrows indicate genes with increased expression, downward arrows indicate genes with decreased expression. Arrows in the Foxo column indicate that the change is specific to Foxo knockout ALDH$^+$ cells.

DISCUSSION

The key finding of this work is the identification of a subpopulation of ALDH$^+$ islet β cells. Based on their impaired insulin secretory properties and transcriptional signature, we propose that ALDH$^+$ cells are failing β cells. They show conjoined features of the two cardinal processes bookending β-cell failure: mitochondrial dysfunction [10] and progenitor-like features [9]. We propose the following model (Fig. 5b): when β cells are subject to increased demand for insulin production, they increase cellular metabolism and substrate flux through mitochondria. Foxo is activated to maintain normal oxidative function and prevent cellular overwork [8, 9]. The tradeoff of increased Foxo function is increased Foxo degradation [8], leading to eventual loss of the protein. As Foxo levels decline, ALDH1A3 is activated; thus, elevated levels of ALDH1A3 are a harbinger of β cell failure. In the progression of the cellular pathology, mitochondrial complex I, IV, and V functions are impaired, leading to reduced ATP production, stalling of protein translation, and reactivation of genes that sustain a cellular progenitor program. When Foxo levels reach their nadir (a situation phenocopied by genetic knockout of Foxo), a further subset of genes becomes altered, including Cyb5r3, Elovl6, and Bach2 (Fig. 5b). We propose that these genes play a pathogenic role in β cell dedifferentiation. Further studies to test their involvement in this process are underway, with the expectation that they are key mediators of progression of β cell failure, and with the ultimate goal of developing therapeutic approaches to ameliorate β cell dysfunction based on this model.

Aldehyde dehydrogenase as a marker of β cell failure. The role of ALDH1A3 in β cell failure will have to be determined through further studies. In oncology, there is no consensus on whether ALDH1A3 is a marker or a pathogenic factor in cancer progression [69]. Our data indicate that ALDH1A3 overexpression doesn't untowardly affect β cell function, but these experiments don't capture the complexity of the potential roles of ALDH1A3 in β cell failure. For example, ALDH1A3 could promote mitochondrial dysfunction–the paramount feature of $ALDH^+$ cells–by activating RAR/RXR signaling via RA production. This can result in increased Pparα function, a feature of metabolically inflexible β cells [10]. This effect may require a specific duration or additional contributors, and would have gone undetected in the experiments carried out so far. To address this and other possibilities, we are generating appropriate models of loss- and gain-of-function.

Mechanisms of cellular failure. A prominent aspect of the gene expression profile of $ALDH^+$ cells is the extent of impairment of mitochondrial gene expression. In addition to decreased complex I, IV, and V subunit expression, ablation of Foxo also causes a profound decrease of Cyb5r3. The latter is likely a Foxo target [87]. Cyb5r3 mutations in humans cause methemoglobinemia [87]. The membrane-bound form localizes to mitochondria and endoplasmic reticulum, where it catalyzes desaturation and elongation of fatty acids, as well as cholesterol biosynthesis. Cyb5r3 generates reducing equivalents NAD^+ and $NADP^+$, and utilizes malonyl CoA and NADPH to make 18:1, 20:1, and 18:0 fatty acids in ratios of 65:20:15. Cyb5r3-deficient cells have decreased

NAD^+/NADH ratios, mitochondrial respiration, ATP production, and mitochondrial electron transport. This results in higher oxidative stress and senescence [87].

Cyb5r3 is a striking candidate as a β cell failure gene. One can envision that in the context of already impaired mitochondrial complex I, IV, and V function in $ALDH^+$ cells, the drop in Cyb5r3 would result in the additional loss of NADH and NADPH reductase activity at the level of complex III, decreasing levels of reduced cytochrome B and C. This may lead to a drop in NAD+ levels to the point where glycolysis is effectively stalled for lack of reducing equivalents. In mice, knockout of the related isoform, Cyb5r4, causes early-onset β cell failure independent of peripheral insulin sensitivity [88]. In yeast, the Cyb5r3 ortholog NQR1 extends lifespan in a SIR2-dependent manner and increases oxidative metabolism [95]. Mitochondrial Cyb5r3 activity is increased by calorie restriction [95] (a condition in which β cells oxidize more FA) and decreased by exposure to elevated glucose levels [96].

In addition to its role in complex III function, Cyb5r3 could prevent β cell failure through its role in fatty acid synthesis, effectively shunting away excess fatty acyl-CoA from mitochondria. This would be achieved in part through activation of the Pparγ program, an interesting feature consistent with the paradoxical increase of Pparγ function in metabolically inflexible β cells [10]. A decrease of Cyb5r3 levels can lead to fatty acid accumulation in the oxidative pathway, and worsen mitochondrial stress through formation of peroxides or other superoxide products. In this regard, it should be noted that another gene specifically affected by Foxo knockout in $ALDH^+$ cells is Elovl6, whose function to increase long-chain fatty acid synthesis complements that of Cyb5r3. While isolated knockout of Elovl6 has no apparent detrimental effect in β cells [97], it

remains to be seen whether this is also true in the context of the failing β cell and in the absence (or deficiency) of Cyb5r3.

An additional interesting candidate emerging from the analysis of Foxo-deficient ALDH$^+$ cells is Bach2. It increases in wild-type ALDH$^+$ cells, but decreases in Foxo knockout ALDH$^+$ cells (Fig. 5b). Our interpretation of these data is that Bach2 is induced by Foxo when the latter undergoes nuclear translocation [8, 9], and decreases as Foxo is cleared from β cells. A transcriptional repressor first identified as a lineage selector of B-lymphocytes [98], Bach2 has emerged as a genetic susceptibility locus in GWAS studies of human type 1 diabetes [92, 93], and has been found to protect β cells from apoptosis and oxidative stress [94]. In addition, its ability to regulate differentiation in the hematopoietic lineage [98] raises the question of whether it has similar effects in endocrine cells, a hypothesis consistent with Bach2's ability to drive transcription from Maf sites, which are known to confer β cell transcriptional features [63, 99].

LncRNAs in ALDH$^+$ cells. ALDH$^+$ cells are strikingly enriched in selected lncRNAs: 6 of the 12 top differentially expressed transcripts belong to this category. At least three of these transcripts have previously been linked to human β cell dysfunction: Malat1, Meg3, and Kcnq1ot1. Malat1 is encoded in an enhancer cluster associated with β cell-specific transcription factors [100]. Meg3 is part of an imprinted locus that confers susceptibility to type 1 diabetes [101] and includes the atypical Notch ligand Dlk1, a negative regulator of adipocyte differentiation, as well as another gene, Rtl1, whose transcripts are also among the top enriched mRNAs in ALDH$^+$ cells (Supplemental Table 1) [81]. Finally, Kcn1qot1 is part of an imprinted locus that includes IGF2 and the

Beckwith-Wiedemann locus [80] and has been linked to type 2 diabetes susceptibility [102]. We don't know the targets, let alone the functional consequences, of these changes in lncRNA profile of $ALDH^+$ cells, but we envision them to herald epigenetic changes leading to dedifferentiation.

In sum, the present work advances our understanding of β cell failure and provides a series of testable targets to explain mechanisms of progression from impaired insulin secretion to cellular dysfunction and dedifferentiation.

CHAPTER I SUPPLEMENTARY INFORMATION

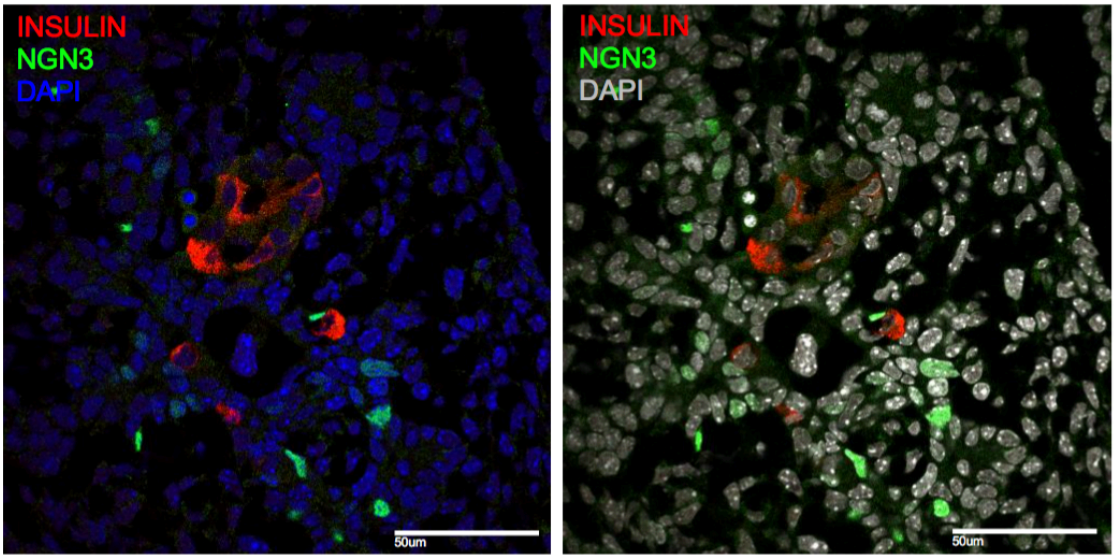

Supplementary Figure 1. Neurogenin3 localization in mouse E12.5 pancreas. Neurogenin3 immunohistochemistry in E12.5 mouse embryos.

The following supplemental tables are available online:

Supplemental Table 1 Complete list of differentially expressed transcripts in wild-type ALDH$^-$ vs. ALDH$^+$ cells. This table lists a complete set of genes differentially expressed between ALDH$^-$ and ALDH$^+$ cells, arranged by p-value.

Supplemental Table 2 Ingenuity analyses of differentially expressed transcripts in wild-type ALDH$^-$ vs. ALDH$^+$ cells. A partial list of different Ingenuity Pathway analyses to identify trends in gene expression in the different islet cell types.

Supplemental Table 3 List of differentially expressed transcripts in ALDH$^+$ cells from wild-type and Foxo knockout mice. This table lists all genes differentially

expressed between wild-type and triple Foxo-deficient $ALDH^+$ cells, arranged by p-value.

CHAPTER II

INTRODUCTION

A hallmark of diabetes is β-cell failure, a state in which chronically increased demand for insulin exceeds the β-cell's secretory capacity and leads to a gradual deterioration of β-cell mass and function. This decline manifests as a mistimed and diminished response to nutrients and, combined with peripheral insulin resistance, gives rise to hyperglycemia. Although current therapies seek to improve β-cell performance or reduce the demand for insulin, they are insufficient to halt disease progression.[103-105]

Recent work established β-cell dedifferentiation as a mechanism of β-cell dysfunction.[106-112] We have proposed that dedifferentiation is the end result of altered mitochondrial substrate utilization, or "metabolic inflexibility".[10] The implication of this model is that acting on the mechanism of mitochondrial dysfunction may prevent dedifferentiation or even promote "re-differentiation" of β-cells as a novel form of therapy. However, the mechanism by which metabolic inflexibility affects mitochondrial function remains unclear. To address this question, we used a combination of marker analysis and RNA profiling to compile a list of potential effector genes of β-cell failure.[113] A strong candidate emerging from this analysis is cytochrome b5 reductase 3 (Cyb5r3).

Cyb5r3 is unique as a candidate β-cell failure gene: it encodes a flavoprotein with membrane-bound and soluble forms, the latter of which is restricted to erythrocytes.[114] Mutations in this form lead to recessive congenital methemoglobinemia (Type I) while mutations in the membrane-bound form can cause severe neurological disease (Type II).[115] Membrane-bound Cyb5r3 has complex functions in fatty acid desaturation,

cholesterol biosynthesis, antioxidant reduction, and mitochondrial electron transport chain (ETC) activity.[114, 116] Notably, knockout of the related isoform Cyb5r4 causes early-onset β-cell failure in mice independent of peripheral insulin sensitivity.[117]

In this study, we report that Cyb5r3 links FoxO1 signaling to β-cell mitochondrial ETC function, affecting the generation of reactive oxygen species, NAD/NADH ratios, and stimulus/secretion coupling. Consistent with the "metabolic inflexibility" hypothesis, these defects are exacerbated when islets are exposed to fatty acids. Mice with β-cell-specific deletion of Cyb5r3 exhibit glucose intolerance due to impaired insulin secretion, a blunted response to insulin secretagogues, and decreased mitochondrial respiration. Moreover, Foxo1 is unable to preserve expression of key markers of β-cell differentiation in Cyb5r3-deficient β-cells, indicating that Cyb5r3 is required for the FoxO1-dependent compensatory response. These data indicate that Cyb5r3 is a key effector of β-cell failure, and highlight a pathway of potential therapeutic import to intervene on disease progression.

MATERIALS AND METHODS

Cell lines: We used the Min6 mouse insulinoma cell line (AddexBio) which was previously characterized for its ability to secrete insulin.[8] Min6 cells were cultured in 15%FBS DMEM media containing penicillin-streptomycin and 0.05mM 2-mercaptoethanol. Min6 media containing 0.5mM palmitate was used for free fatty acid challenge. 0.5mM palmitate media was prepared by first dissolving free fatty acid (FFA)-free BSA (Fisher Scientific) in Min6 media to a final concentration of 600uM, then adding sodium palmitate (Sigma). This solution was then incubated at 50°C and shaken overnight at 250rpm, then filtered before use.

Adenoviral Vectors: Dominant negative FoxO1 adenovirus (DN256) and constitutively active FoxO1 (FoxO1-ADA) have been previously described.[76] shCyb5r3 adenovirus, containing the effective shRNA sequence of 5'- GATTGGAGACACCATTGAAT -3', was generated by cloning the shRNA sequence into the pEQU6-vector with LR Clonase II enzyme (Invitrogen) and ligating it to a pAd-REP plasmid that contained the remaining adenovirus genome. The recombination products were transformed into *E. coli* cells. After incubation overnight, the positive clones were selected, and cosmid DNA was purified. The purified cosmid DNA (2 µg) was digested with Pac1 and then transfected into 293 cells with Lipofectamine 2000 according to manufacturer's instructions. The 293 cells were grown at 37°C with 5% CO_2. The adenovirus plaques were seen 7 days after transfection. The low titer virus was further amplified to 1012 vp/ml using a cesium chloride gradient.

Mice: Genotyping was performed as previously described for RIP-Cre$^+$ FoxO1/3/4-floxed mice, Glut4-Cre$^+$ Insulin Receptor KO, and leptin receptor-deficient Db/db mice.[1, 58, 59] RIP-Cre$^+$ mice (Jackson Laboratories) were crossed with Cyb5r3-floxed *mice* (Knockout Mouse Project) to generate RIP-Cre$^+$ Cyb5r3-floxed mice and were maintained on a C57BL/6 background. The floxed Cyb5r3 allele was genotyped using the primers 5'-ACAGTCCAGCTTTGGCTTTACCC-3' and 5'-ATAGGGCTAGAAAAGGAGCAGAGAGC-3' yielding a 456bp product. We derived Cre$^+$ controls from the same litters. Sample size calculations were based on the variance observed in prior experiments.[10, 31] All mice were fed normal chow (NC) except where stated otherwise, and maintained on a 12–hour light–dark cycle (lights on at 7 AM). NC had 62.1% calories from carbohydrates, 24.6% from protein and 13.2% from fat (PicoLab rodent diet 20, 5053; Purina Mills); high fat diet (HFD) had 20% calories from carbohydrates, 20% from protein and 60% from fat (D12492; Research Diets). The Columbia University Institutional Animal Care and Utilization Committee approved all experiments.

Metabolic Analyses:

We performed intraperitoneal glucose tolerance tests (ipGTT) by injecting glucose (2 g/kg) after an overnight (16h) fast, and we performed intraperitoneal insulin tolerance tests by injecting insulin (0.75 units/kg) after a 5h fast.[118, 119] We measured insulin by ELISA (Mercodia). We performed hyperglycemic glucose clamps as previously described.[10] We measured body composition by NMR (Bruker Optics). For determination of nonesterified fatty acids and triglycerides, we used commercially

available colorimetric assays (for NEFA: Wako; and for TG: Thermo Scientific).

Islet Isolation and Fluorescence-Activated Cell Sorting: We isolated islets by collagenase digestion from mice as previously described.[10] Sorting of β cells was performed as previously described.[113] Briefly, we incubated cells with the fluorescent ALDH substrate BODIPY™-aminoacetaldehyde (Aldefluor) for 1 hr prior to flow cytometry. Thereafter, cells were applied to a BD Influx sorter and analyzed with a BD LSRII instrument. We gated cells for RFP (red) and aldefluor (green) fluorescence, yielding three sub-populations: $RFP^{-}ALDH^{-}$ (non-β cells), $RFP^{+}ALDH^{-}$ (β cells), and $RFP^{+}ALDH^{+}$ (ALDH-positive β cells).

Glucose-stimulated insulin secretion (GSIS) assays:

For insulin secretion assays, we placed islets in ice-cold Krebs buffer (119 mM NaCl, 2.5 mM $CaCl_2$, 1.19 mM KH_2PO_4, 1.19 mM Mg_2SO_4, 10 mM HEPES (pH 7.4), 2% BSA and 2.8 mM glucose) and incubated at 37 °C for 1hr. We then stimulated islets with varying glucose concentrations (2.8, 16.8 mM) and secretagogues (L-Arginine (30mM), KCl (40mM)) for 1hr at 37 °C. At the end of the incubation, we collected islets by centrifugation and assayed the supernatant for insulin content by radioimmunoassay.[118, 120] Insulin levels were then normalized to total protein or total insulin content. To assay insulin secretion in adherent Min6 cells, we used the same protocol but with an overnight pre-incubation period in low (2.8mM) glucose media.

Single-Cell Intracellular Calcium Microfluimetry:

Primary islets were isolated from RIP-Cre^{+}:Cyb5r3$^{fl/fl}$ (B-Cyb5r3) mice and their controls then allowed to rest overnight in RPMI media containing 15% FBS and penicillin-streptomycin. Islets were then treated with shScramble or shCyb5r3 adenovirus at 6 x 10^{8} PFU/10cm dish of islets, with each dish containing islets from a single mouse (~150-200 islets). After overnight incubation at 37°C, the islets were washed with RPMI+15% FBS, then allowed to rest for an additional day, allowing for expression of the adenoviral construct. The next day, islets were dispersed to single cells using trypsin digestion in a 37°C water bath, and then plated on 35mm glass bottom dishes with 20mm microwells pre-coated with fibronectin (Sigma, F1141). Cells were allowed to attach overnight, then loaded in the dark with fura2-AM (5 μM) in KRBH buffer. The cells were washed and then transferred into a perifusion chamber placed in the light path of a Zeiss Axiovert fluorescence microscope (Zeiss, USA), and perifused with low glucose (2.8mM), high glucose (16.8mM), or KCl (40mM) -containing KRBH buffer. β cells were excited by a Lambda DG-4 150 Watt xenon light source (Sutter, Novato, USA), using alternating wavelengths of 340 and 380 nm at 0.5 s intervals, and imaged at 510 nm. For each data set, regions of interest corresponding to the locations of 10-20 individual cells were selected and digital images were captured using an AxioCam camera controlled by Stallion SB.4.1.0 PC software (Intelligent Imaging Innovations, USA). Single-cell intracellular Ca^{2+} mobilization data consisted of excitation ratios (F340/F380) plotted against time (min).

Lactate measurement: Lactate levels were measured by a commercially available kit according to manufacturer's instructions (Abcam, Ab65331). In brief, Min6 cells were

washed, homogenized, and the supernatant collected. Ice-cold perchloric acid (4M) was added to each sample to a final concentration of 1M. Samples were incubated on ice for 5 min. then spun down at 13,000 x g for 2 min at 4°C. Following neutralization with KOH, the supernatant was collected for colorimetric assay (read at 450nm).

NAD^+/NADH measurement: NAD^+ and NADH levels were quantified by commercially available kit according to the manufacturer's instructions (BioVision). In brief, cells were lysed by freeze/thaw. To determine NADH levels, samples were heated at 60°C for 30 min to decompose NAD. For the detection of total NAD, samples were incubated with the NAD cycling enzyme mix to convert NAD^+ to NADH. Both samples were then mixed with NADH developer and incubated at room temperature for 1h before colorimetric reading absorbance at 450 nm. NAD levels were calculated by subtracting NADH from total NAD.

Reactive Oxygen Species (ROS) Measurement: Levels of intracellular ROS were measured in Min6 cells by conversion of the acetyl ester CM-H_2DCFDA into a fluorescent product (excitation/emission 485nm/520nm). Min6 cells were grown in 24-well plates and washed once with warm Hanks buffered salt solution (HBSS). Immediately before the assay, 50ug of CM-H_2DCFDA was reconstituted in 8.6ul DMSO to make a 10mM stock solution. The HBSS was then replaced with 0.8ml HBSS containing 1uM CM-H_2DCFDA and incubated at 37°C for 30 min. The plate was then placed on ice and all wells were washed with cold HBSS. Cells were then scraped in 0.5ml of cold HBSS and 200ul of the cell suspension was loaded into a black uncoated

96-well plate for reading. The remainder of the sample was used to assay for total protein (BCA protein assay kit, Pierce) to correct for total cellular content per well.

Mitochondrial Complex Activity Assays: Complex I-IV activity was measured as previously described, with some modification detailed below.[121] Mitochondrial-enriched fractions were used for all assay measurements. For Complex I activity, mitochondrial preparations were resuspended in NADH dehydrogenase assay buffer (1X PBS, 0.35% BSA, 200μM NADH, 240μM KCN, 60μM DCIP, 70μM decylubiquinone, 25μM Antimycin A) containing 200μM Rotenone or water. Complex I activity was measured as the rate of decrease in absorbance at 600nm. Specific Complex I enzyme activity was calculated by subtracting the rotenone resistant activity from the total enzyme activity. For Complex II activity, mitochondrial preparations were resuspended in succinate dehydrogenase assay buffer (25mM K3PO4 pH 7.2, 0.35% BSA, 2mM EDTA, 5mM sodium succinate, 60μM DCIP, 25μM Antimycin A, 240μM KCN, 2μM Rotenone and 150μM phenazine methosulfate). Complex II activity was measured as the rate of decrease in absorbance at 600nm. Complex III activity was measured as described previously.[121] For Complex IV activity, mitochondrial preparations were resuspended in cytochrome C oxidase assay buffer (20mM K3PO4 pH 7.2, 0.35% BSA, 1mM EDTA, 25μM Antimycin A, 100μg/mL reduced cytochrome C) containing either 10mM KCN or water. Complex IV activity was measured as the rate of decrease in absorbance at 550nm. Specific Complex IV enzyme activity was calculated by subtracting the KCN resistant activity from the total enzyme activity. For each assay, absorbance was measured at the given wavelength every 10 sec for 20 min at 25°C using a SpectraMax

Paradigm Multi-Mode Microplate Reader (Molecular Devices LLC., Sunnyvale, CA). Enzymatic activities were normalized to protein concentrations, as determined with a Bradford Protein Assay Kit (Bio Rad-Laboratories, Hercules, CA) following manufacturer protocols. Enzyme activity was calculated using previously described equations.[121]

Chromatin Immunoprecipitation (ChIP) Assay: ChIP was performed as described previously by Son *et al*., 2013.[122] Briefly, Min6 cells were cross-linked, lysed, and sonicated. Immunoprecipitation reactions were set up using 4 µg of anti-Foxo1 or IgG antibody per immunoprecipitation. The immunocomplexes were recovered with protein G-dynabeads, washed under stringent conditions and reverse-crosslinked. The precipitated DNA was analyzed by quantitative PCR using primers for mCyb5r3 (F: 5'-CATCTAGTGGAATGGGTACGTG -3', R: 5'- TAGTGCAGAACGGTCTTTGTAG -3').

Immunoblot and Immunohistochemistry: We performed immunoblotting and immunohistochemistry as previously described.[9] Antibodies used are listed with supplementary information.

Mitochondrial Function: We used the XF24-3 respirometer (Seahorse Bioscience) with 24-well plates. We used the F_1F_0 ATP synthase inhibitor oligomycin to assess uncoupling, FCCP to estimate maximum respiration, and rotenone to measure non-mitochondrial respiration.[61]

RNA Measurements: We used standard techniques for mRNA isolation and SYBR green quantitative PCR. Primers for mCyb5r3 were: (F: 5'-CAGGGCTTCGTGAATGAGGAG -3', R: 5'- TCCACACATCAGTATCAGCGG -3'). All other PCR primer sequences have been published.[9]

Statistical Analyses and General Methods. Sample sizes were estimated from expected effect size based on previous experiments. No randomization or blinding was used. We present data as means ± SEM. We used two-tailed Student's t-test, one-way ANOVA, or two-way ANOVA for data analysis, and the customary threshold of $p < 0.05$ to declare statistically significant differences.

RESULTS

Cyb5r3 expression decreases in diabetic islets in a FoxO1-dependent manner

During the progression of β-cell failure, FoxO1 is first activated in response to metabolic stress, and then becomes gradually inactivated.[8] Subsequently, we have proposed that Cyb5r3 is a marker of dedifferentiating β-cells with a bimodal regulation.[113] It's induced in stressed β-cells with active FoxO1, and decreased in dedifferentiating β-cells when FoxO1 levels fall, as defined by increased Aldh1a3 activity ($ALDH^{hi}$).[113] To test this model, including the dependence of Cyb5r3 on FoxO1, we measured Cyb5r3 levels under different metabolic conditions. As observed previously, *Cyb5r3* mRNA levels were induced in $Aldh^{hi}$ β-cells, whereas this induction was blunted in $Aldh^{hi}$ β-cells from *Foxo1* knockout mice (Fig. 6a). Moreover, when Cyb5r3 expression was assessed by immunohistochemistry of pancreatic tissue, it was reduced in multiple models of murine diabetes, including β cell-specific *FoxO* knockout,[10] diabetic GIRKO,[1] high fat diet (HFD)-fed, and S961 insulin receptor antagonist-treated mice[123] (Fig. 6b, Supp. Fig. 1a-c).

We next tested whether Cyb5r3 is a FoxO1 target. Chromatin immunoprecipitation (ChIP) with an anti-FoxO1 antibody showed enrichment at a putative FoxO1 binding site (5'-ATAAACA-3', position -661 to -667) in the *Cyb5r3* promoter (Fig. 6c). To assess the effect of FoxO1 activity on *Cyb5r3* expression in β-cells, we treated mouse insulinoma (Min6) cells with adenovirus encoding a constitutively active (FoxO1-ADA) or dominant negative (FoxO1-DN256) FoxO1.[124] Constitutively active FoxO1 caused a ~5-fold increase in *Cyb5r3* expression, while

dominant negative FoxO1 suppressed it by 60% (Fig. 6d). These data indicate that FoxO1 can directly activate *Cyb5r3* expression.

Chapter II, Figure 6

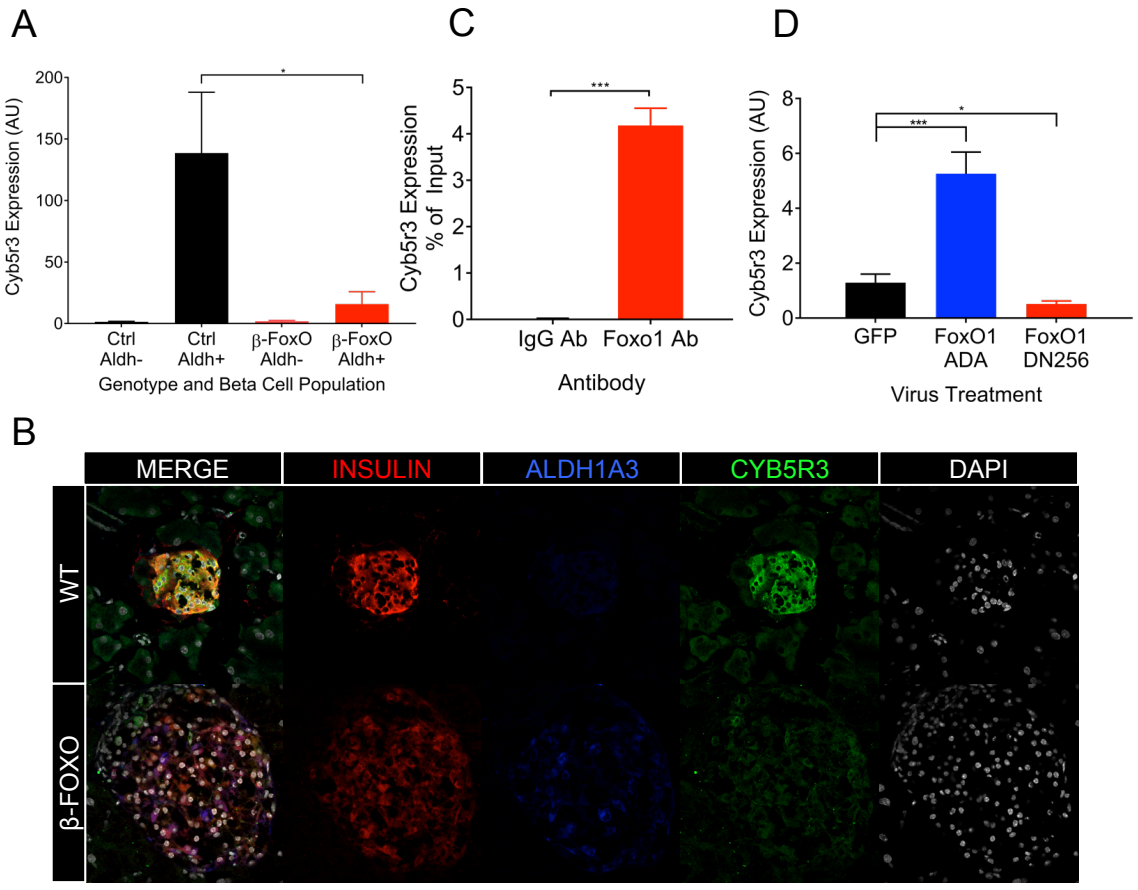

Cyb5r3 maintains β-cell secretory function

To determine whether Cyb5r3 is required for proper β-cell function, we treated Min6 cells with adenovirus expressing a short hairpin RNA against Cyb5r3 (Ad-shCyb5r3). The shRNA effectively lowered Cyb5r3 mRNA and protein by 95%, and 80%, respectively, without affecting Cyb5r4 expression (Supp. Fig. 2a-d). We then assessed glucose-stimulated insulin secretion. Min6 cells treated with shCyb5r3 adenovirus

showed an impaired insulin secretory response compared to control cells treated with shScramble adenovirus (Fig. 7a). Because Cyb5r3 is thought to participate in mitochondrial function, we measured basal respiration, and showed that Min6 cells stably expressing the shCyb5r3 construct had a ~25% decrease in basal respiration (Fig. 7b).

The second phase of insulin secretion in response to glucose requires mitochondrial ATP production.[125] Although Cyb5r3 can affect mitochondrial ETC activity, the mechanism by which it does so is unclear.[87, 116] It can alter the availability of NADH for electron transfer, pass reducing equivalents to coenzyme Q, or reduce cytochrome b protein subunits or heme groups located in ETC complex III.[2] Thus, we sought to determine whether loss of Cyb5r3 activity in β-cells affects ETC activity through complex III, or whether it had a broader impact on all ETC complexes. Enzymatic assays for complexes I-IV revealed that mitochondria isolated from Ad-shCyb5r3-treated Min6 cells had 4-15% reduced activity in complexes I, II, and IV, and a much more severe ~50% decrease in complex III activity (Fig. 7c-f). These data are consistent with a primary effect of Cyb5r3 on complex III, with lesser effects facilitating efficient electron flux through the other complexes.

We have proposed that a constitutive increase in β-cell lipid oxidation paves the way for β-cell failure and dedifferentiation, possibly by increasing ROS formation.[10, 113] ETC complexes I and III are the major producers of mitochondrial ROS, and production of ROS at these sites is increased in states of stymied electron flow.[126] Because we observed that complex I and III activities were affected by shCyb5r3 treatment, we tested the effect of shCyb5r3 knockdown on lipid-induced ROS formation. To do this,

we measured ROS production in Ad-shCyb5r3-treated Min6 cells cultured with and without palmitate, a condition that increases fatty acid oxidation and mimics the metabolic inflexibility of failing β-cells. Consistent with our hypothesis, an increase in ROS generation was only observed when Min6 cells expressing Ad-shCyb5r3 were treated with 0.5mM palmitate (Fig. 7g).

Cyb5r3 is an NADH-dependent oxidoreductase, and loss of its activity can perturb cellular NAD:NADH ratios. Min6 cells treated with Ad-shCyb5r3 had a decrease in NAD:NADH ratio, while overexpression of Cyb5r3-GFP led to an increase, consistent with Cyb5r3's NADH-consuming activity (Fig. 7h,i). Furthermore, we hypothesized that upon knockdown of Cyb5r3, β-cells would compensate for increased NADH concentrations (or decreased NAD:NADH ratio) by increasing lactate production via lactate dehydrogenase to convert excess NADH to NAD^+. Indeed, Ad-shCyb5r3-treated Min6 cells showed increased lactate levels when cultured in 0.5mM palmitate (Fig. 7j). In the setting of increased β-cell lipid oxidation, the disturbances in NAD:NADH ratio, combined with increased ROS production and reduced electron transport, may generate enough cellular stress so as to induce β-cell failure.

Chapter II, Figure 7

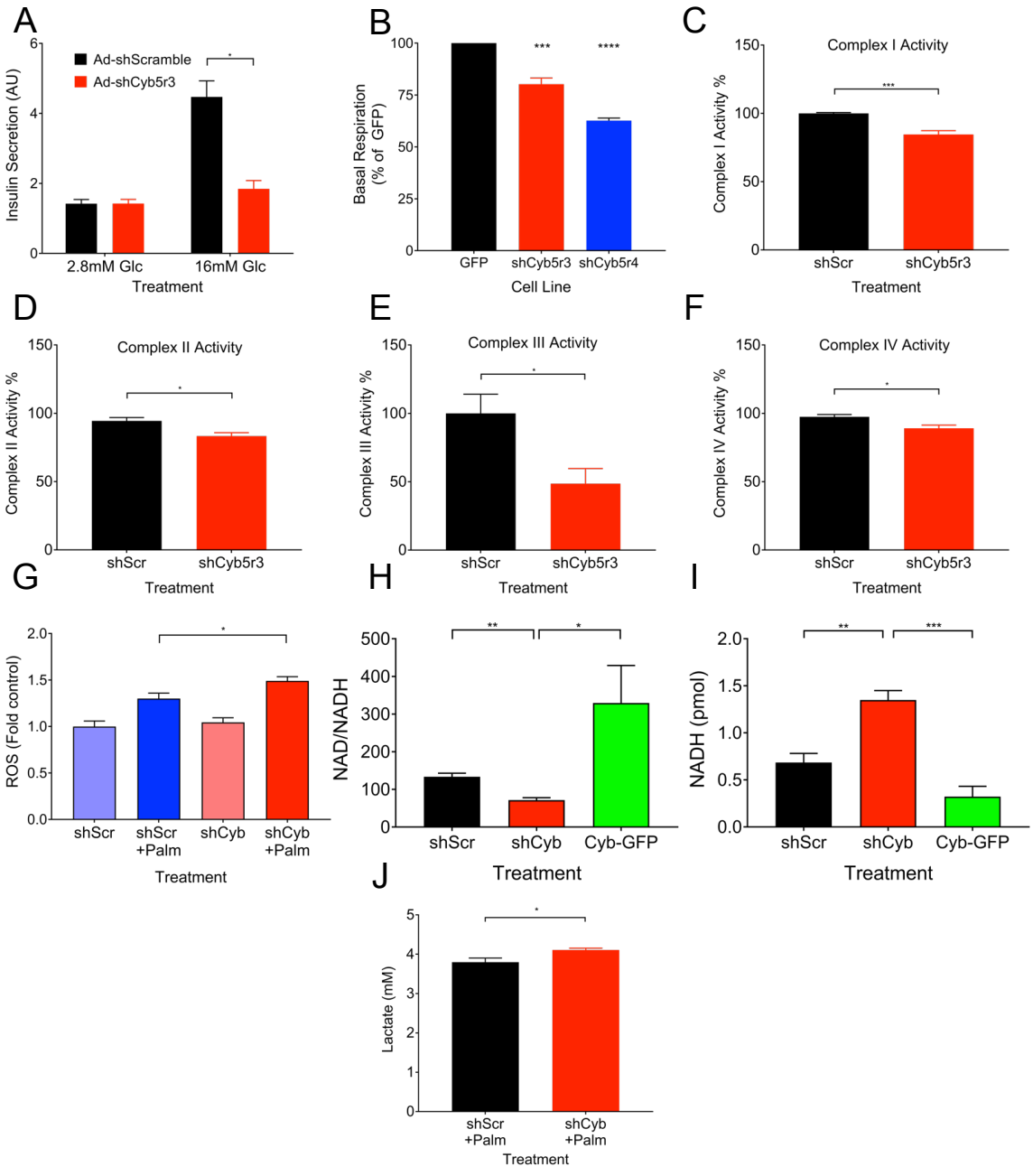

Cyb5r3 is necessary for islet insulin secretory function *ex vivo*

Although we observed defects in glucose-stimulated insulin secretion in Min6 cells with Cyb5r3 knockdown, it remained unclear whether Cyb5r3 played a similar critical role

within the islet. To test this point, we isolated primary islets from wildtype mice, treated them with shCyb5r3 or shScramble adenoviruses, then performed *ex vivo* glucose-stimulated insulin secretion assays. Consistent with findings in Min6 cells, Ad-shCyb5r3-treated islets displayed blunted insulin secretion in response to glucose that was not due to differences in insulin content (Fig. 8a,b).

To examine whether loss of Cyb5r3 impinges on processes upstream or downstream of intracellular calcium release, we performed single-cell Fura2AM calcium flux imaging on β-cells exposed to glucose and KCl. To chemically identify β-cells, we isolated islets from *Insulin2-GFP* mice[74], dissociated to single cells, treated with Ad-shCyb5r3 or Ad-shScramble, then gated single β-cells by GFP-expression for fluorescence measurements. Remarkably, Ad-shCyb5r3-treated β-cells displayed a severely blunted calcium flux in response to glucose and, to a lesser extent, KCl (Fig. 8c,d). Given the *in vitro* data supporting Cyb5r3's role in ETC function, these findings suggest that Cyb5r3 is required for efficient ATP production from glucose.

Chapter II, Figure 8

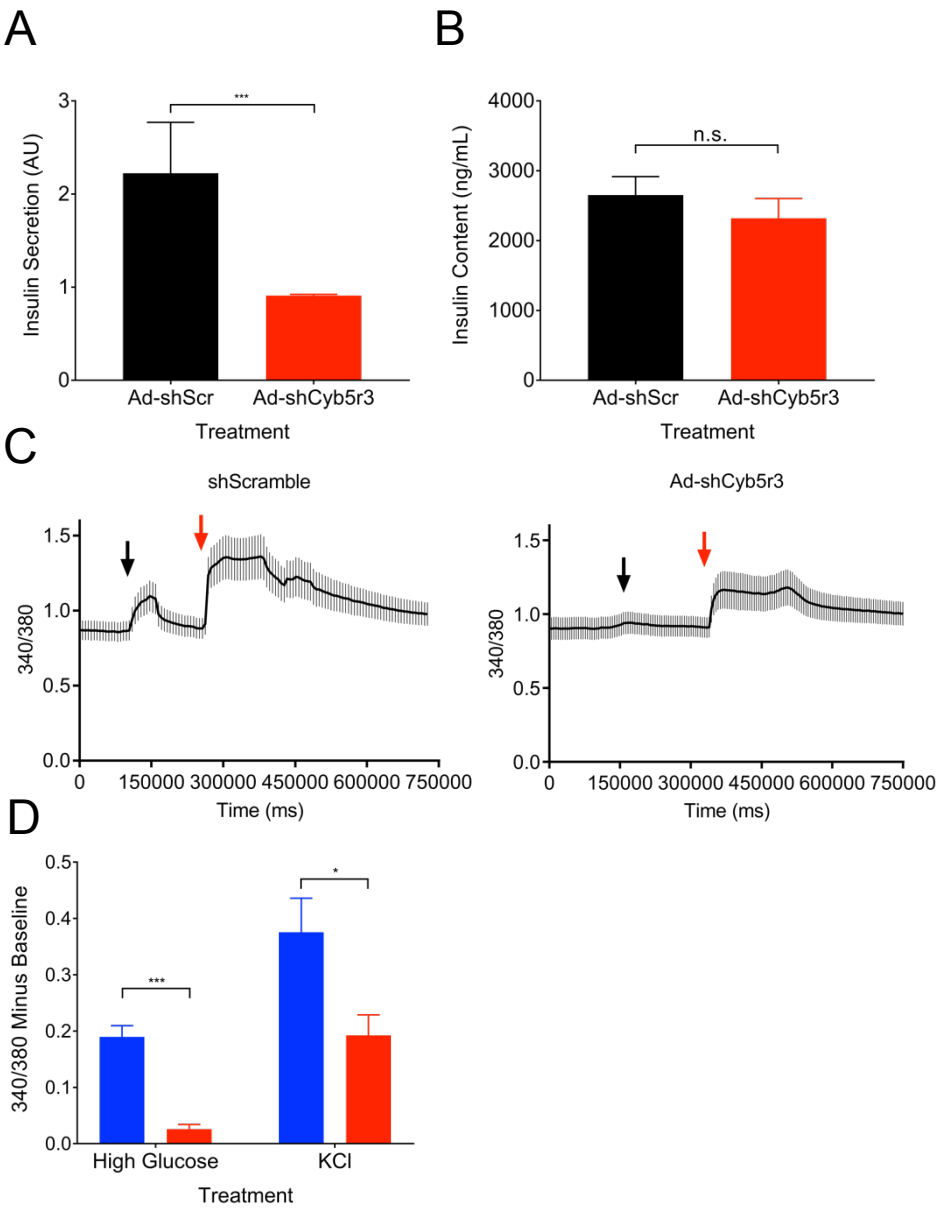

β-cell dysfunction following Cyb5r3 ablation in mice

To examine the effects of the loss of Cyb5r3 in β-cells *in vivo*, we generated rat insulin promoter (RIP)-Cre-Cyb5r3$^{fl/fl}$ mice (B-Cyb5r3). These mice were born at Mendelian ratios with no gross morphological defects or differences in body weight, lean

mass, fat mass, or tissue water content (Supp. Fig. 3a). Immunostaining for Cyb5r3 in pancreas sections of B-Cyb5r3 mice revealed 80-100% Cre recombinase efficiency, consistent with previous findings (Fig. 9a).[9] Notably, Cre recombinase efficiency was less in male mice, with some islets still retaining Cyb5r3 expression in the majority of β-cells (Supp. Fig. 4a). Islets from 2-month-old B-Cyb5r3 mice had normal β and δ/PP cell ratios (quantified together) compared to RIP-Cre+ controls (Supp. Fig. 5a). However, B-Cyb5r3 islets had a greater proportion of α cells compared to controls (17% vs. 11% of total islet area, p=0.032) (Fig. 10b, Supp. Fig. 5a).

Chapter II, Figure 9

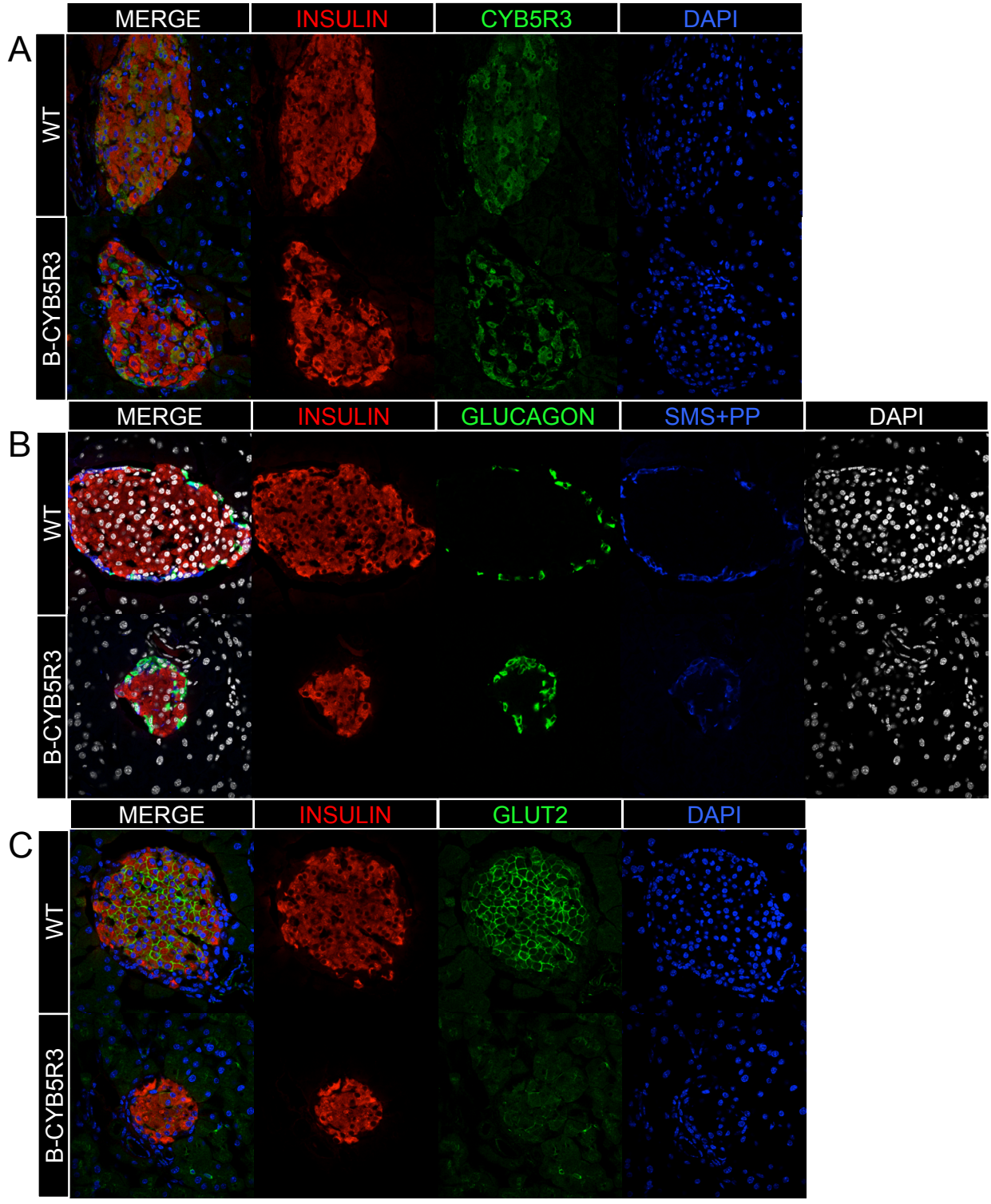

Chapter II, Figure 9 Continued

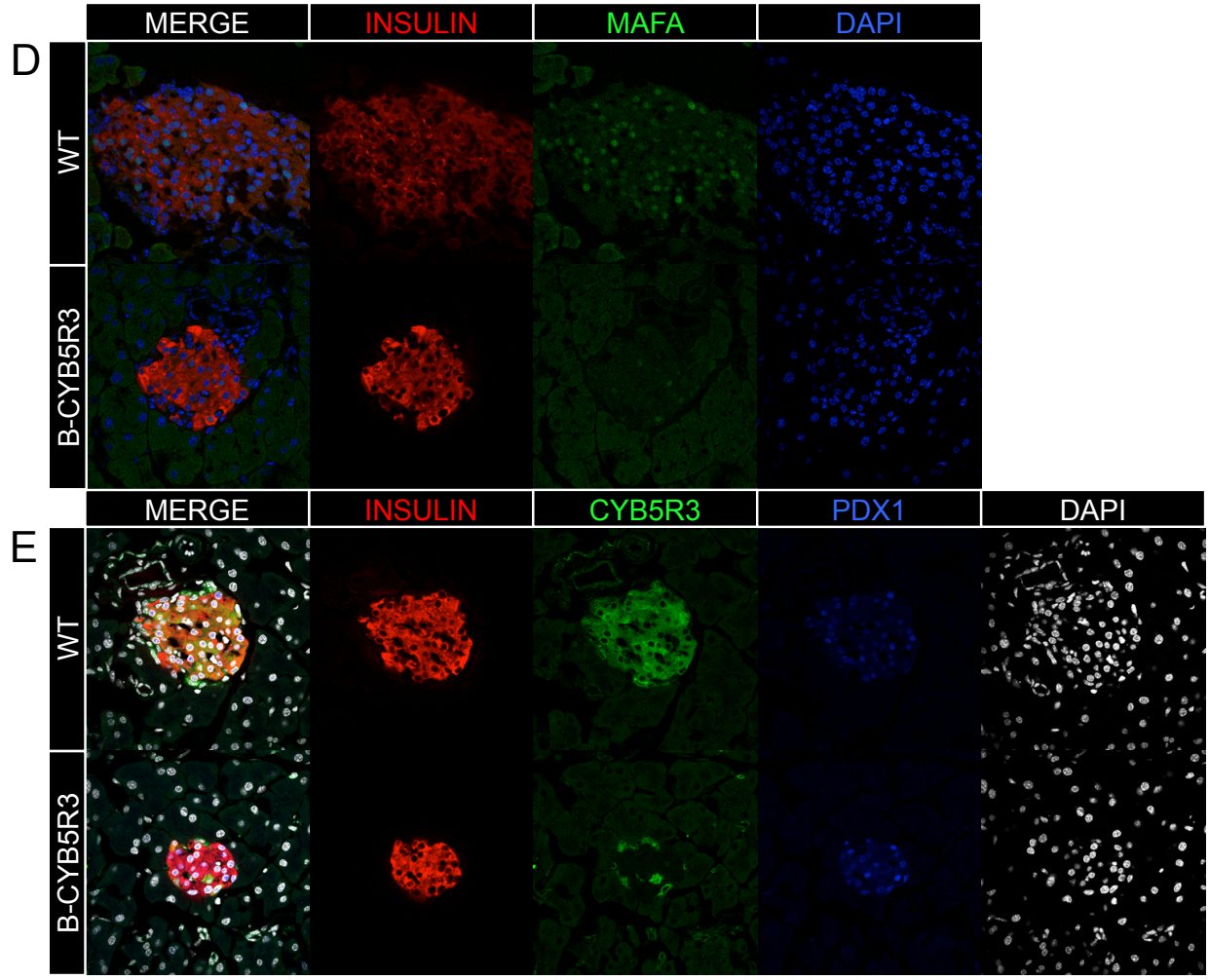

Chapter II, Figure 10

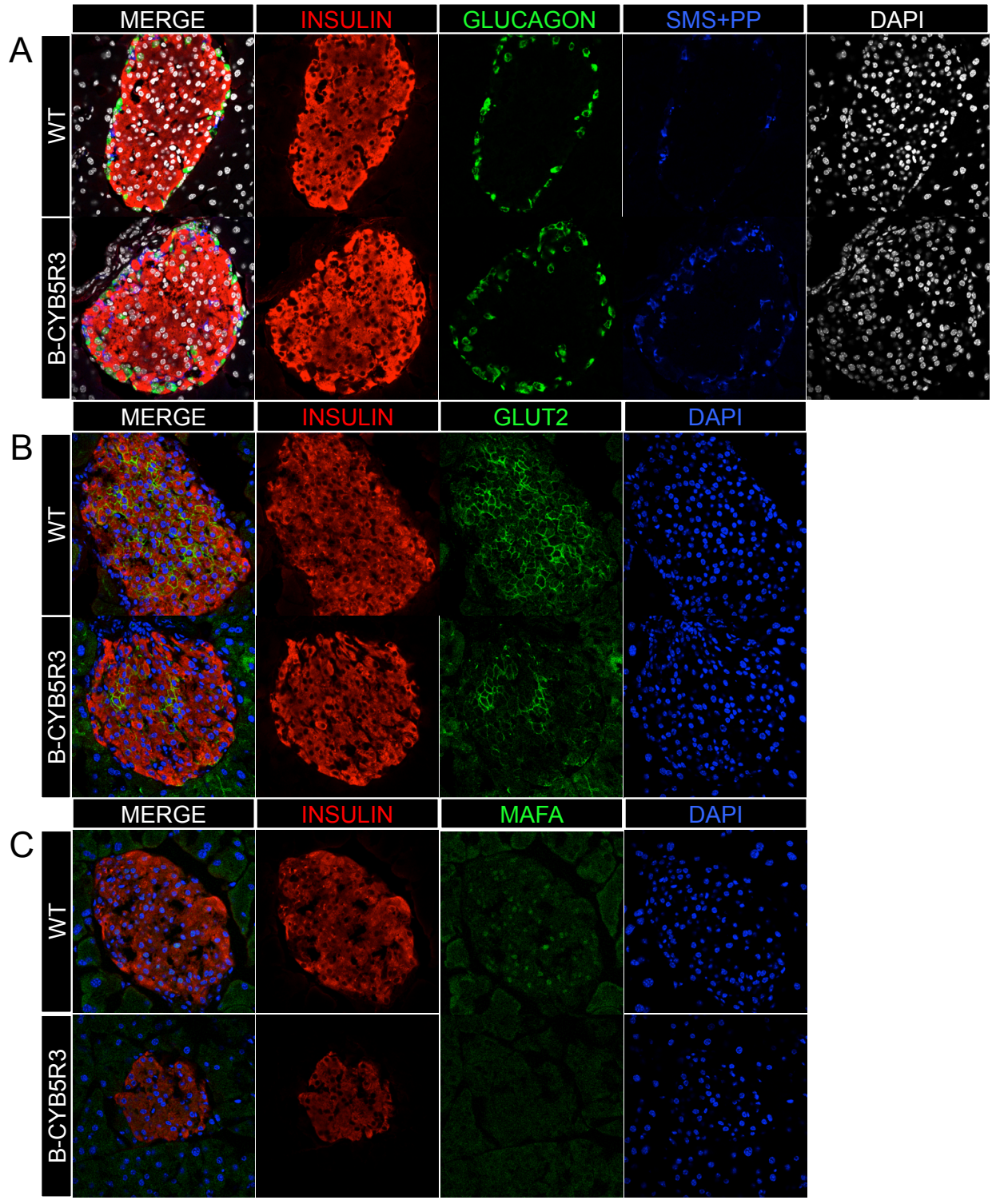

Chapter II, Figure 10 Continued

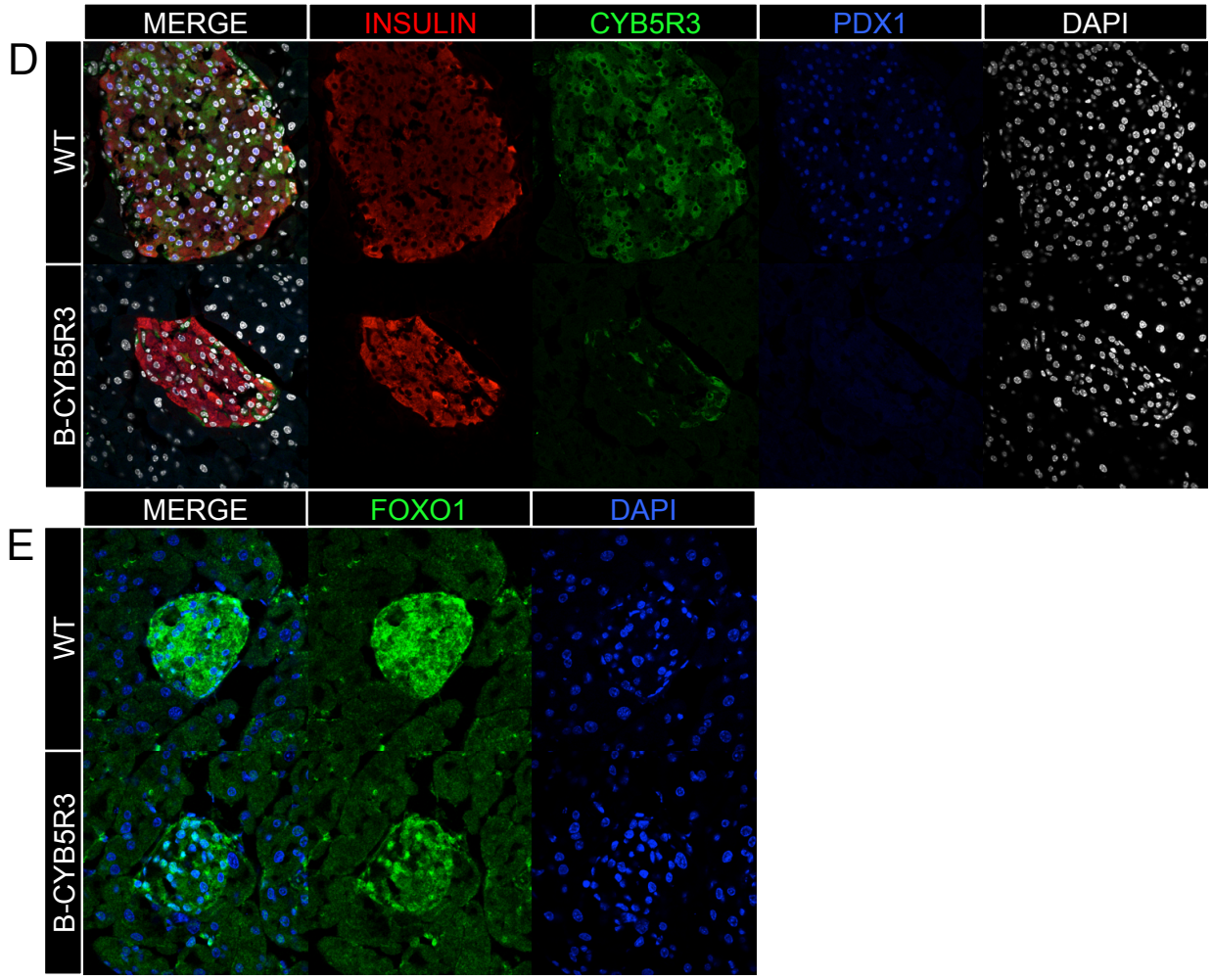

Chapter II, Figure 11

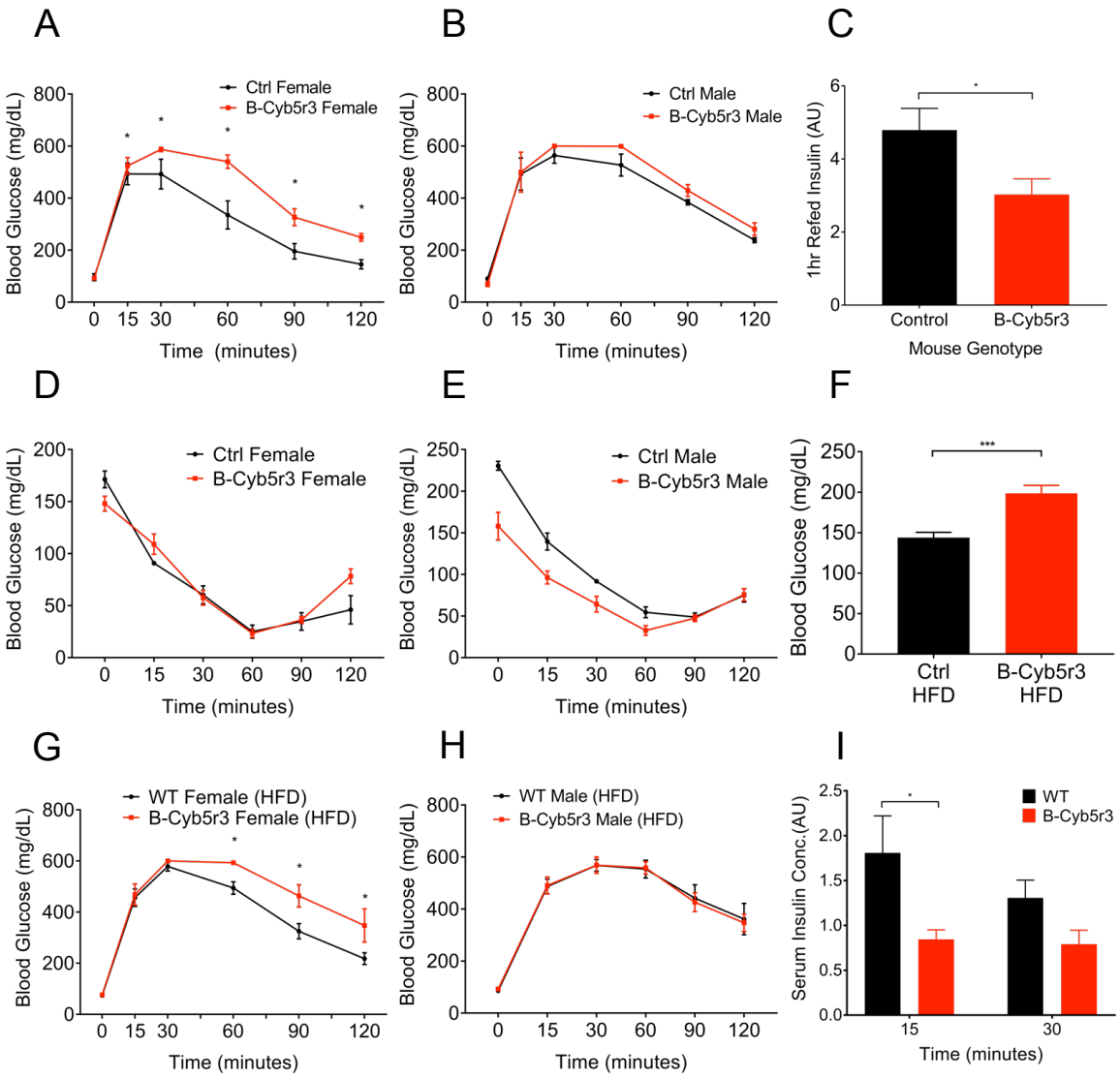

Chapter II, Figure 12

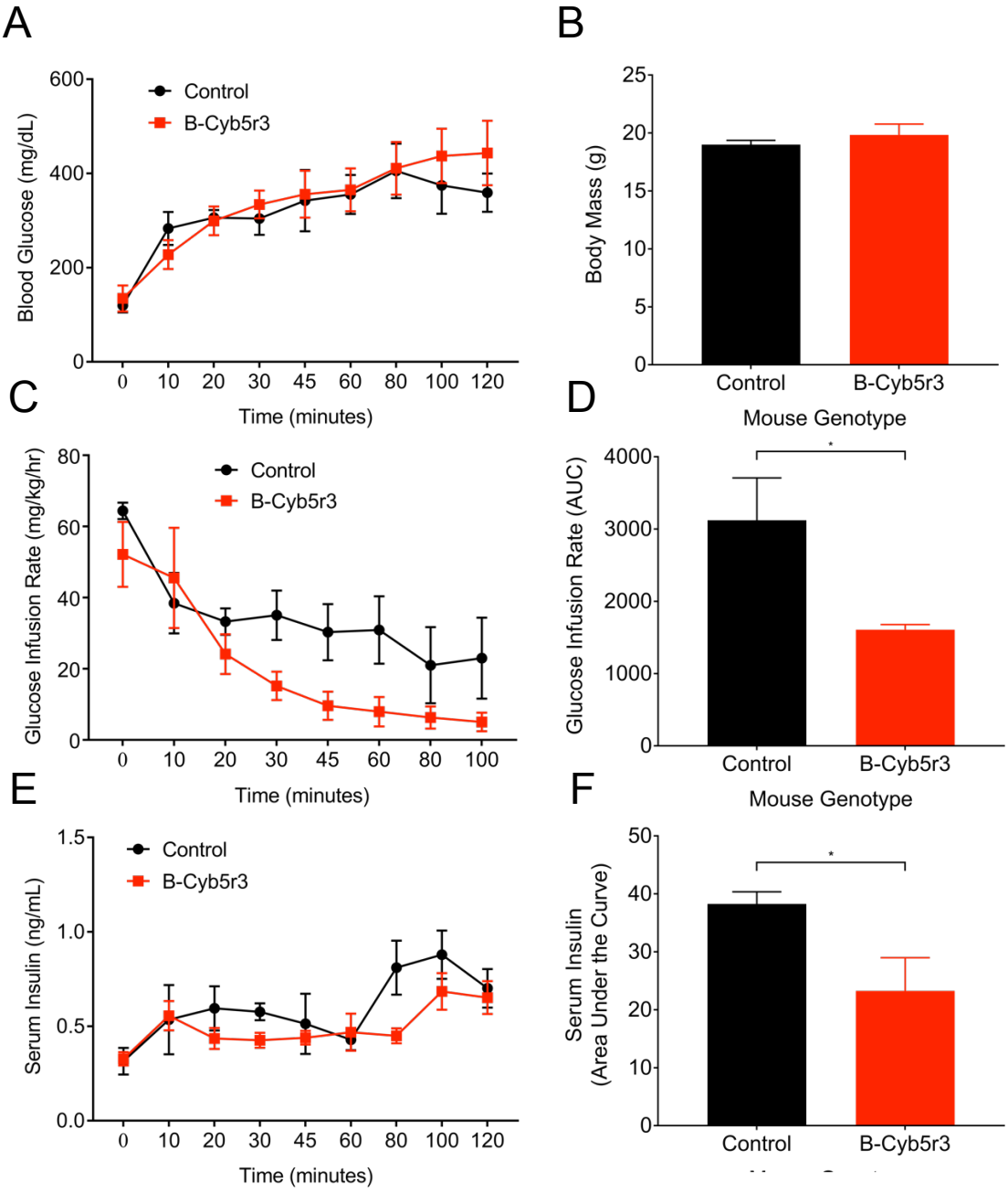

We analyzed the metabolic features of B-Cyb5r3 mice. Although plasma glucose levels in 4-month-old animals were normal, females demonstrated glucose intolerance relative to RIP-Cre^{+} controls as assessed by intraperitoneal glucose tolerance tests

(IPGTT), as well as lower refed insulin levels after a 4-hour fast (Fig. 11a,c). Male mice did not display glucose intolerance at 4 months of age, but showed mild glucose intolerance at 8 months of age (Fig. 11b, Supp. Fig. 4b). We observed similar results in oral glucose tolerance tests (OGTT), effectively ruling out an incretin effect (Supp. Fig. 3c,d). In contrast, insulin tolerance tests, fasting or re-fed free fatty acids, and triglyceride levels revealed no differences between B-Cyb5r3 and control mice (Fig. 11d,e, Supp. Fig. 3e,f).

Next, we tested the effects of diet on B-Cyb5r3 animals. Within 1 week of being placed on a diet consisting of 60% fat (HFD), female B-Cyb5r3 mice began to exhibit significant hyperglycemia (Fig. 11f). Glucose tolerance tests confirmed that 4-month-old female B-Cyb5r3 mice on HFD develop glucose intolerance relative to controls (Fig. 11g,h). By 6 months of age, both male and female mice showed impaired insulin secretion 15 minutes after a glucose gavage (Fig. 11i). To directly assess insulin secretory function in vivo, we performed hyperglycemic clamps. B-Cyb5r3 mice required a lower glucose infusion rate to maintain hyperglycemia and had a commensurate decrease in plasma insulin levels, suggestive of a primary insulin secretory defect (Fig. 12a-f).

We next analyzed islet composition and markers of β-cell functional maturity. Interestingly, islets from 2-month-old B-Cyb5r3 mice showed decreased expression of Glut2 and MafA (Fig. 9c,d), but preserved expression of Pdx1, suggesting that β-cells partly maintain their differentiated features (Fig. 9e). However, in 6-month-old B-Cyb5r3 animals islet architecture was disrupted, with α– and δ/PP-cells appearing in the islet core (Fig. 10a), and the greater relative proportion of α-cells persisted (Supp. Fig. 5b).

In addition to the previously established lack of Glut2 and MafA (Fig. 10b,c), the majority of β-cells now showed a substantial decrease in Pdx1 expression (Fig. 10d). We also investigated FoxO1 expression and localization. As expected based on the incipient hyperglycemia, there was increased nuclear FoxO1 staining in B-Cyb5r3 islets (Fig. 10e). However, this increase didn't result in improved expression of β-cell differentiation markers, such as MafA and Pdx1. These data indicate that B-Cyb5r3 is required for FoxO1 induction of MafA (the relationship between FoxO1 and Pdx1 being more complex), and suggest that the β-cell's redox status or mitochondrial function regulates MafA. These data indicate that B-Cyb5r3 β-cells are trying to compensate for impaired function by increasing FoxO1 activity, but since they lack Cyb5r3 they are unable to do so.

Chapter II, Figure 13

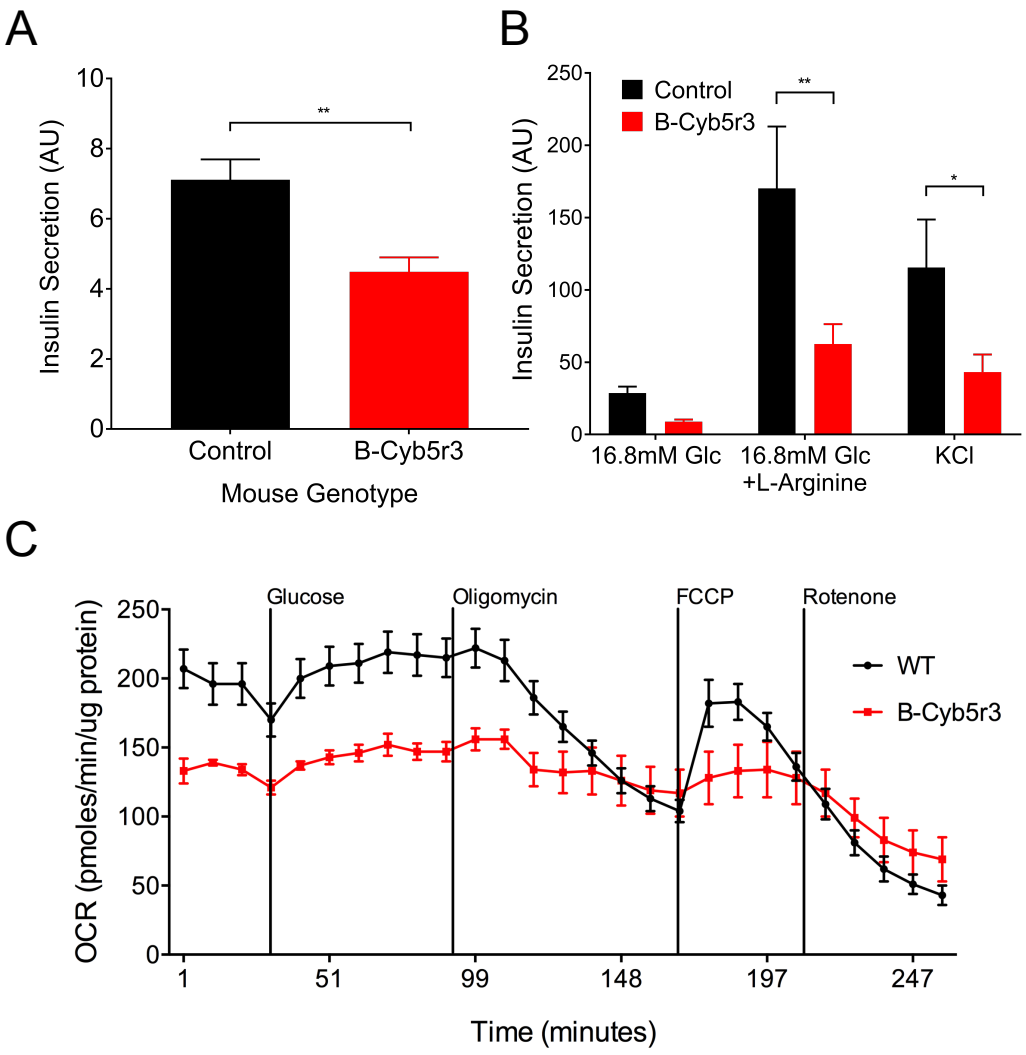

Impaired islet function in B-Cyb5r3 mice

To assess islet function in B-Cyb5r3 mice, we isolated primary islets and performed glucose-stimulated insulin secretion assays. Consistent with data from Min6 cells and islets treated with Ad-shCyb5r3, B-Cyb5r3 mouse islets showed decreased insulin secretion in response to glucose compared to RIP-Cre+ controls, as well as a blunted response to the depolarizing agents L-arginine and KCl (Fig. 13a,b). To determine whether this impairment occurred in the context of mitochondrial dysfunction,

we assessed basal respiration in B-Cyb5r3 primary islets and found a nearly ~50% decrease compared to controls (Fig. 13c). Thus, the data indicate that lack of Cyb5r3 results in profound mitochondrial dysfunction leading to impaired insulin secretion.

DISCUSSION

The paramount challenge in defining the progression of β cell dedifferentiation has been identifying molecular pathways that contribute to the clinically silent, or reversible, phase of pathogenesis. What events initiate the slow creep to hyperglycemia, and at what point do β cells begin to lose their "β cell-ness"? Answering these questions is essential for the development of therapeutics aimed at the prevention or reversal of dedifferentiation. Current literature continues to characterize dedifferentiation as the loss of classical β cell markers such as Insulin, FoxO1, MafA, Nkx6.1, and Pdx1, or conversely, as the acquisition of progenitor markers such as Neurogenin3, L-Myc, Nanog, and Oct4.[9, 44, 46, 99] Some degree of temporal resolution has been achieved as to the order of transcription factor downregulation. For example, in *db/db* mice, FoxO1 nuclear translocation occurs at 6 weeks of age, while depletion of MafA and Glut2 occurs at 8 weeks, followed by Nkx6.1 at 10 weeks.[99] Although the loss of these transcription factors acts as landmarks on the path to β cell dedifferentiation, it is not clear why one precedes another, or perhaps more importantly, how one may beget another. From a therapeutic standpoint, we still don't know which downstream effectors are critical contributors to targetable cellular processes in β cell function.

To address this question, we identified a marker of β cell dysfunction that could be used to isolate and study the early phase of dedifferentiation. Using the FoxO β cell conditional knockout mouse (β-FoxO), a MODY-like murine model of diabetes known to display β cell dedifferentiation with age,[10] we found that expression of Aldh1a3 was uniquely increased in dysfunctional β cells.[113] RNA sequencing of the Aldh1a3+ β cell population then identified Cyb5r3 as the top down-regulated gene.

The key contribution of this work is the identification of Cyb5r3 as a novel FoxO1-regulated oxidoreductase that is essential to β cell function. *In vitro*, β cells with Cyb5r3 knockdown display impaired glucose-stimulated insulin secretion, decreased basal respiration, impaired mitochondrial complex activity, decreased NAD:NADH ratio, and increased ROS production. *Ex vivo*, primary islets with Cyb5r3 knockdown also displayed impaired glucose-stimulated insulin secretion and impaired calcium flux in response to high glucose. Mice with β cell-specific Cyb5r3 deletion show impaired glucose tolerance and blunted insulin secretion, the onset of which is hastened by high fat diet feeding. Islets from B-Cyb5r3 mice have impaired glucose stimulated insulin secretion, decreased basal respiration, and loss of the mature β cell markers Glut2, MafA, and Pdx1. Both *in vitro* and *in vivo* findings suggest that loss of Cyb5r3 causes profound mitochondrial dysfunction. Therefore, Cyb5r3 acts as a potential mechanistic link between the loss of FoxO, cellular stress, and dedifferentiation.

Mitochondria are critical fuel sensors in β cells that allow the coupling of nutrient metabolism with insulin secretion. Their essential role in β cell metabolism-secretion coupling is evidenced by the maternally-inherited mutations in mitochondrial DNA that are known to cause functional impairment of the ETC and insulin-deficient forms of diabetes.[127, 128] Perhaps unsurprisingly then, mitochondrial dysfunction has been found in many rodent models of diabetes and in human patients.[10, 113, 127, 129-131] In particular, β cells are susceptible to ROS damage because they produce relatively low levels of the free-radical quenching enzymes superoxide dismutase, catalase, and glutathione peroxidase.[39, 132, 133] The mitochondrial genome, inner membrane proteins (such as ATP

synthase), and inner membrane lipids are especially vulnerable to oxidative damage due to their proximity to free radicals. Oxidation of the mitochondrial membrane lipid cardiolipin has been shown to alter the activity of adenine nucleotide transporter and cytochrome c oxidase, both of which are critical to ATP synthesis and insulin secretion.[134] Furthermore, in alveolar epithelial cells, mitochondrial complex III-generated ROS has been shown to induce cell death through the activation of ASK1-JNK pathways.[135] Our findings show that deletion of β cell Cyb5r3 causes impaired mitochondrial complex activity and increased ROS production, reducing glucose-stimulated insulin secretion and predisposing to β cell failure in B-Cyb5r3 mice. The decrease in mitochondrial complex activity we observe could be due to a direct effect on electron transport (i.e. through the production of reducing equivalents), or an indirect effect via the assembly of ETC complexes, as Cyb5r3's flavin domain is known to reduce heme groups which are found in the cytochrome b and cytochrome c subunits of Complex III, as well as in Complex IV.[136] In light of these data, we propose the following model: in the setting of incipient metabolic stress, β cell FoxO1 translocates to the nucleus to initiate a protective response.[8] As a part of this repertoire, Cyb5r3 expression is increased to facilitate electron transport, ATP production, antioxidant reduction, and to shunt excess fatty acyl-CoA away from the oxidative pathway. However, as previously shown, FoxO1 is eventually degraded with chronic stress, leading to a concomitant decrease in Cyb5r3 expression.[9] Therefore, loss of Cyb5r3 activity with subsequent mitochondrial dysfunction may initiate a cycle of impaired stimulus-secretion coupling, worsened hyperglycemia, and increased biosynthetic demand for insulin, eventually causing the loss of β cell function and identity.

There are many parallels between the β-FoxO and B-Cyb5r3 models. Islets from both show impaired glucose-stimulated insulin secretion and loss of mature β cell markers MafA, Glut2, and Pdx1 before the onset of β cell dedifferentiation as defined by expression of endocrine progenitor markers.[9, 113] At a cellular level, both knockout models display defects in mitochondrial respiration and glucose-stimulated calcium flux and in mice, glucose intolerance occurs in adulthood and worsens with age.[10] These similarities suggest that the mitochondrial phenotype observed in β-FoxO knockouts is driven by the loss of Cyb5r3, and that restoration of Cyb5r3 in β-FoxO mice might prevent the β cell dedifferentiation observed with aging and multiparity.

Cyb5r3 is expressed in nearly all tissues and has been implicated in a wide range of cellular redox reactions.[87] The yeast ortholog of Cyb5r3, NADH-Coenzyme Q reductase 1 (NQR1), reduces fasting-induced apoptosis by increasing levels of reduced Coenzyme Q and extends lifespan through a SIR2-dependent mechanism that increases oxidative metabolism.[95] Yeast NQR1 activity increases in calorie restriction, a condition usually accompanied by increased FA oxidation. In mammals, Cyb5r3 is localized predominantly to mitochondrial and endoplasmic reticulum membranes and plays a role in many cellular processes, including the reduction of cytochrome b5 and coenzyme Q, fatty acid desaturation/elongation, cholesterol biosynthesis, metabolism of xenobiotics, and antioxidant reduction, making it likely that it contributes to β cell function in multiple ways. Mice with global overexpression of Cyb5r3 have moderate lifespan extension, increased insulin sensitivity, increased complex I and III activity, a greater proportion of unsaturated very long chain FAs in TGs, and reduced ROS

production.[116] It is still unknown whether β cells from these mice are protected from dedifferentiation.

Although our study has focused on Cyb5r3's role in the mitochondria, it is likely that cellular lipid compositions are altered in B-Cyb5r3 mice, which in itself can impair the function of critical organelles, such as the ER and mitochondria.[137, 138] Cyb5r3's lipid desaturation/elongation function may also stimulate triglyceride synthesis and shunt free fatty acid metabolism away from toxic lipid species such as ceramide. As mechanistic precedence, Min6 cells with higher expression of stearoyl-CoA desaturase 1 (SCD1), the rate-limiting enzyme in the formation of monounsaturated fatty acids, are protected from lipid-induced toxicity.[139]

Cyb5r3's role in reducing antioxidants such as coenzyme Q, α-tocopherol, and ascorbate may be especially critical in oxidative stress-prone β cells. In response to oxidative stress, FoxO1 protects against β cell failure by translocating to the nucleus and inducing expression of NeuroD and MafA, two transcription factors regulating the Insulin2 gene.[8] However, with prolonged stress or hyperglycemia, the loss of FoxO1-dependent Cyb5r3 expression may hasten the depletion of what little antioxidant reserves remain. It is known that Cyb5r3 expression can be stimulated by oxidative stress: binding of the activating transcription factor Nrf2 (in complex with FoxO3a) to two antioxidant response elements in the human Cyb5r3 promoter is increased by exposure to diquat.[87] In our study, Min6 cells with Cyb5r3 knockdown showed increased ROS production only when exposed to the fatty acid palmitate. These findings suggest that Cyb5r3's role in reducing antioxidants may be a safeguard against conditions that increase mitochondrial free radical production.

Clinical guidelines for the treatment of diabetes continue to reinforce the importance of "β cell rest." [7, 53, 54] In patients with type II diabetes, early intensive insulin therapy has been shown to improve β cell function, glycemic control, and lower remission rates, consistent with a model in which β cells dedifferentiate then redifferentiate upon recovery.[140] It is our hope that as the progression of β cell identity loss continues to be mapped out, more molecular targets amenable to pharmacological intervention will arise. The results of this study suggest that Cyb5r3 may be one such target and that therapies that improve mitochondrial plasticity and optimize ETC function may be particularly beneficial for the prevention of β cell dedifferentiation. Membrane permeable peptides that target cardiolipin on the inner mitochondrial membrane to facilitate electron transfer from cytochrome c to complex IV are currently in clinical trials for multiple indications ranging from congestive heart failure to Leber's Hereditary Optic Neuropathy.[141] Although the effect of this type of intervention on β cell failure remains unknown, these peptides have been shown to improve the function of aged islets post-transplantation and to facilitate the transplant of islets by preserving mitochondrial polarization and reducing islet cell apoptosis.[142] The discovery of such peptides highlights the possibility that a novel class of mitochondrial therapeutics may be able to selectively enhance ETC complex functions as a way to prevent β cell dedifferentiation.

CHAPTER II SUPPLEMENTARY INFORMATION

Chapter II, Supplemental Figure 1

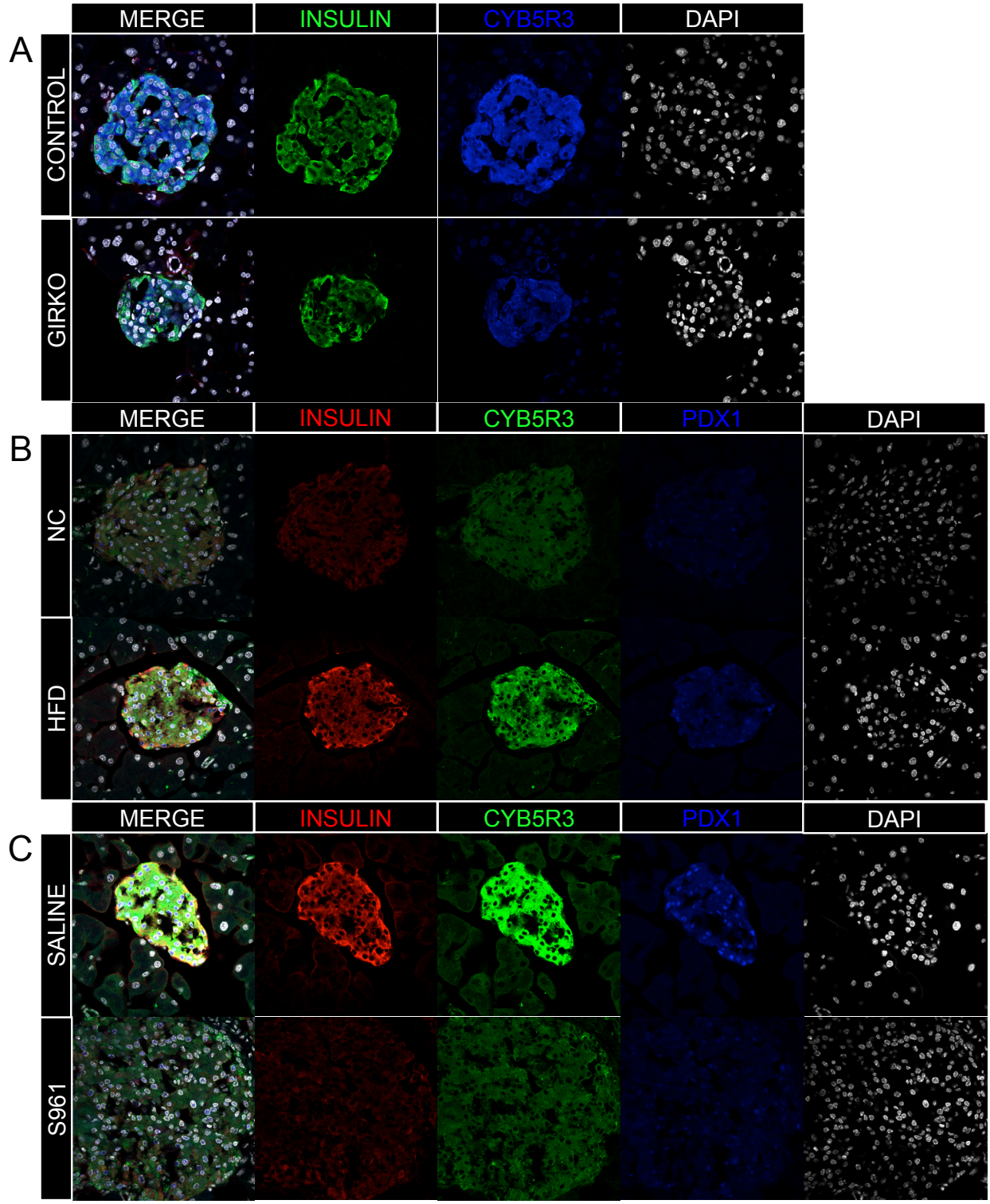

Chapter II, Supplemental Figure 2

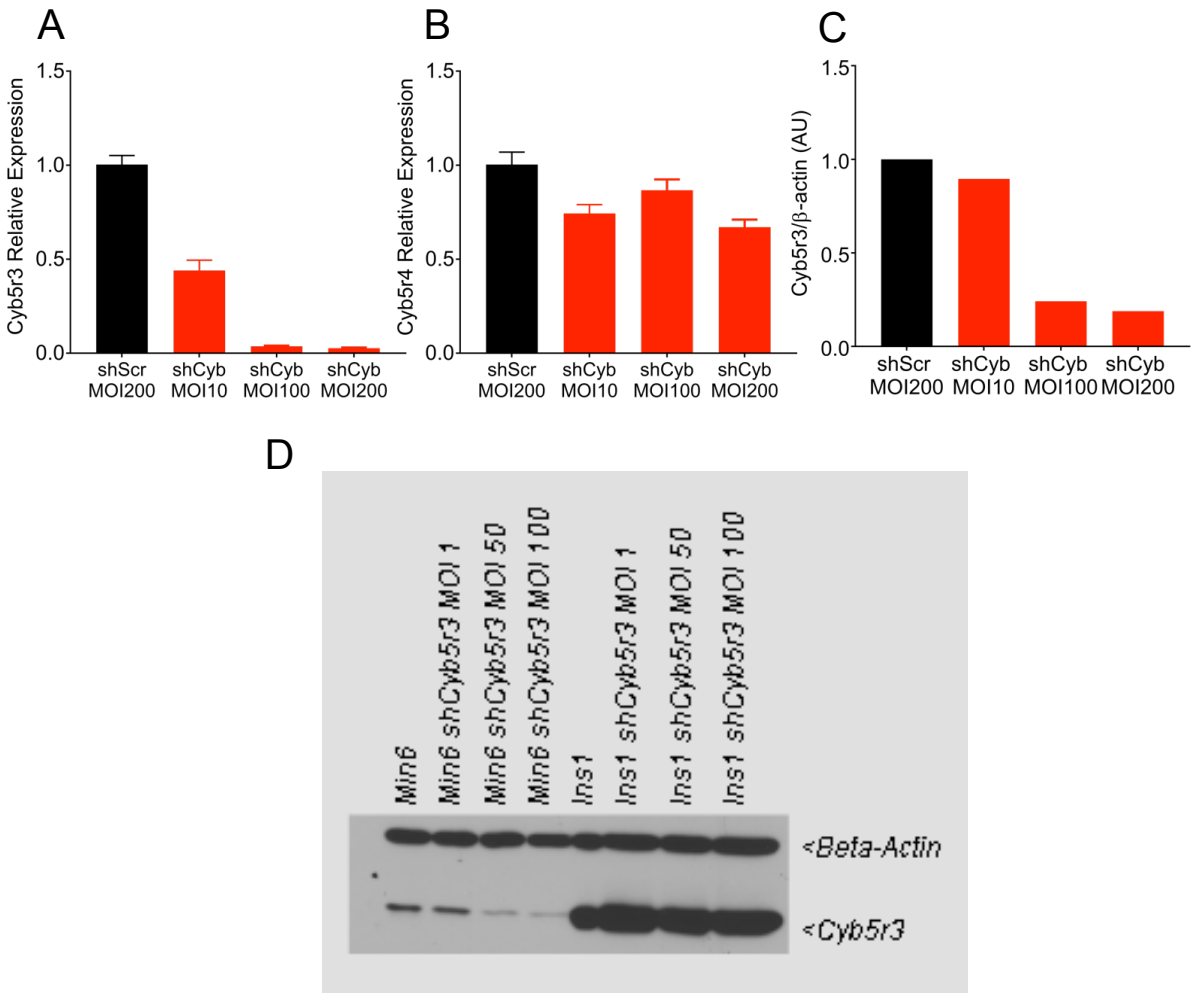

Chapter II, Supplemental Figure 3

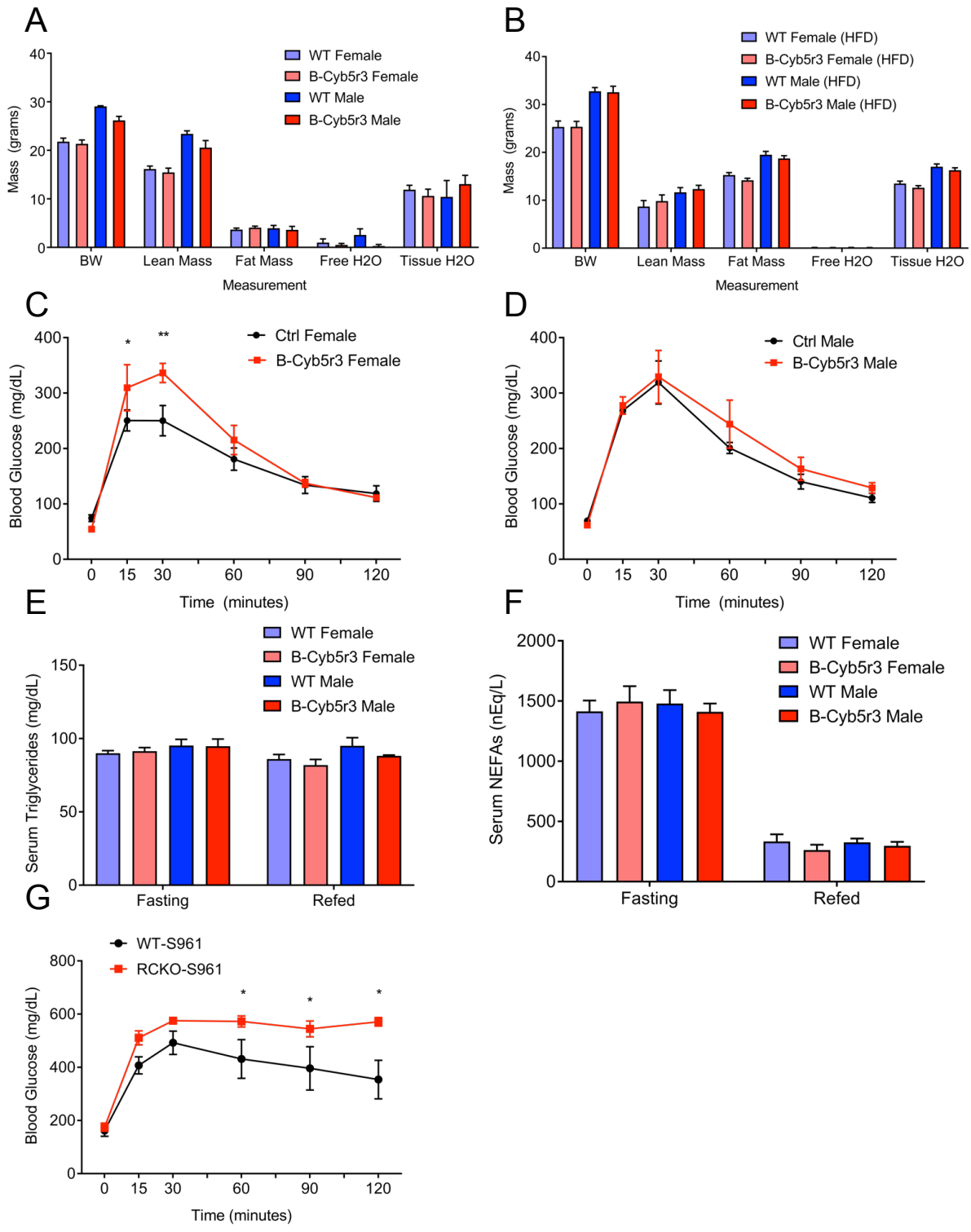

Chapter II, Supplemental Figure 4

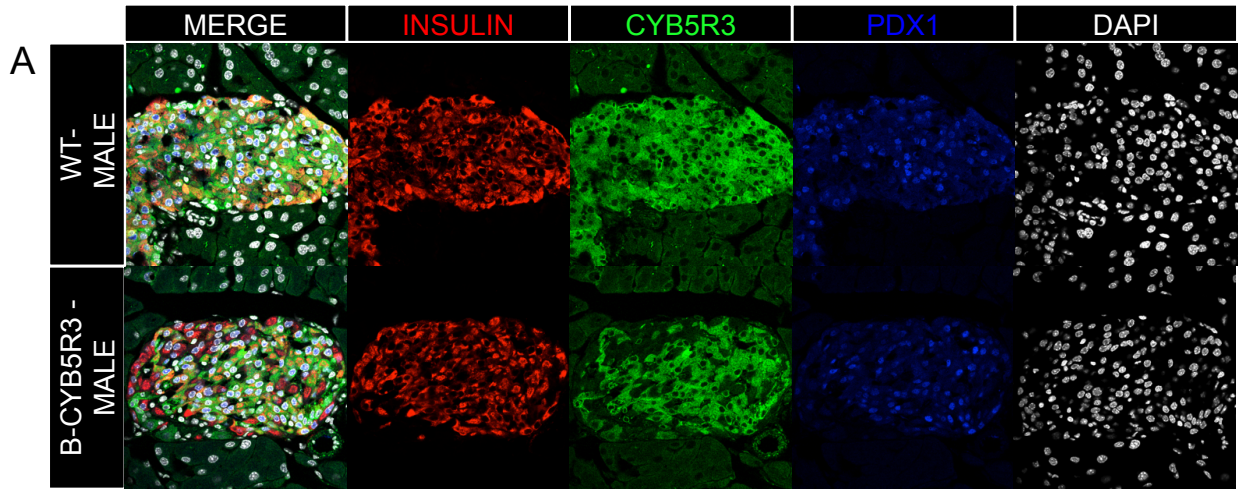

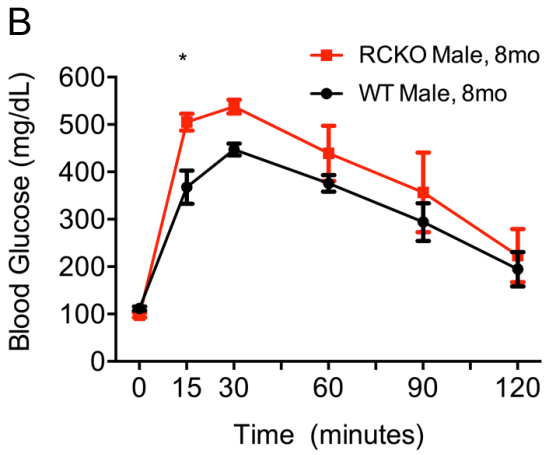

Chapter II, Supplemental Figure 5

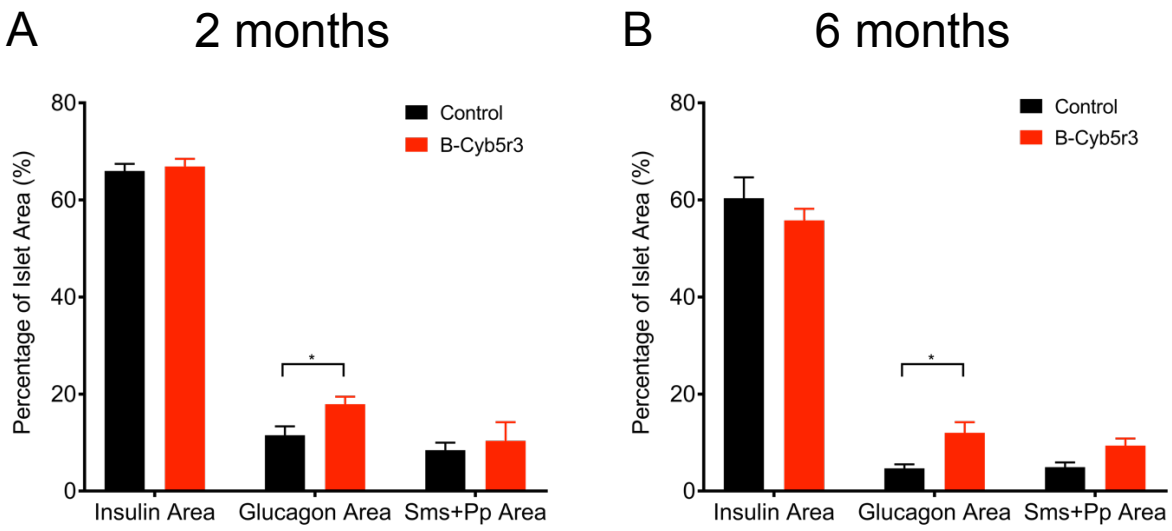

Chapter II, Supplemental Figure 6

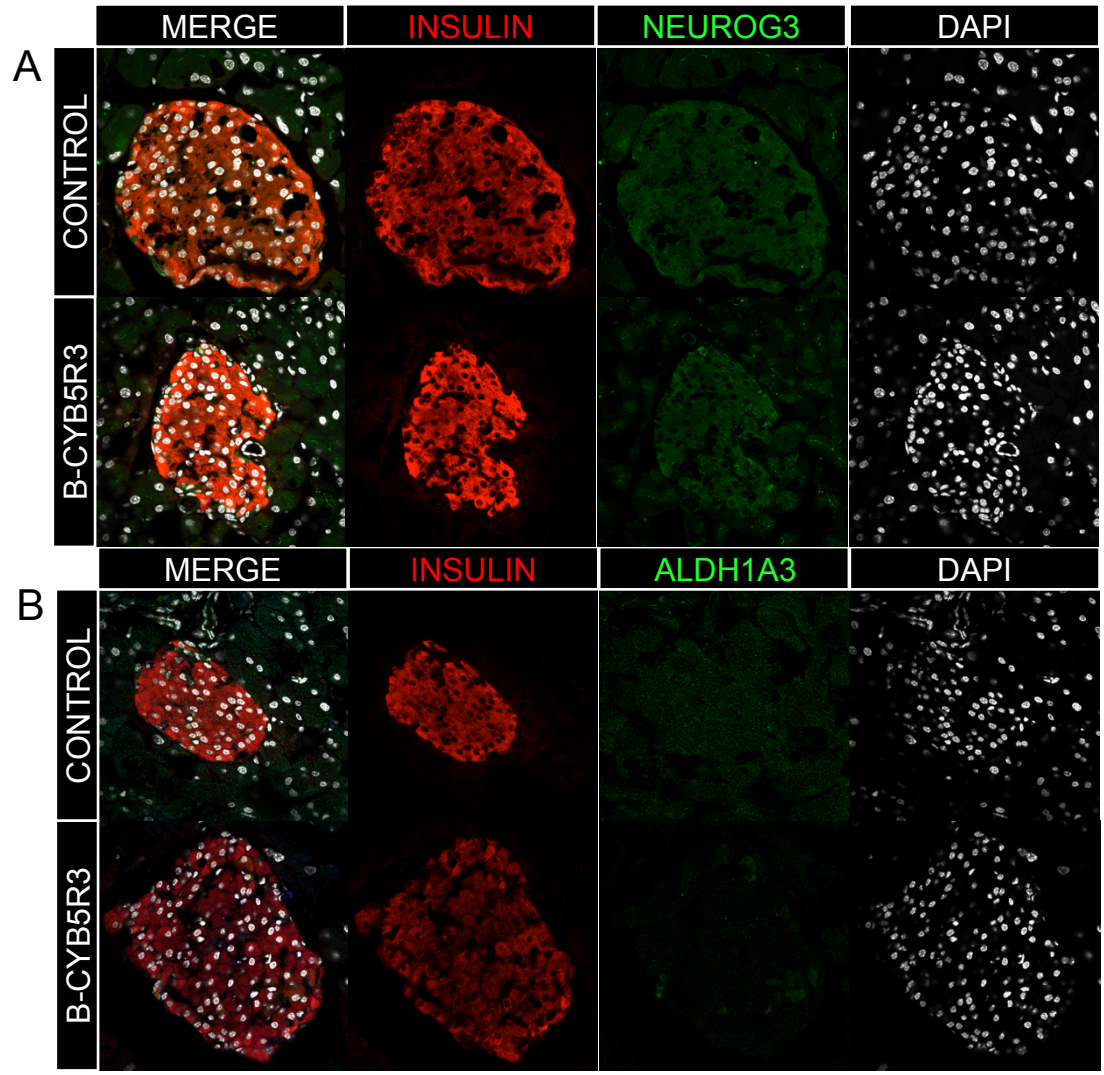

Chapter II, Supplemental Table 1

Antigen	Species	Dilution	Product Number	Company
Insulin	Guinea Pig	1:2000	A0564	DAKO
Aldh1a3	Rabbit	1:100	NBP2-15339	Novus
Cyb5r3	Rabbit	1:100	10894-1-AP	Proteintech
Proglucagon	Rabbit	1:500	#8233	Cell Signaling
Somatostatin	Goat	1:1000	SC-7819	Santa Cruz
Pancreatic Polypeptide	Goat	1:500	AB77192	Abcam
Glut2	Rabbit	1:200	AB54460	Abcam
MafA	Rabbit	1:200	IHC00352	Bethyl
Pdx1	Goat	1:100	AF2419	R&D
FoxO1	Rabbit	1:100	CST 2880S	Cell Signaling
Neurogenin3	Rabbit	1:100	AB2011	BCBC

CONCLUSIONS AND FUTURE DIRECTIONS

Chapter I described the characterization of Aldh1a3 as a marker of dysfunctional β-cells**.** Identification of the top differentially-regulated transcripts in murine models of diabetes characterized by dedifferentiation (ie Pdx1-FoxO KO and β-FoxO KO mice) showed an increase in Aldh1a3 expression. Quantification of transcript, protein, and retinoic acid species confirmed that Aldh1a3 was induced in diabetic islets. Moreover, by immunohistochemistry, Aldh1a3-high cells were found to have lower expression of MafA, Nkx6.1, Insulin, but higher expression of the progenitor markers L-myc and Ngn3.

Treatment of β-cells with Aldefluor allowed for the isolation of β-cells based on their aldehyde dehydrogenase activity. Comparison of insulin secretion in Aldh-low and Aldh-high populations revealed that Aldh-high β-cells have a functional defect in insulin secretion. RNA sequencing was performed on these populations from RIP-Cre^{+} control and β-FoxO mice. In both genotypes, the Aldh-high population was characterized by the sole induction of the Aldh1a3 isoform (and not other Aldh enzymes), as well as defects in oxidative phosphorylation and mitochondrial function.

To assess whether increased Aldh1a3 activity alters β-cell function, we overexpressed Aldh1a3 in Min6 cells by adenoviral infection. These cells showed no change in insulin secretion, leading us to the tentative conclusion that Aldh1a3 was solely a marker of dysfunction, rather than a contributor. From these data, we conclude that Aldh1a3 is a marker of dysfunctional β-cells characterized by the loss of mature β-cell markers, the

expression of endocrine progenitor markers, and an insulin secretory defect likely due to mitochondrial dysfunction.

Additional studies are required to determine whether Aldh1a3 induction has a functional role in the failing β-cell. Mice with β-specific Aldh1a3 overexpression have now been generated and are currently being characterized. The question remains as to where in the progression of diabetes/dedifferentiation Aldh1a3 induction occurs. Although our studies placed one more signpost on the road to dedifferentiation, additional markers need to be identified. The loss of MafA, Insulin, and Nkx6.1 expression in Aldh-high β-cells suggest that Aldh1a3 may not be an early marker of dysfunction, but rather a later marker of ongoing dedifferentiation. Co-staining of Aldh1a3 and Ngn3/L-myc in a subset of Aldh-high β-cells supports this hypothesis.

Chapter II extended the work in Chapter I by characterizing the role of Cyb5r3 in the β-cell. Cyb5r3 was found to be the second-most differentially regulated transcript by RNA sequencing in a comparison of Aldh-high β-cells from RIP-Cre^{+} control versus β-FoxO mice. Immunohistochemistry confirmed that Cyb5r3 expression is reduced in β-cells from multiple models of diabetes. ChIP and treatment of Min6 cells with constitutively active or dominant negative forms of FoxO1 confirmed that Cyb5r3 expression is directly activated by FoxO1.

Knockdown of Cyb5r3 expression had a wide array of effects *in vitro.* Treatment of Min6 cells with an shCyb5r3-expressing adenovirus showed that these cells had decreased

insulin secretion, basal respiration, mitochondrial complex III activity, NAD/NADH ratio, but increased ROS production with palmitate exposure. *Ex vivo*, primary islets treated with the same shCyb5r3 adenovirus showed impaired insulin secretion with no change in total insulin content, as well as impaired calcium flux in response to high glucose and KCl.

Mice with β-cell-specific knockout of Cyb5r3 showed impaired glucose tolerance due to a primary β-cell defect. Hyperglycemic clamp confirmed that reduced glucose disposal occurred in the setting of impaired insulin secretion. Challenge with HFD feeding caused elevated glucose levels in female B-Cyb5r3 mice within one week. Primary islets from B-Cyb5r3 mice were functionally impaired, as stimulated insulin secretion assays revealed a blunted response to high glucose, the secretagogue l-arginine, and the depolarizing agent KCl. Respirometry of primary islets showed a reduction in respiration, consistent with the findings in shCyb5r3-treated Min6 cells.

Analysis of islets by immunohistochemistry revealed that B-Cyb5r3 islets had reduced Glut2 and MafA expression by 2 months of age, but still retained expression of Pdx1. By 6 months of age, Glut2, MafA, and Pdx1 expression were all decreased, and a compensatory increase in nuclear FoxO1 staining was observed. These findings suggest that Cyb5r3 is required for FoxO1's maintenance of β-cell identity.

From these data, we conclude that Cyb5r3 is the missing link between FoxO1 and mitochondrial function. As previously mentioned, β-cells lacking FoxO are characterized

by metabolic inflexibility and mitochondrial dysfunction. Although it is now clear that Cyb5r3 contributes to β-cell mitochondrial function, it is not known whether Cyb5r3 plays a role in substrate selection/utilization. Culturing of shCyb5r3-treated Min6 cells in palmitate increases the production of ROS, but it is possible that Cyb5r3 might also influence pathways linked to glucose versus FFA oxidation. Alternatively, mitochondrial dysfunction in general might cause a preference for lipid versus glucose oxidation in the β-cell.

It also remains unclear whether restoration of Cyb5r3 activity can rescue the mitochondrial dysfunction observed in failing β-cells. Future experiments could attempt to answer this by overexpressing Cyb5r3 in FoxO knockout Min6 cells, or by introducing a β-cell-specific Cyb5r3 overexpression allele into the β-FoxO mouse. In terms of translational relevance, there are currently no known pharmacological activators of Cyb5r3. However, treatment of B-Cyb5r3 or β-FoxO islets with the SS-31 peptide might reveal whether an improvement of ETC function can rescue the impairment in insulin secretion.

Finally, Cyb5r3 may contribute to β-cell function independent of its role in the mitochondria. For example, it is unclear whether Cyb5r3's maintenance of NAD/NADH ratio might influence the activity of sirtuins and protein acetylation. Cyb5r3 might also affect the function of multiple organelles through its lipid elongation/desaturation function. Loss of Cyb5r3 could lead to a preponderance of saturated phospholipids in

ER, plasma, or mitochondrial membranes and cause several types of organelle stress. These functions remain unexplored and will be addressed in future experiments.

In summary, Chapter I of this thesis identifies a novel marker of dysfunctional β-cells, with sequencing of this dysfunctional population yielding potential contributors to β-cell dedifferentiation. Chapter II validates one such contributor, Cyb5r3, an oxidoreductase shown to be critical to β-cell mitochondrial function as well as FoxO1-mediated β-cell lineage stability.

REFERENCES

1. Lin, H.V., Ren, H., Samuel, V.T., Lee, H.Y., Lu, T.Y., Shulman, G.I., and Accili, D. Diabetes in mice with selective impairment of insulin action in Glut4-expressing tissues. *Diabetes*. **60**(3): p. 700-9(2011).
2. Cook, J.R., Matsumoto, M., Banks, A.S., Kitamura, T., Tsuchiya, K., and Accili, D. A mutant allele encoding DNA binding-deficient FoxO1 differentially regulates hepatic glucose and lipid metabolism. *Diabetes*. **64**(6): p. 1951-65(2015).
3. Pajvani, U.B. and Accili, D. The new biology of diabetes. *Diabetologia*. **58**(11): p. 2459-68(2015).
4. Ferrannini, E. The stunned beta cell: a brief history. *Cell metabolism*. **11**(5): p. 349-52(2010).
5. Weyer, C., Bogardus, C., Mott, D.M., and Pratley, R.E. The natural history of insulin secretory dysfunction and insulin resistance in the pathogenesis of type 2 diabetes mellitus. *J Clin Invest*. **104**(6): p. 787-94(1999).
6. Prentki, M., Matschinsky, F.M., and Madiraju, S.R. Metabolic signaling in fuel-induced insulin secretion. *Cell Metab*. **18**(2): p. 162-85(2013).
7. Savage, P.J., Bennion, L.J., Flock, E.V., Nagulesparan, M., Mott, D., Roth, J., Unger, R.H., and Bennett, P.H. Diet-induced improvement of abnormalities in insulin and glucagon secretion and in insulin receptor binding in diabetes mellitus. *J Clin Endocrinol Metab*. **48**(6): p. 999-1007(1979).
8. Kitamura, Y.I., Kitamura, T., Kruse, J.P., Raum, J.C., Stein, R., Gu, W., and Accili, D. FoxO1 protects against pancreatic beta cell failure through NeuroD and MafA induction. *Cell Metab*. **2**(3): p. 153-63(2005).

9. Talchai, C., Xuan, S., Lin, H.V., Sussel, L., and Accili, D. Pancreatic beta cell dedifferentiation as a mechanism of diabetic beta cell failure. *Cell*. **150**(6): p. 1223-34(2012).

10. Kim-Muller, J.Y., Zhao, S., Srivastava, S., Mugabo, Y., Noh, H.L., Kim, Y.R., Madiraju, S.R., Ferrante, A.W., Skolnik, E.Y., Prentki, M., and Accili, D. Metabolic inflexibility impairs insulin secretion and results in MODY-like diabetes in triple FoxO-deficient mice. *Cell Metab*. **20**(4): p. 593-602(2014).

11. Talchai, S.C. and Accili, D. Legacy Effect of Foxo1 in Pancreatic Endocrine Progenitors on Adult beta-Cell Mass and Function. *Diabetes*. **64**(8): p. 2868-79(2015).

12. Kaestner, K.H., Knochel, W., and Martinez, D.E. Unified nomenclature for the winged helix/forkhead transcription factors. *Genes Dev*. **14**(2): p. 142-6(2000).

13. Lin, K., Dorman, J.B., Rodan, A., and Kenyon, C. daf-16: An HNF-3/forkhead family member that can function to double the life-span of Caenorhabditis elegans. *Science*. **278**(5341): p. 1319-1322(1997).

14. Ogg, S., Paradis, S., Gottlieb, S., Patterson, G.I., Lee, L., Tissenbaum, H.A., and Ruvkun, G. The Fork head transcription factor DAF-16 transduces insulin-like metabolic and longevity signals in C. elegans. *Nature*. **389**(6654): p. 994-999(1997).

15. Accili, D. and Arden, K.C. FoxOs at the crossroads of cellular metabolism, differentiation, and transformation. *Cell*. **117**(4): p. 421-6(2004).

16. Haeusler, R.A., Hartil, K., Vaitheesvaran, B., Arrieta-Cruz, I., Knight, C.M., Cook, J.R., Kammoun, H.L., Febbraio, M.A., Gutierrez-Juarez, R., Kurland, I.J., and

Accili, D. Integrated control of hepatic lipogenesis versus glucose production requires FoxO transcription factors. *Nat Commun*. **5**: p. 5190(2014).

17. Kitamura, T., Feng, Y., Kitamura, Y.I., Chua, S.C., Jr., Xu, A.W., Barsh, G.S., Rossetti, L., and Accili, D. Forkhead protein FoxO1 mediates Agrp-dependent effects of leptin on food intake. *Nat Med*. **12**(5): p. 534-40(2006).
18. Plum, L., Lin, H.V., Dutia, R., Tanaka, J., Aizawa, K.S., Matsumoto, M., Kim, A.J., Cawley, N.X., Paik, J.H., Loh, Y.P., DePinho, R.A., Wardlaw, S.L., and Accili, D. The obesity susceptibility gene Cpe links FoxO1 signaling in hypothalamic pro-opiomelanocortin neurons with regulation of food intake. *Nat Med*. **15**(10): p. 1195-201(2009).
19. Ren, H., Orozco, I.J., Su, Y., Suyama, S., Gutierrez-Juarez, R., Horvath, T.L., Wardlaw, S.L., Plum, L., Arancio, O., and Accili, D. FoxO1 target Gpr17 activates AgRP neurons to regulate food intake. *Cell*. **149**(6): p. 1314-26(2012).
20. Chakrabarti, P. and Kandror, K.V. FoxO1 controls insulin-dependent adipose triglyceride lipase (ATGL) expression and lipolysis in adipocytes. *J Biol Chem*. **284**(20): p. 13296-300(2009).
21. Matsumoto, M., Pocai, A., Rossetti, L., Depinho, R.A., and Accili, D. Impaired regulation of hepatic glucose production in mice lacking the forkhead transcription factor Foxo1 in liver. *Cell Metab*. **6**(3): p. 208-16(2007).
22. Tsuchiya, K., Banks, A.S., Liang, C.P., Tabas, I., Tall, A.R., and Accili, D. Homozygosity for an allele encoding deacetylated FoxO1 protects macrophages from cholesterol-induced inflammation without increasing apoptosis. *Arterioscler Thromb Vasc Biol*. **31**(12): p. 2920-8(2011).

23. Tsuchiya, K., Tanaka, J., Shuiqing, Y., Welch, C.L., DePinho, R.A., Tabas, I., Tall, A.R., Goldberg, I.J., and Accili, D. FoxOs integrate pleiotropic actions of insulin in vascular endothelium to protect mice from atherosclerosis. *Cell Metab*. **15**(3): p. 372-81(2012).

24. Tsuchiya, K., Westerterp, M., Murphy, A.J., Subramanian, V., Ferrante, A.W., Jr., Tall, A.R., and Accili, D. Expanded granulocyte/monocyte compartment in myeloid-specific triple FoxO knockout increases oxidative stress and accelerates atherosclerosis in mice. *Circ Res*. **112**(7): p. 992-1003(2013).

25. Wang, Z., York, N.W., Nichols, C.G., and Remedi, M.S. Pancreatic beta cell dedifferentiation in diabetes and redifferentiation following insulin therapy. *Cell Metab*. **19**(5): p. 872-82(2014).

26. Kitamura, T., Nakae, J., Kitamura, Y., Kido, Y., Biggs, W.H., 3rd, Wright, C.V., White, M.F., Arden, K.C., and Accili, D. The forkhead transcription factor Foxo1 links insulin signaling to Pdx1 regulation of pancreatic beta cell growth. *J Clin Invest*. **110**(12): p. 1839-47(2002).

27. Martinez, S.C., Cras-Meneur, C., Bernal-Mizrachi, E., and Permutt, M.A. Glucose regulates Foxo1 through insulin receptor signaling in the pancreatic islet beta-cell. *Diabetes*. **55**(6): p. 1581-91(2006).

28. Kawamori, D., Kaneto, H., Nakatani, Y., Matsuoka, T.A., Matsuhisa, M., Hori, M., and Yamasaki, Y. The forkhead transcription factor Foxo1 bridges the JNK pathway and the transcription factor PDX-1 through its intracellular translocation. *J Biol Chem*. **281**(2): p. 1091-8(2006).

29. Banks, A.S., Kon, N., Knight, C., Matsumoto, M., Gutierrez-Juarez, R., Rossetti, L., Gu, W., and Accili, D. SirT1 gain of function increases energy efficiency and prevents diabetes in mice. *Cell Metab*. **8**(4): p. 333-41(2008).

30. Qiang, L., Banks, A.S., and Accili, D. Uncoupling of acetylation from phosphorylation regulates FoxO1 function independent of its subcellular localization. *J Biol Chem*. **285**(35): p. 27396-401(2010).

31. Kim-Muller, J.Y., Kim, Y.J., Fan, J., Zhao, S., Banks, A.S., Prentki, M., and Accili, D. FoxO1 deacetylation decreases fatty acid oxidation in beta-cells and sustains insulin secretion in diabetes. *J Biol Chem*. (2016).

32. Matschinsky, F.M. Banting Lecture 1995. A lesson in metabolic regulation inspired by the glucokinase glucose sensor paradigm. *Diabetes*. **45**(2): p. 223-241(1996).

33. Odegaard, M.L., Joseph, J.W., Jensen, M.V., Lu, D., Ilkayeva, O., Ronnebaum, S.M., Becker, T.C., and Newgard, C.B. The mitochondrial 2-oxoglutarate carrier is part of a metabolic pathway that mediates glucose- and glutamine-stimulated insulin secretion. *J Biol Chem*. **285**(22): p. 16530-7(2010).

34. Eto, K., Tsubamoto, Y., Terauchi, Y., Sugiyama, T., Kishimoto, T., Takahashi, N., Yamauchi, N., Kubota, N., Murayama, S., Aizawa, T., Akanuma, Y., Aizawa, S., Kasai, H., Yazaki, Y., and Kadowaki, T. Role of NADH shuttle system in glucose-induced activation of mitochondrial metabolism and insulin secretion. *Science*. **283**(5404): p. 981-985(1999).

35. Schuit, F., De Vos, A., Farfari, S., Moens, K., Pipeleers, D., Brun, T., and Prentki, M. Metabolic fate of glucose in purified islet cells. Glucose-regulated anaplerosis in beta cells. *J Biol Chem*. **272**(30): p. 18572-9(1997).

36. Gheni, G., Ogura, M., Iwasaki, M., Yokoi, N., Minami, K., Nakayama, Y., Harada, K., Hastoy, B., Wu, X., Takahashi, H., Kimura, K., Matsubara, T., Hoshikawa, R., Hatano, N., Sugawara, K., Shibasaki, T., Inagaki, N., Bamba, T., Mizoguchi, A., Fukusaki, E., Rorsman, P., and Seino, S. Glutamate acts as a key signal linking glucose metabolism to incretin/cAMP action to amplify insulin secretion. *Cell Rep*. **9**(2): p. 661-73(2014).

37. Ivarsson, R., Quintens, R., Dejonghe, S., Tsukamoto, K., in 't Veld, P., Renstrom, E., and Schuit, F.C. Redox control of exocytosis: regulatory role of NADPH, thioredoxin, and glutaredoxin. *Diabetes*. **54**(7): p. 2132-42(2005).

38. MacDonald, M.J., Fahien, L.A., Brown, L.J., Hasan, N.M., Buss, J.D., and Kendrick, M.A. Perspective: emerging evidence for signaling roles of mitochondrial anaplerotic products in insulin secretion. *Am J Physiol Endocrinol Metab*. **288**(1): p. E1-15(2005).

39. Maechler, P., Li, N., Casimir, M., Vetterli, L., Frigerio, F., and Brun, T. Role of mitochondria in beta-cell function and dysfunction. *Adv Exp Med Biol*. **654**: p. 193-216(2010).

40. Buteau, J., Shlien, A., Foisy, S., and Accili, D. Metabolic diapause in pancreatic beta-cells expressing a gain-of-function mutant of the forkhead protein Foxo1. *J Biol Chem*. **282**(1): p. 287-93(2007).

41. Kelley, D.E. and Mandarino, L.J. Fuel selection in human skeletal muscle in insulin resistance: a reexamination. *Diabetes*. **49**(5): p. 677-83(2000).

42. Puri, S., Akiyama, H., and Hebrok, M. VHL-mediated disruption of Sox9 activity compromises beta-cell identity and results in diabetes mellitus. *Genes Dev*. **27**(23): p. 2563-75(2013).

43. Taylor, B.L., Liu, F.F., and Sander, M. Nkx6.1 is essential for maintaining the functional state of pancreatic beta cells. *Cell Rep*. **4**(6): p. 1262-75(2013).

44. Blum, B., Roose, A.N., Barrandon, O., Maehr, R., Arvanites, A.C., Davidow, L.S., Davis, J.C., Peterson, Q.P., Rubin, L.L., and Melton, D.A. Reversal of beta cell de-differentiation by a small molecule inhibitor of the TGFbeta pathway. *Elife*. **3**: p. e02809(2014).

45. Chera, S., Baronnier, D., Ghila, L., Cigliola, V., Jensen, J.N., Gu, G., Furuyama, K., Thorel, F., Gribble, F.M., Reimann, F., and Herrera, P.L. Diabetes recovery by age-dependent conversion of pancreatic delta-cells into insulin producers. *Nature*. **514**(7523): p. 503-7(2014).

46. Casellas, A., Mallol, C., Salavert, A., Jimenez, V., Garcia, M., Agudo, J., Obach, M., Haurigot, V., Vila, L., Molas, M., Lage, R., Morro, M., Casana, E., Ruberte, J., and Bosch, F. Insulin-like Growth Factor 2 Overexpression Induces beta-Cell Dysfunction and Increases Beta-cell Susceptibility to Damage. *J Biol Chem*. **290**(27): p. 16772-85(2015).

47. Nathan, G., Kredo-Russo, S., Geiger, T., Lenz, A., Kaspi, H., Hornstein, E., and Efrat, S. MiR-375 promotes redifferentiation of adult human beta cells expanded in vitro. *PloS one*. **10**(4): p. e0122108(2015).

48. Toren-Haritan, G. and Efrat, S. TGFbeta Pathway Inhibition Redifferentiates Human Pancreatic Islet beta Cells Expanded In Vitro. *PloS one*. **10**(9): p. e0139168(2015).

49. Friedman-Mazursky, O., Elkon, R., and Efrat, S. Redifferentiation of expanded human islet beta cells by inhibition of ARX. *Sci Rep*. **6**: p. 20698(2016).

50. Fiori, J.L., Shin, Y.K., Kim, W., Krzysik-Walker, S.M., Gonzalez-Mariscal, I., Carlson, O.D., Sanghvi, M., Moaddel, R., Farhang, K., Gadkaree, S.K., Doyle, M.E., Pearson, K.J., Mattison, J.A., de Cabo, R., and Egan, J.M. Resveratrol prevents beta-cell dedifferentiation in nonhuman primates given a high-fat/high-sugar diet. *Diabetes*. **62**(10): p. 3500-13(2013).

51. Gerstein, H.C., Bosch, J., Dagenais, G.R., Diaz, R., Jung, H., Maggioni, A.P., Pogue, J., Probstfield, J., Ramachandran, A., Riddle, M.C., Ryden, L.E., and Yusuf, S. Basal insulin and cardiovascular and other outcomes in dysglycemia. *N Engl J Med*. **367**(4): p. 319-28(2012).

52. Kim-Muller, J.Y. and Accili, D. Cell biology. Selective insulin sensitizers. *Science*. **331**(6024): p. 1529-31(2011).

53. Doar, J.W., Wilde, C.E., Thompson, M.E., and Sewell, P.F. Influence of treatment with diet alone on oral glucose-tolerance test and plasma sugar and insulin levels in patients with maturity-onset diabetes mellitus. *Lancet*. **1**(7919): p. 1263-6(1975).

54. Greenwood, R.H., Mahler, R.F., and Hales, C.N. Improvement in insulin secretion in diabetes after diazoxide. *Lancet*. **1**(7957): p. 444-7(1976).

55. U.K. Prospective Diabetes Study Group. Intensive blood-glucose control with sulphonylureas or insulin compared with conventional treatment and risk of complications in patients with type 2 diabetes (UKPDS 33). . *Lancet*. **352**(9131): p. 837-53(1998).

56. White, M.G., Marshall, H.L., Rigby, R., Huang, G.C., Amer, A., Booth, T., White, S., and Shaw, J.A. Expression of mesenchymal and alpha-cell phenotypic markers in islet beta-cells in recently diagnosed diabetes. *Diabetes Care*. **36**(11): p. 3818-20(2013).

57. Marselli, L., Suleiman, M., Masini, M., Campani, D., Bugliani, M., Syed, F., Martino, L., Focosi, D., Scatena, F., Olimpico, F., Filipponi, F., Masiello, P., Boggi, U., and Marchetti, P. Are we overestimating the loss of beta cells in type 2 diabetes? *Diabetologia*. **57**(2): p. 362-5(2014).

58. Kitamura, T., Kitamura, Y.I., Kobayashi, M., Kikuchi, O., Sasaki, T., Depinho, R.A., and Accili, D. Regulation of pancreatic juxtaductal endocrine cell formation by FoxO1. *Molecular and cellular biology*. **29**(16): p. 4417-30(2009).

59. Tsuchiya, K., Tanaka, J., Shuiqing, Y., Welch, C.L., Depinho, R.A., Tabas, I., Tall, A.R., Goldberg, I.J., and Accili, D. FoxOs Integrate Pleiotropic Actions of Insulin in Vascular Endothelium to Protect Mice from Atherosclerosis. *Cell metabolism*. **15**(3): p. 372-81(2012).

60. Xuan, S., Kitamura, T., Nakae, J., Politi, K., Kido, Y., Fisher, P.E., Morroni, M., Cinti, S., White, M.F., Herrera, P.L., Accili, D., and Efstratiadis, A. Defective insulin secretion in pancreatic beta cells lacking type 1 IGF receptor. *The Journal of clinical investigation*. **110**(7): p. 1011-9(2002).

61. Qiang, L., Wang, L., Kon, N., Zhao, W., Lee, S., Zhang, Y., Rosenbaum, M., Zhao, Y., Gu, W., Farmer, S.R., and Accili, D. Brown remodeling of white adipose tissue by SirT1-dependent deacetylation of Ppargamma. *Cell*. **150**(3): p. 620-32(2012).

62. Fajans, S.S. and Bell, G.I. MODY: history, genetics, pathophysiology, and clinical decision making. *Diabetes Care*. **34**(8): p. 1878-84(2011).

63. Hang, Y., Yamamoto, T., Benninger, R.K., Brissova, M., Guo, M., Bush, W., Piston, D.W., Powers, A.C., Magnuson, M., Thurmond, D.C., and Stein, R. The MafA transcription factor becomes essential to islet beta-cells soon after birth. *Diabetes*. **63**(6): p. 1994-2005(2014).

64. Clee, S.M., Yandell, B.S., Schueler, K.M., Rabaglia, M.E., Richards, O.C., Raines, S.M., Kabara, E.A., Klass, D.M., Mui, E.T., Stapleton, D.S., Gray-Keller, M.P., Young, M.B., Stoehr, J.P., Lan, H., Boronenkov, I., Raess, P.W., Flowers, M.T., and Attie, A.D. Positional cloning of Sorcs1, a type 2 diabetes quantitative trait locus. *Nature genetics*. **38**(6): p. 688-93(2006).

65. https://www.t1dbase.org/page/AtlasHome. 2016; Available from: https://www.t1dbase.org/page/AtlasHome.

66. Cinti, F., Bouchi, R., Kim-Muller, J.Y., Ohmura, Y., Rodrigo Sandoval, P., Masini, M., Marselli, L., Suleiman, M., Ratner, L.E., Marchetti, P., and Accili, D. Evidence of beta-cell Dedifferentiation in Human Type 2 Diabetes. *The Journal of clinical endocrinology and metabolism*. p. jc20152860(2015).

67. Ginestier, C., Hur, M.H., Charafe-Jauffret, E., Monville, F., Dutcher, J., Brown, M., Jacquemier, J., Viens, P., Kleer, C.G., Liu, S., Schott, A., Hayes, D.,

Birnbaum, D., Wicha, M.S., and Dontu, G. ALDH1 is a marker of normal and malignant human mammary stem cells and a predictor of poor clinical outcome. *Cell Stem Cell*. **1**(5): p. 555-67(2007).

68. Fleischman, A.G. ALDH marks leukemia stem cell. *Blood*. **119**(15): p. 3376-7(2012).

69. Marcato, P., Dean, C.A., Giacomantonio, C.A., and Lee, P.W. Aldehyde dehydrogenase: its role as a cancer stem cell marker comes down to the specific isoform. *Cell Cycle*. **10**(9): p. 1378-84(2011).

70. Awad, O., Yustein, J.T., Shah, P., Gul, N., Katuri, V., O'Neill, A., Kong, Y., Brown, M.L., Toretsky, J.A., and Loeb, D.M. High ALDH activity identifies chemotherapy-resistant Ewing's sarcoma stem cells that retain sensitivity to EWS-FLI1 inhibition. *PloS one*. **5**(11): p. e13943(2010).

71. Huang, E.H., Hynes, M.J., Zhang, T., Ginestier, C., Dontu, G., Appelman, H., Fields, J.Z., Wicha, M.S., and Boman, B.M. Aldehyde dehydrogenase 1 is a marker for normal and malignant human colonic stem cells (SC) and tracks SC overpopulation during colon tumorigenesis. *Cancer Res*. **69**(8): p. 3382-9(2009).

72. Croker, A.K., Goodale, D., Chu, J., Postenka, C., Hedley, B.D., Hess, D.A., and Allan, A.L. High aldehyde dehydrogenase and expression of cancer stem cell markers selects for breast cancer cells with enhanced malignant and metastatic ability. *J Cell Mol Med*. **13**(8B): p. 2236-52(2009).

73. Zhang, W., Liu, Y., Hu, H., Huang, H., Bao, Z., Yang, P., Wang, Y., You, G., Yan, W., Jiang, T., Wang, J., and Zhang, W. ALDH1A3: A Marker of Mesenchymal

Phenotype in Gliomas Associated with Cell Invasion. *PloS one*. **10**(11): p. e0142856(2015).

74. Talchai, C., Xuan, S., Kitamura, T., DePinho, R.A., and Accili, D. Generation of functional insulin-producing cells in the gut by Foxo1 ablation. *Nat Genet*. **44**(4): p. 406-12, S1(2012).

75. Morgan, C.A., Parajuli, B., Buchman, C.D., Dria, K., and Hurley, T.D. N,N-diethylaminobenzaldehyde (DEAB) as a substrate and mechanism-based inhibitor for human ALDH isoenzymes. *Chem Biol Interact*. **234**: p. 18-28(2015).

76. Nakae, J., Kitamura, T., Silver, D.L., and Accili, D. The forkhead transcription factor Foxo1 (Fkhr) confers insulin sensitivity onto glucose-6-phosphatase expression. *J Clin Invest*. **108**(9): p. 1359-67(2001).

77. Kitamura, T., Kitamura, Y.I., Funahashi, Y., Shawber, C.J., Castrillon, D.H., Kollipara, R., DePinho, R.A., Kitajewski, J., and Accili, D. A Foxo/Notch pathway controls myogenic differentiation and fiber type specification. *J Clin Invest*. **117**(9): p. 2477-85(2007).

78. Brun, P.J., Grijalva, A., Rausch, R., Watson, E., Yuen, J.J., Das, B.C., Shudo, K., Kagechika, H., Leibel, R.L., and Blaner, W.S. Retinoic acid receptor signaling is required to maintain glucose-stimulated insulin secretion and beta-cell mass. *The FASEB journal : official publication of the Federation of American Societies for Experimental Biology*. **29**(2): p. 671-83(2015).

79. Dorrell, C., Schug, J., Lin, C.F., Canaday, P.S., Fox, A.J., Smirnova, O., Bonnah, R., Streeter, P.R., Stoeckert, C.J., Jr., Kaestner, K.H., and Grompe, M.

Transcriptomes of the major human pancreatic cell types. *Diabetologia*. **54**(11): p. 2832-44(2011).

80. Moran, I., Akerman, I., van de Bunt, M., Xie, R., Benazra, M., Nammo, T., Arnes, L., Nakic, N., Garcia-Hurtado, J., Rodriguez-Segui, S., Pasquali, L., Sauty-Colace, C., Beucher, A., Scharfmann, R., van Arensbergen, J., Johnson, P.R., Berry, A., Lee, C., Harkins, T., Gmyr, V., Pattou, F., Kerr-Conte, J., Piemonti, L., Berney, T., Hanley, N., Gloyn, A.L., Sussel, L., Langman, L., Brayman, K.L., Sander, M., McCarthy, M.I., Ravassard, P., and Ferrer, J. Human beta cell transcriptome analysis uncovers lncRNAs that are tissue-specific, dynamically regulated, and abnormally expressed in type 2 diabetes. *Cell Metab*. **16**(4): p. 435-48(2012).

81. Kameswaran, V., Bramswig, N.C., McKenna, L.B., Penn, M., Schug, J., Hand, N.J., Chen, Y., Choi, I., Vourekas, A., Won, K.J., Liu, C., Vivek, K., Naji, A., Friedman, J.R., and Kaestner, K.H. Epigenetic regulation of the DLK1-MEG3 microRNA cluster in human type 2 diabetic islets. *Cell Metab*. **19**(1): p. 135-45(2014).

82. Stecca, B. and Ruiz i Altaba, A. A GLI1-p53 inhibitory loop controls neural stem cell and tumour cell numbers. *The EMBO journal*. **28**(6): p. 663-76(2009).

83. Virbasius, J.V. and Scarpulla, R.C. Activation of the human mitochondrial transcription factor A gene by nuclear respiratory factors: a potential regulatory link between nuclear and mitochondrial gene expression in organelle biogenesis. *Proc Natl Acad Sci U S A*. **91**(4): p. 1309-13(1994).

84. Dinkova-Kostova, A.T. and Abramov, A.Y. The emerging role of Nrf2 in mitochondrial function. *Free Radic Biol Med*. **88**(Pt B): p. 179-88(2015).

85. Gu, Y., Lindner, J., Kumar, A., Yuan, W., and Magnuson, M.A. Rictor/mTORC2 is essential for maintaining a balance between beta-cell proliferation and cell size. *Diabetes*. **60**(3): p. 827-37(2011).

86. Tessem, J.S., Moss, L.G., Chao, L.C., Arlotto, M., Lu, D., Jensen, M.V., Stephens, S.B., Tontonoz, P., Hohmeier, H.E., and Newgard, C.B. Nkx6.1 regulates islet beta-cell proliferation via Nr4a1 and Nr4a3 nuclear receptors. *Proc Natl Acad Sci U S A*. **111**(14): p. 5242-7(2014).

87. Siendones, E., SantaCruz-Calvo, S., Martin-Montalvo, A., Cascajo, M.V., Ariza, J., Lopez-Lluch, G., Villalba, J.M., Acquaviva-Bourdain, C., Roze, E., Bernier, M., de Cabo, R., and Navas, P. Membrane-bound CYB5R3 is a common effector of nutritional and oxidative stress response through FOXO3a and Nrf2. *Antioxid Redox Signal*. **21**(12): p. 1708-25(2014).

88. Xie, J., Zhu, H., Larade, K., Ladoux, A., Seguritan, A., Chu, M., Ito, S., Bronson, R.T., Leiter, E.H., Zhang, C.Y., Rosen, E.D., and Bunn, H.F. Absence of a reductase, NCB5OR, causes insulin-deficient diabetes. *Proc Natl Acad Sci U S A*. **101**(29): p. 10750-5(2004).

89. Matsuzaka, T., Shimano, H., Yahagi, N., Kato, T., Atsumi, A., Yamamoto, T., Inoue, N., Ishikawa, M., Okada, S., Ishigaki, N., Iwasaki, H., Iwasaki, Y., Karasawa, T., Kumadaki, S., Matsui, T., Sekiya, M., Ohashi, K., Hasty, A.H., Nakagawa, Y., Takahashi, A., Suzuki, H., Yatoh, S., Sone, H., Toyoshima, H., Osuga, J., and Yamada, N. Crucial role of a long-chain fatty acid elongase,

Elovl6, in obesity-induced insulin resistance. *Nat Med*. **13**(10): p. 1193-202(2007).

90. Takiishi, T., Van Belle, T., Gysemans, C., and Mathieu, C. Effects of vitamin D on antigen-specific and non-antigen-specific immune modulation: relevance for type 1 diabetes. *Pediatr Diabetes*. **14**(2): p. 81-9(2013).

91. Fadista, J., Vikman, P., Laakso, E.O., Mollet, I.G., Esguerra, J.L., Taneera, J., Storm, P., Osmark, P., Ladenvall, C., Prasad, R.B., Hansson, K.B., Finotello, F., Uvebrant, K., Ofori, J.K., Di Camillo, B., Krus, U., Cilio, C.M., Hansson, O., Eliasson, L., Rosengren, A.H., Renstrom, E., Wollheim, C.B., and Groop, L. Global genomic and transcriptomic analysis of human pancreatic islets reveals novel genes influencing glucose metabolism. *Proc Natl Acad Sci U S A*. **111**(38): p. 13924-9(2014).

92. Cooper, J.D., Smyth, D.J., Smiles, A.M., Plagnol, V., Walker, N.M., Allen, J.E., Downes, K., Barrett, J.C., Healy, B.C., Mychaleckyj, J.C., Warram, J.H., and Todd, J.A. Meta-analysis of genome-wide association study data identifies additional type 1 diabetes risk loci. *Nature genetics*. **40**(12): p. 1399-401(2008).

93. Winkler, C., Krumsiek, J., Buettner, F., Angermuller, C., Giannopoulou, E.Z., Theis, F.J., Ziegler, A.G., and Bonifacio, E. Feature ranking of type 1 diabetes susceptibility genes improves prediction of type 1 diabetes. *Diabetologia*. **57**(12): p. 2521-9(2014).

94. Marroqui, L., Santin, I., Dos Santos, R.S., Marselli, L., Marchetti, P., and Eizirik, D.L. BACH2, a candidate risk gene for type 1 diabetes, regulates apoptosis in

pancreatic beta-cells via JNK1 modulation and crosstalk with the candidate gene PTPN2. *Diabetes*. **63**(7): p. 2516-27(2014).

95. Jimenez-Hidalgo, M., Santos-Ocana, C., Padilla, S., Villalba, J.M., Lopez-Lluch, G., Martin-Montalvo, A., Minor, R.K., Sinclair, D.A., de Cabo, R., and Navas, P. NQR1 controls lifespan by regulating the promotion of respiratory metabolism in yeast. *Aging Cell*. **8**(2): p. 140-51(2009).

96. Ahmed, M., Muhammed, S.J., Kessler, B., and Salehi, A. Mitochondrial proteome analysis reveals altered expression of voltage dependent anion channels in pancreatic beta-cells exposed to high glucose. *Islets*. **2**(5): p. 283-92(2010).

97. Tang, N., Matsuzaka, T., Suzuki, M., Nakano, Y., Zao, H., Yokoo, T., Suzuki-Kemuriyama, N., Kuba, M., Okajima, Y., Takeuchi, Y., Kobayashi, K., Iwasaki, H., Yatoh, S., Takahashi, A., Suzuki, H., Sone, H., Shimada, M., Nakagawa, Y., Yahagi, N., Yamada, N., and Shimano, H. Ablation of Elovl6 protects pancreatic islets from high-fat diet-induced impairment of insulin secretion. *Biochem Biophys Res Commun*. **450**(1): p. 318-23(2014).

98. Kamio, T., Toki, T., Kanezaki, R., Sasaki, S., Tandai, S., Terui, K., Ikebe, D., Igarashi, K., and Ito, E. B-cell-specific transcription factor BACH2 modifies the cytotoxic effects of anticancer drugs. *Blood*. **102**(9): p. 3317-22(2003).

99. Guo, S., Dai, C., Guo, M., Taylor, B., Harmon, J.S., Sander, M., Robertson, R.P., Powers, A.C., and Stein, R. Inactivation of specific beta cell transcription factors in type 2 diabetes. *J Clin Invest*. **123**(8): p. 3305-16(2013).

100. Pasquali, L., Gaulton, K.J., Rodriguez-Segui, S.A., Mularoni, L., Miguel-Escalada, I., Akerman, I., Tena, J.J., Moran, I., Gomez-Marin, C., van de Bunt,

M., Ponsa-Cobas, J., Castro, N., Nammo, T., Cebola, I., Garcia-Hurtado, J., Maestro, M.A., Pattou, F., Piemonti, L., Berney, T., Gloyn, A.L., Ravassard, P., Gomez-Skarmeta, J.L., Muller, F., McCarthy, M.I., and Ferrer, J. Pancreatic islet enhancer clusters enriched in type 2 diabetes risk-associated variants. *Nature genetics*. **46**(2): p. 136-43(2014).

101. Wallace, C., Smyth, D.J., Maisuria-Armer, M., Walker, N.M., Todd, J.A., and Clayton, D.G. The imprinted DLK1-MEG3 gene region on chromosome 14q32.2 alters susceptibility to type 1 diabetes. *Nature genetics*. **42**(1): p. 68-71(2010).

102. Yasuda, K., Miyake, K., Horikawa, Y., Hara, K., Osawa, H., Furuta, H., Hirota, Y., Mori, H., Jonsson, A., Sato, Y., Yamagata, K., Hinokio, Y., Wang, H.Y., Tanahashi, T., Nakamura, N., Oka, Y., Iwasaki, N., Iwamoto, Y., Yamada, Y., Seino, Y., Maegawa, H., Kashiwagi, A., Takeda, J., Maeda, E., Shin, H.D., Cho, Y.M., Park, K.S., Lee, H.K., Ng, M.C., Ma, R.C., So, W.Y., Chan, J.C., Lyssenko, V., Tuomi, T., Nilsson, P., Groop, L., Kamatani, N., Sekine, A., Nakamura, Y., Yamamoto, K., Yoshida, T., Tokunaga, K., Itakura, M., Makino, H., Nanjo, K., Kadowaki, T., and Kasuga, M. Variants in KCNQ1 are associated with susceptibility to type 2 diabetes mellitus. *Nature genetics*. **40**(9): p. 1092-7(2008).

103. Maedler, K., Carr, R.D., Bosco, D., Zuellig, R.A., Berney, T., and Donath, M.Y. Sulfonylurea induced beta-cell apoptosis in cultured human islets. *Journal of Clinical Endocrinology and Metabolism*. **90**(1): p. 501-6(2005).

104. Abdulreda, M.H., Rodriguez-Diaz, R., Caicedo, A., and Berggren, P.O. Liraglutide Compromises Pancreatic beta Cell Function in a Humanized Mouse Model. *Cell Metab*. (2016).

105. Kahn, S.E., Haffner, S.M., Heise, M.A., Herman, W.H., Holman, R.R., Jones, N.P., Kravitz, B.G., Lachin, J.M., O'Neill, M.C., Zinman, B., Viberti, G., and Group, A.S. Glycemic durability of rosiglitazone, metformin, or glyburide monotherapy. *N Engl J Med*. **355**(23): p. 2427-43(2006).

106. Talchai, C., Xuan, S., Lin, H.V., Sussel, L., and Accili, D. Pancreatic β cell dedifferentiation as a mechanism of diabetic β cell failure. *Cell*. **150**(6): p. 1223-1234(2012).

107. Wang, Z., York, N.W., Nichols, C.G., and Remedi, M.S. Pancreatic β cell dedifferentiation in diabetes and redifferentiation following insulin therapy. *Cell Metab.* **19**(5): p. 872-882(2014).

108. Spijker, H.S., Song, H., Ellenbroek, J.H., Roefs, M.M., Engelse, M.A., Bos, E., Koster, A.J., Rabelink, T.J., Hansen, B.C., Clark, A., Carlotti, F., and de Koning, E.J.P. Loss of β-Cell Identity Occurs in Type 2 Diabetes and Is Associated With Islet Amyloid Deposits. - PubMed - NCBI. *Diabetes*. **64**(8): p. 2928-2938(2015).

109. Jonas, J.C., Sharma, A., Hasenkamp, W., Ilkova, H., Patanè, G., Laybutt, R., Bonner-Weir, S., and Weir, G.C. Chronic hyperglycemia triggers loss of pancreatic beta cell differentiation in an animal model of diabetes. *Journal of Biological Chemistry*. **274**(20): p. 14112-14121(1999).

110. Guo, S., Dai, C., Guo, M., Taylor, B., Harmon, J.S., Sander, M., Robertson, R.P., Powers, A.C., and Stein, R., *Inactivation of specific β cell transcription factors in type 2 diabetes*, in *Journal of Clinical Investigation*. 2013, American Society for Clinical Investigation. p. 3305-3316.

111. Taylor, B.L., Liu, F.-F., and Sander, M. Nkx6.1 Is Essential for Maintaining the Functional State of Pancreatic Beta Cells. *Cell Rep*. **4**(6): p. 1262-1275(2013).

112. Puri, S., Akiyama, H., and Hebrok, M. VHL-mediated disruption of Sox9 activity compromises β-cell identity and results in diabetes mellitus. *Genes & Development*. **27**(23): p. 2563-2575(2013).

113. Kim-Muller, J.Y., Fan, J., Kim, Y.J., Lee, S.A., Ishida, E., Blaner, W.S., and Accili, D. Aldehyde dehydrogenase 1a3 defines a subset of failing pancreatic beta cells in diabetic mice. *Nat Commun*. **7**: p. 12631(2016).

114. Siendones, E., SantaCruz-Calvo, S., Martín-Montalvo, A., Cascajo, M.V., Ariza, J., López-Lluch, G., M, V., José, Acquaviva-Bourdain, C., Roze, E., Bernier, M., de Cabo, R., and Navas, P. Membrane-Bound CYB5R3 Is a Common Effector of Nutritional and Oxidative Stress Response Through FOXO3a and Nrf2. *Antioxidants and Redox Signaling*. **21**(12): p. 1708-1725(2014).

115. Shirabe, K., Landi, M.T., Takeshita, M., Uziel, G., Fedrizzi, E., and Borgese, N. A novel point mutation in a 3' splice site of the NADH-cytochrome b5 reductase gene results in immunologically undetectable enzyme and impaired NADH-dependent ascorbate regeneration in cultured fibroblasts of a patient with type II hereditary methemoglobinemia. *Am J Hum Genet*. **57**(2): p. 302-10(1995).

116. Martin-Montalvo, A., Sun, Y., Diaz-Ruiz, A., Ali, A., Gutierrez, V., Palacios, H.H., Curtis, J., Siendones, E., Ariza, J., Abulwerdi, G.A., Sun, X., Wang, A.X., Pearson, K.J., Fishbein, K.W., Spencer, R.G., Wang, M., Han, X., Scheibye-Knudsen, M., Baur, J.A., Shertzer, H.G., Navas, P., Villalba, J.M., Zou, S.,

Bernier, M., and de Cabo, R. Cytochrome b5 reductase and the control of lipid metabolism and healthspan. *NPJ Aging Mech Dis*. **2**: p. 16006(2016).

117. Xie, J., Zhu, H., Larade, K., Ladoux, A., Seguritan, A., Chu, M., Ito, S., Bronson, R.T., Leiter, E.H., Zhang, C.-Y., Rosen, E.D., and Bunn, H.F. Absence of a reductase, NCB5OR, causes insulin-deficient diabetes. *Proc. Natl. Acad. Sci. U.S.A.* **101**(29): p. 10750-10755(2004).

118. Nakae, J., Biggs, W.H., 3rd, Kitamura, T., Cavenee, W.K., Wright, C.V., Arden, K.C., and Accili, D. Regulation of insulin action and pancreatic beta-cell function by mutated alleles of the gene encoding forkhead transcription factor Foxo1. *Nat Genet*. **32**(2): p. 245-53(2002).

119. Haeusler, R.A., Kaestner, K.H., and Accili, D. FoxOs function synergistically to promote glucose production. *J Biol Chem*. **285**(46): p. 35245-8(2010).

120. Kitamura, T., Kido, Y., Nef, S., Merenmies, J., Parada, L.F., and Accili, D. Preserved pancreatic beta-cell development and function in mice lacking the insulin receptor-related receptor. *Mol Cell Biol*. **21**(16): p. 5624-30(2001).

121. Spinazzi, M., Casarin, A., Pertegato, V., Salviati, L., and Angelini, C. Assessment of mitochondrial respiratory chain enzymatic activities on tissues and cultured cells. *Nat Protoc*. **7**(6): p. 1235-46(2012).

122. Son, J., Shen, S.S., Margueron, R., and Reinberg, D. Nucleosome-binding activities within JARID2 and EZH1 regulate the function of PRC2 on chromatin. *Genes Dev*. **27**(24): p. 2663-77(2013).

123. Schaffer, L., Brand, C.L., Hansen, B.F., Ribel, U., Shaw, A.C., Slaaby, R., and Sturis, J. A novel high-affinity peptide antagonist to the insulin receptor. *Biochem Biophys Res Commun*. **376**(2): p. 380-3(2008).

124. Nakae, J., Kitamura, T., Kitamura, Y., Biggs, W.H., 3rd, Arden, K.C., and Accili, D. The forkhead transcription factor Foxo1 regulates adipocyte differentiation. *Dev Cell*. **4**(1): p. 119-29(2003).

125. Wollheim, C.B. and Maechler, P. Beta-cell mitochondria and insulin secretion: messenger role of nucleotides and metabolites. *Diabetes*. **51 Suppl 1**: p. S37-42(2002).

126. St-Pierre, J., Buckingham, J.A., Roebuck, S.J., and Brand, M.D. Topology of superoxide production from different sites in the mitochondrial electron transport chain. *J Biol Chem*. **277**(47): p. 44784-90(2002).

127. Lowell, B.B. and Shulman, G.I. Mitochondrial dysfunction and type 2 diabetes. *Science*. **307**(5708): p. 384-7(2005).

128. Maassen, J.A., LM, T.H., Van Essen, E., Heine, R.J., Nijpels, G., Jahangir Tafrechi, R.S., Raap, A.K., Janssen, G.M., and Lemkes, H.H. Mitochondrial diabetes: molecular mechanisms and clinical presentation. *Diabetes*. **53 Suppl 1**: p. S103-9(2004).

129. Anello, M., Lupi, R., Spampinato, D., Piro, S., Masini, M., Boggi, U., Del Prato, S., Rabuazzo, A.M., Purrello, F., and Marchetti, P. Functional and morphological alterations of mitochondria in pancreatic beta cells from type 2 diabetic patients. *Diabetologia*. **48**(2): p. 282-9(2005).

130. Bindokas, V.P., Kuznetsov, A., Sreenan, S., Polonsky, K.S., Roe, M.W., and Philipson, L.H. Visualizing superoxide production in normal and diabetic rat islets of Langerhans. *J Biol Chem*. **278**(11): p. 9796-801(2003).

131. Gauthier, B.R., Wiederkehr, A., Baquie, M., Dai, C., Powers, A.C., Kerr-Conte, J., Pattou, F., MacDonald, R.J., Ferrer, J., and Wollheim, C.B. PDX1 deficiency causes mitochondrial dysfunction and defective insulin secretion through TFAM suppression. *Cell Metab*. **10**(2): p. 110-8(2009).

132. Tiedge, M., Lortz, S., Drinkgern, J., and Lenzen, S. Relation between antioxidant enzyme gene expression and antioxidative defense status of insulin-producing cells. *Diabetes*. **46**(11): p. 1733-42(1997).

133. Lenzen, S., Drinkgern, J., and Tiedge, M. Low antioxidant enzyme gene expression in pancreatic islets compared with various other mouse tissues. *Free Radic Biol Med*. **20**(3): p. 463-6(1996).

134. Hoch, F.L. Cardiolipins and biomembrane function. *Biochim Biophys Acta*. **1113**(1): p. 71-133(1992).

135. Soberanes, S., Urich, D., Baker, C.M., Burgess, Z., Chiarella, S.E., Bell, E.L., Ghio, A.J., De Vizcaya-Ruiz, A., Liu, J., Ridge, K.M., Kamp, D.W., Chandel, N.S., Schumacker, P.T., Mutlu, G.M., and Budinger, G.R. Mitochondrial complex III-generated oxidants activate ASK1 and JNK to induce alveolar epithelial cell death following exposure to particulate matter air pollution. *J Biol Chem*. **284**(4): p. 2176-86(2009).

136. Elahian, F., Sepehrizadeh, Z., Moghimi, B., and Mirzaei, S.A. Human cytochrome b5 reductase: structure, function, and potential applications. *Crit Rev Biotechnol*. **34**(2): p. 134-43(2014).

137. Fu, S., Yang, L., Li, P., Hofmann, O., Dicker, L., Hide, W., Lin, X., Watkins, S.M., Ivanov, A.R., and Hotamisligil, G.S. Aberrant lipid metabolism disrupts calcium homeostasis causing liver endoplasmic reticulum stress in obesity. *Nature*. **473**(7348): p. 528-31(2011).

138. Hazel, J.R. and Williams, E.E. The role of alterations in membrane lipid composition in enabling physiological adaptation of organisms to their physical environment. *Prog Lipid Res*. **29**(3): p. 167-227(1990).

139. Busch, A.K., Gurisik, E., Cordery, D.V., Sudlow, M., Denyer, G.S., Laybutt, D.R., Hughes, W.E., and Biden, T.J. Increased fatty acid desaturation and enhanced expression of stearoyl coenzyme A desaturase protects pancreatic beta-cells from lipoapoptosis. *Diabetes*. **54**(10): p. 2917-24(2005).

140. Weng, J., Li, Y., Xu, W., Shi, L., Zhang, Q., Zhu, D., Hu, Y., Zhou, Z., Yan, X., Tian, H., Ran, X., Luo, Z., Xian, J., Yan, L., Li, F., Zeng, L., Chen, Y., Yang, L., Yan, S., Liu, J., Li, M., Fu, Z., and Cheng, H. Effect of intensive insulin therapy on beta-cell function and glycaemic control in patients with newly diagnosed type 2 diabetes: a multicentre randomised parallel-group trial. *Lancet*. **371**(9626): p. 1753-60(2008).

141. Szeto, H.H. and Birk, A.V. Serendipity and the discovery of novel compounds that restore mitochondrial plasticity. *Clin Pharmacol Ther*. **96**(6): p. 672-83(2014).

142. Thomas, D.A., Stauffer, C., Zhao, K., Yang, H., Sharma, V.K., Szeto, H.H., and Suthanthiran, M. Mitochondrial targeting with antioxidant peptide SS-31 prevents mitochondrial depolarization, reduces islet cell apoptosis, increases islet cell yield, and improves posttransplantation function. *J Am Soc Nephrol*. **18**(1): p. 213-22(2007).